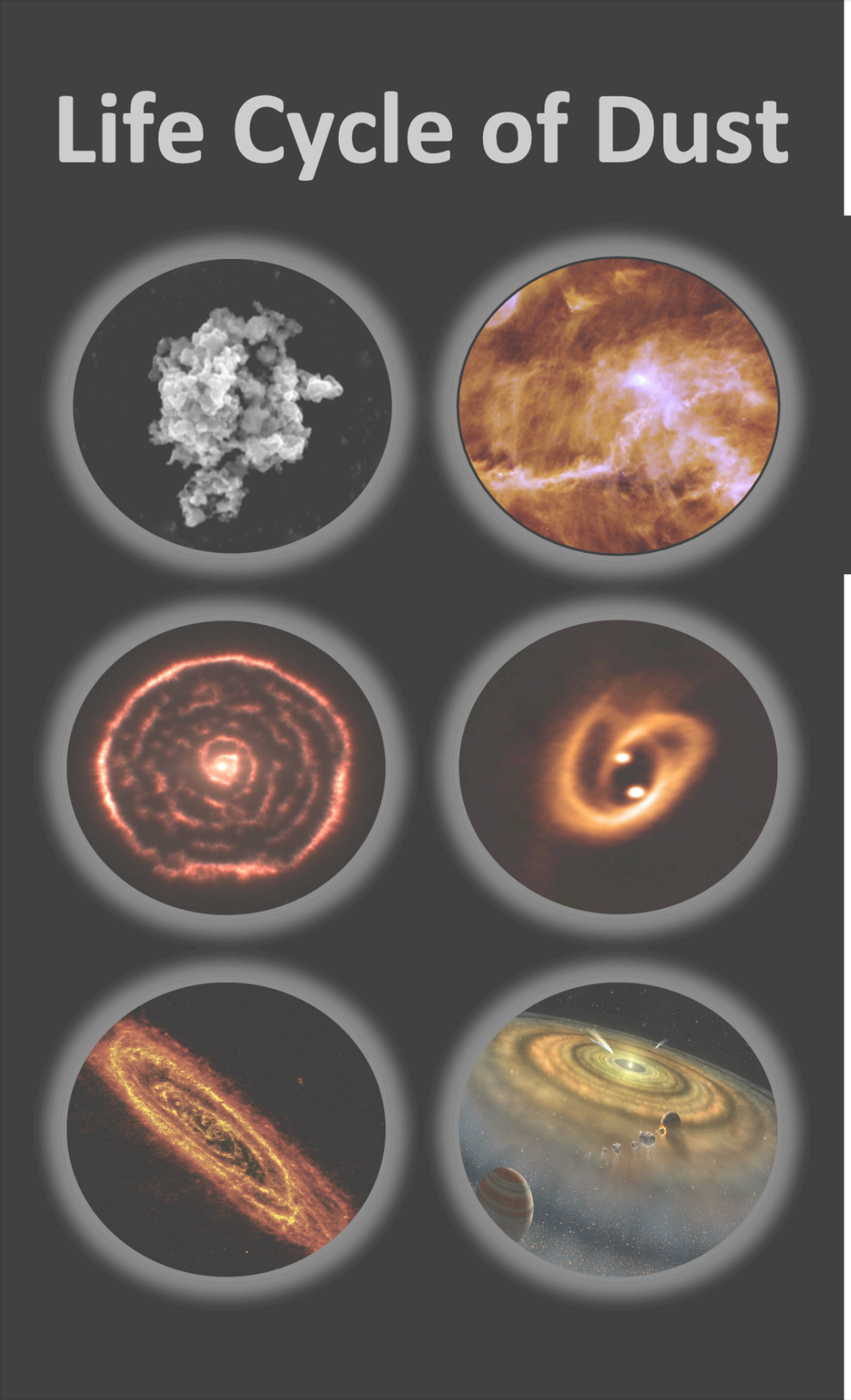

Astronomical facilities to study the dust

Josep Miquel Girart

Institute of Space Sciences (ICE-CSIC / IEEC)

Institute of Space Sciences
EXCELENCIA MARÍA DE MAEZTU
CSIC

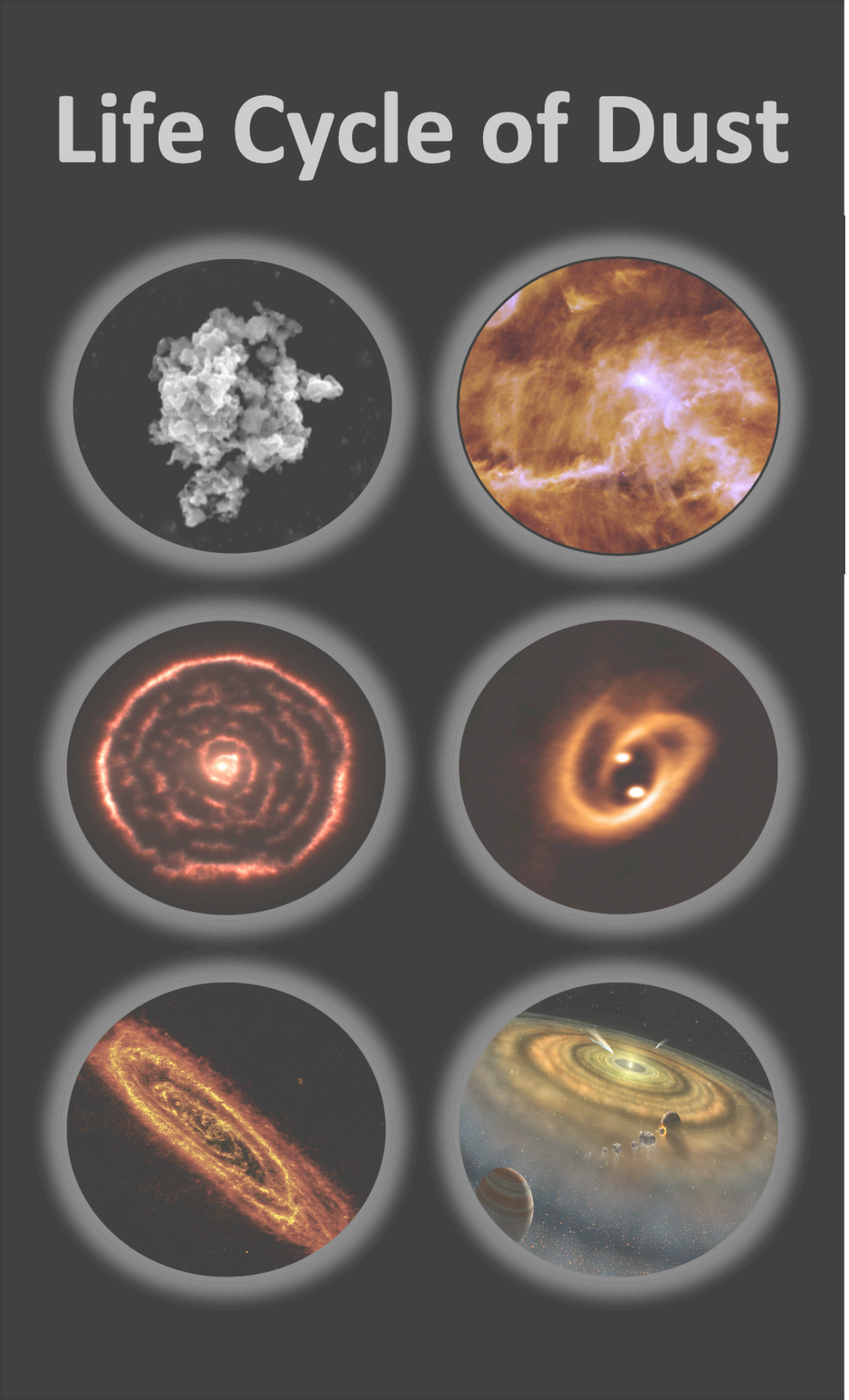

- Dust observational features
- Telescopes basics
- Facilities: from Radio to Optical wavelengths

Life Cycle of Dust

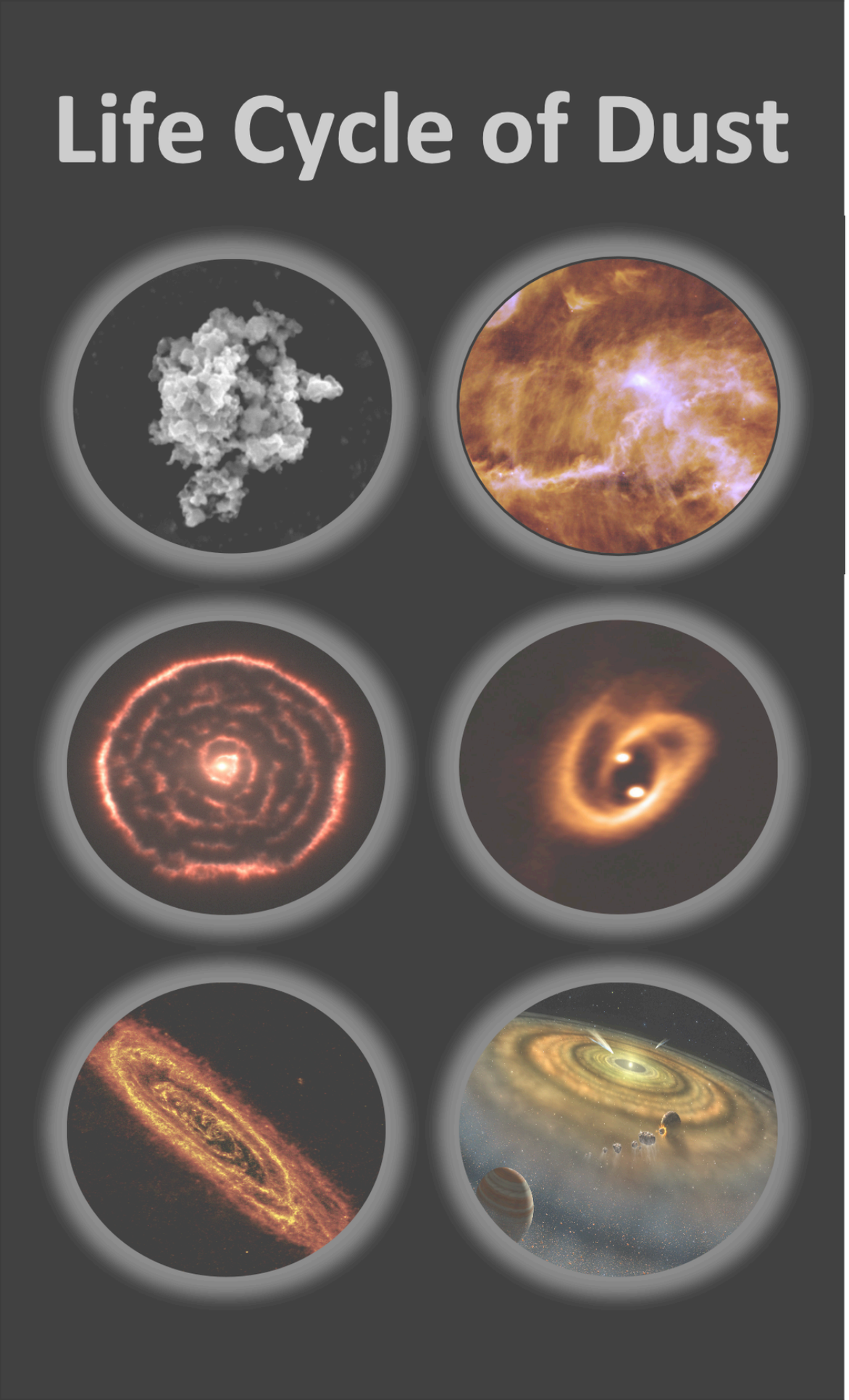

★ Dust observational features

- Continuum
  - ➡ The black body
  - ➡ The grey body
    - ➡ Protostellar cores
    - ➡ Protoplanetary disks
  - ➡ Scattering
  - ➡ Polarization
  - ➡ Anomalous microwave emission
- Spectral features
  - ➡ Absorption & Emission

Life Cycle of Dust

★ Dust observational features

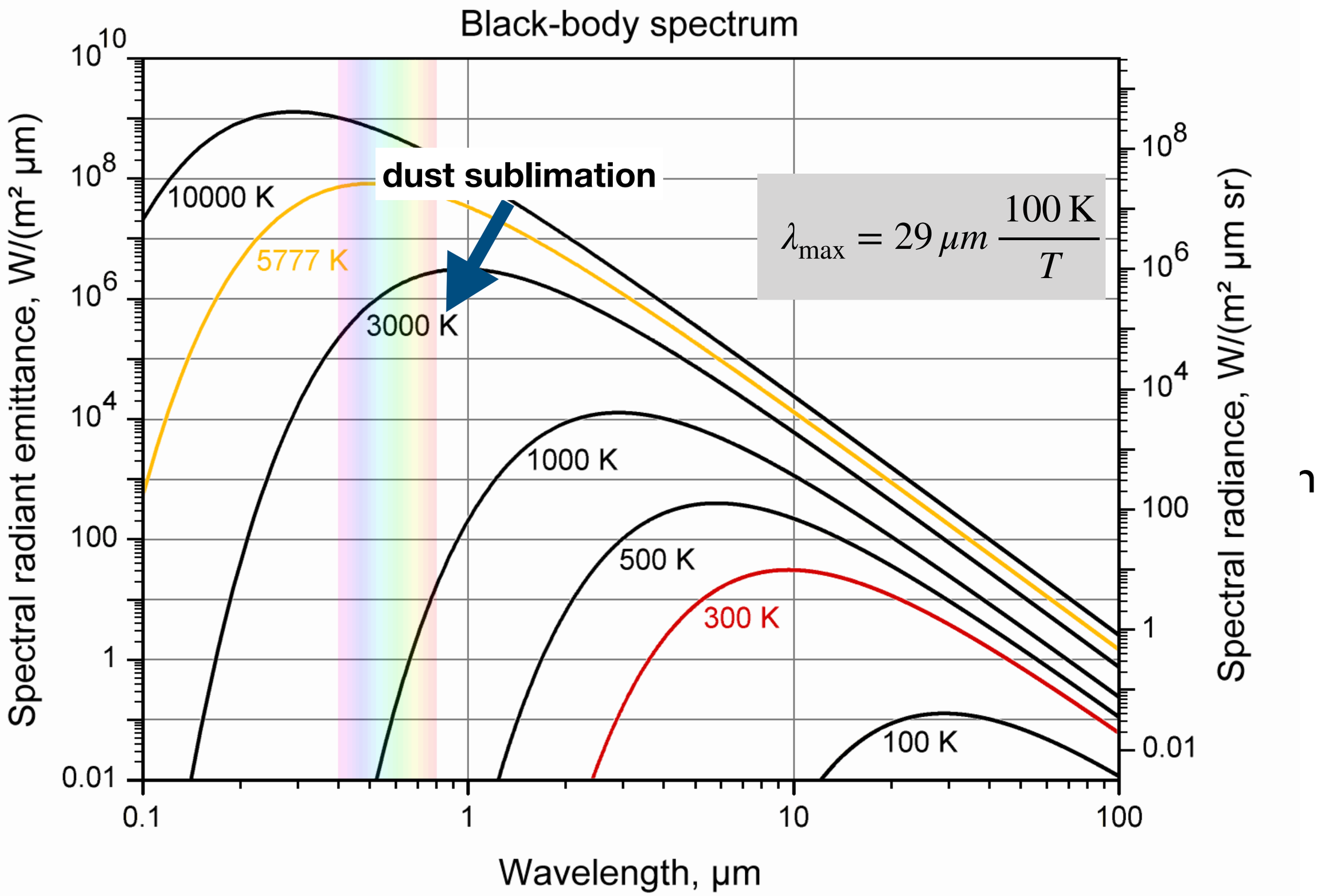

Life Cycle of Dust

★ Dust observational features

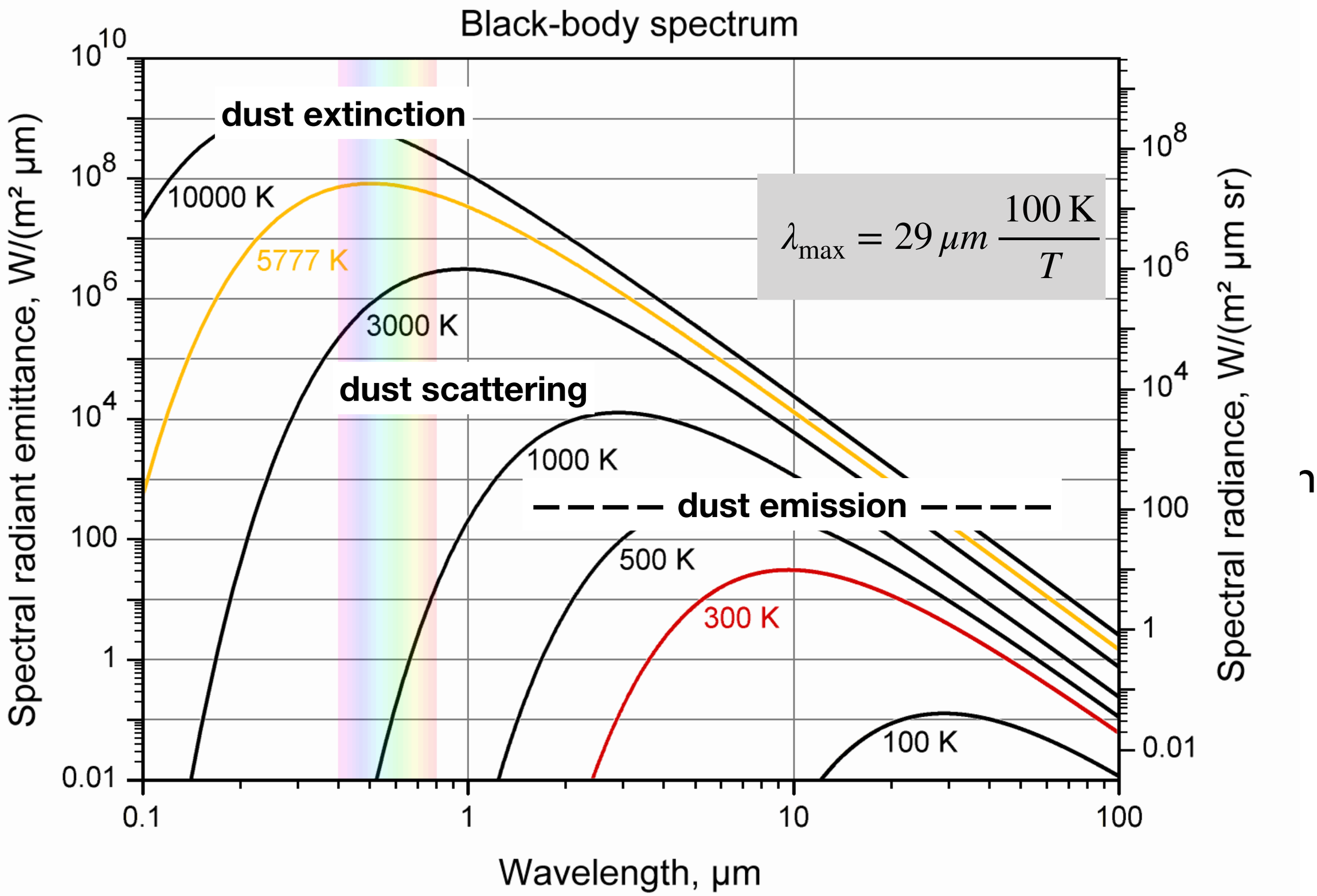

SED of collapsing cloud + star + disk. Protostellar phase.

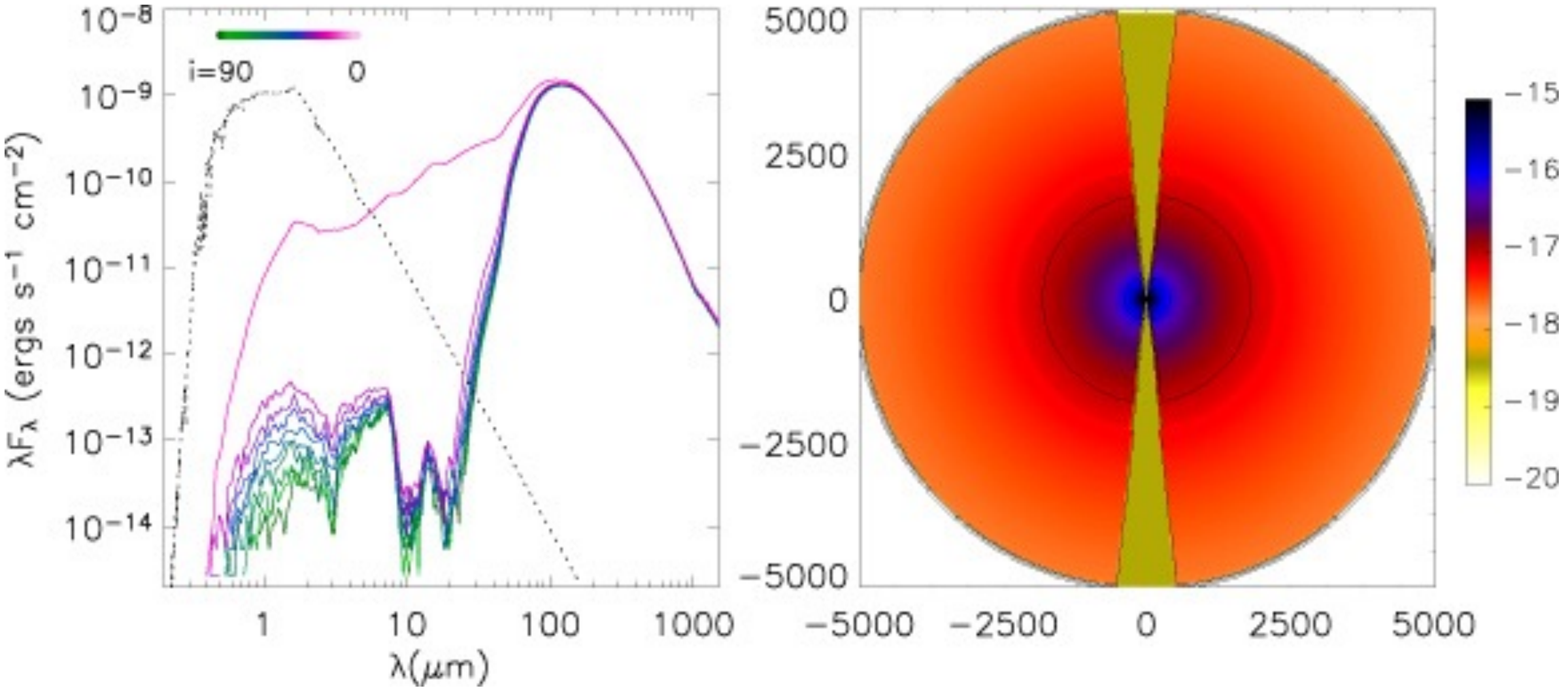

Most of the mass is in the dense and extended envelope surrounding the disk+protostar system.
Very hard to observationally characterize the disks.

Class 0

Whitney et al. 2003

SED B335 Protostar

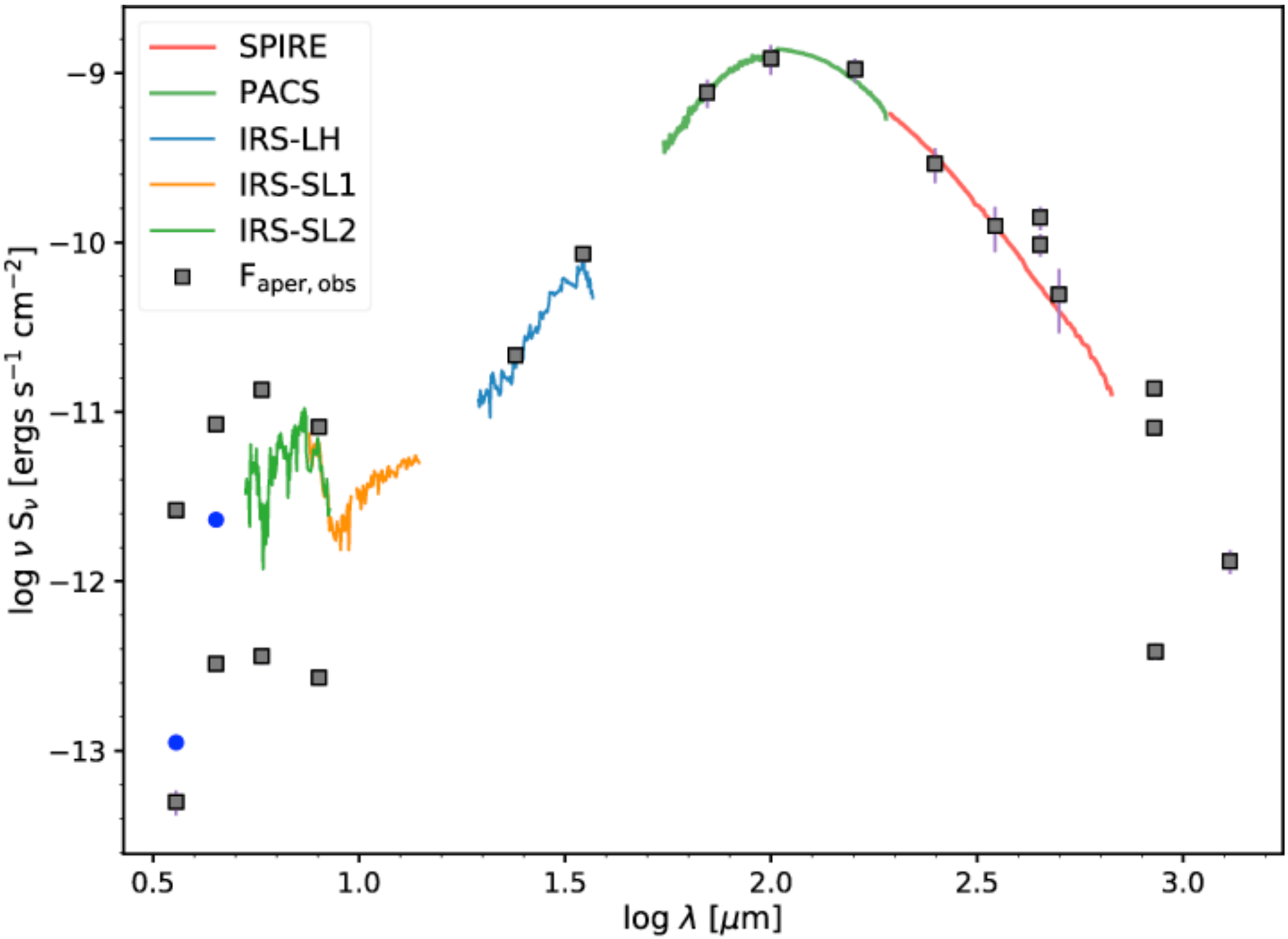

Evans et al. 2023

Imaging dust in a protostar: B335

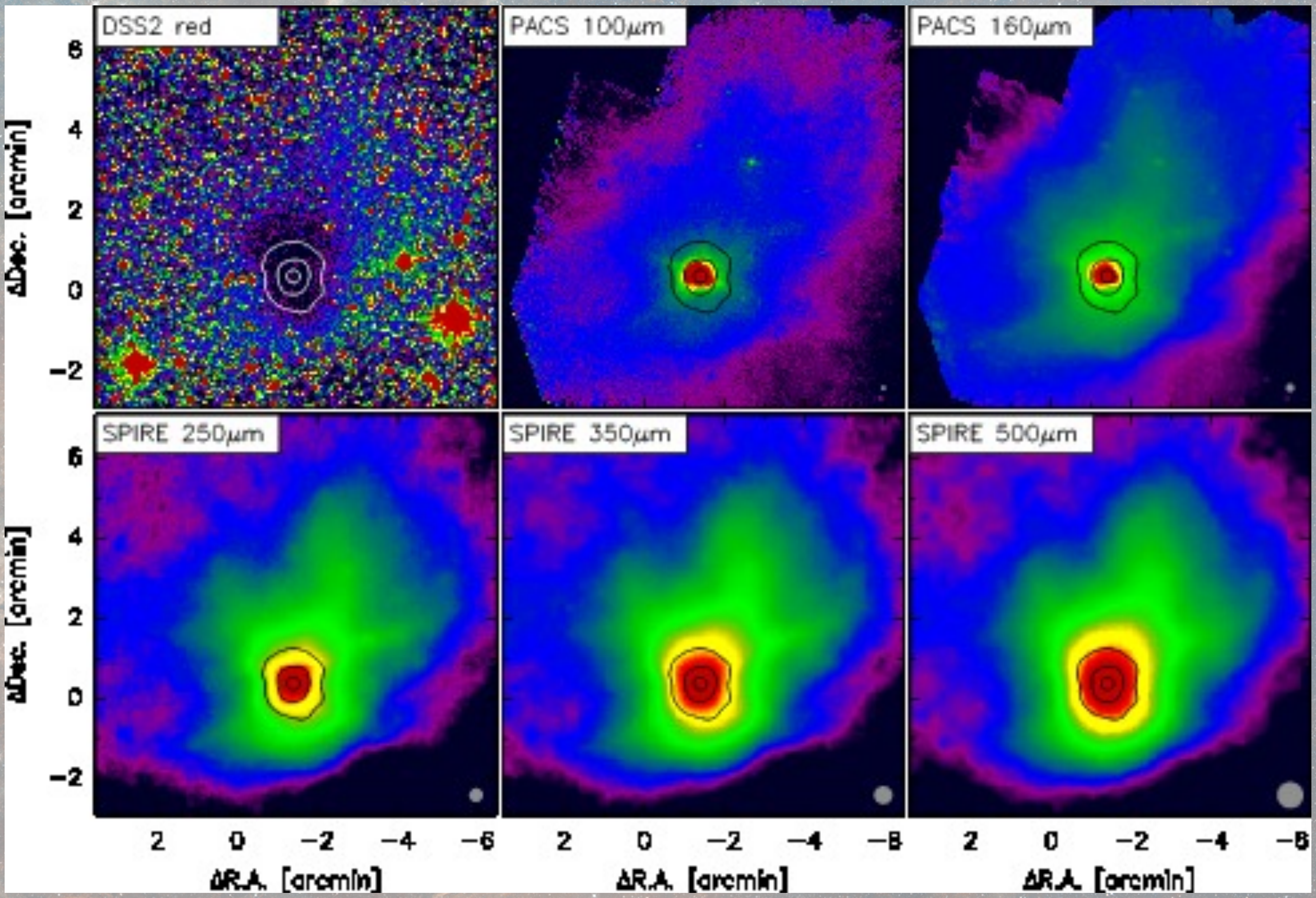

Imaging dust in a protostar: B335

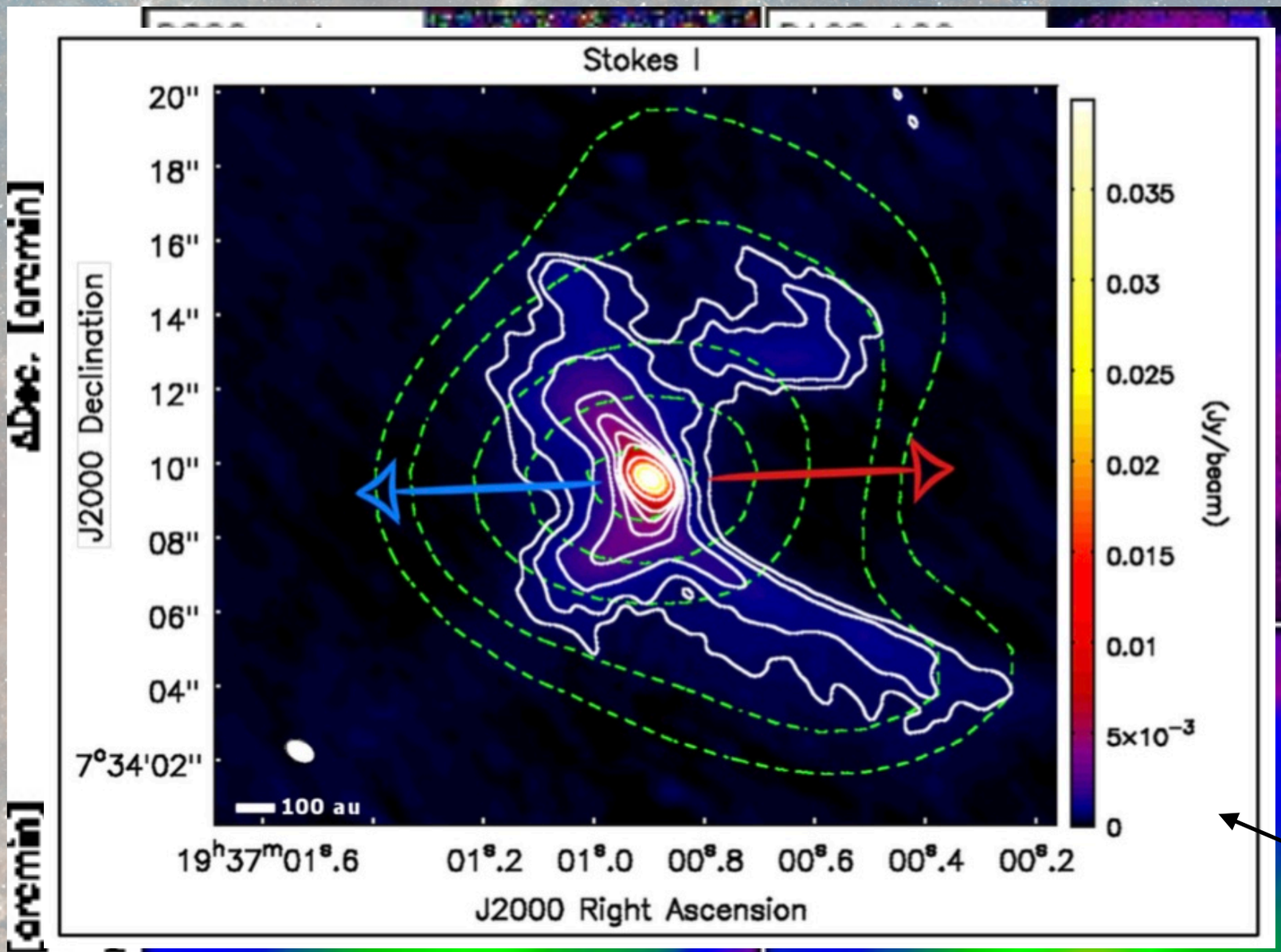

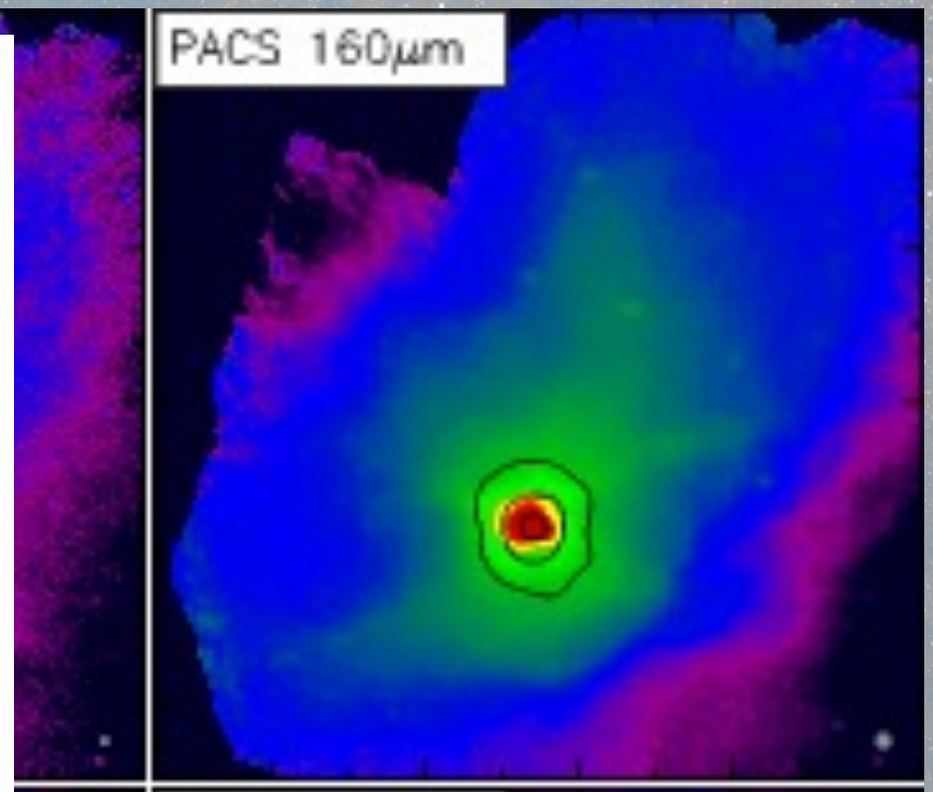

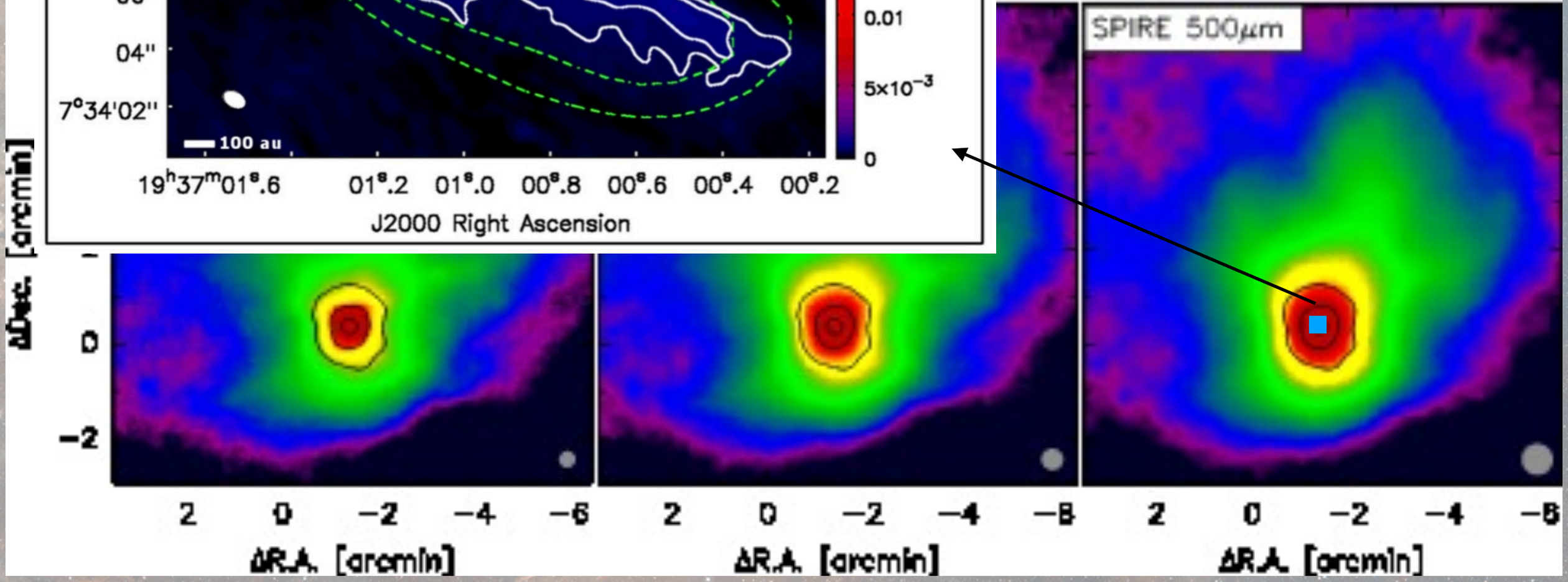

Imaging dust in in z ~ 5 galaxies

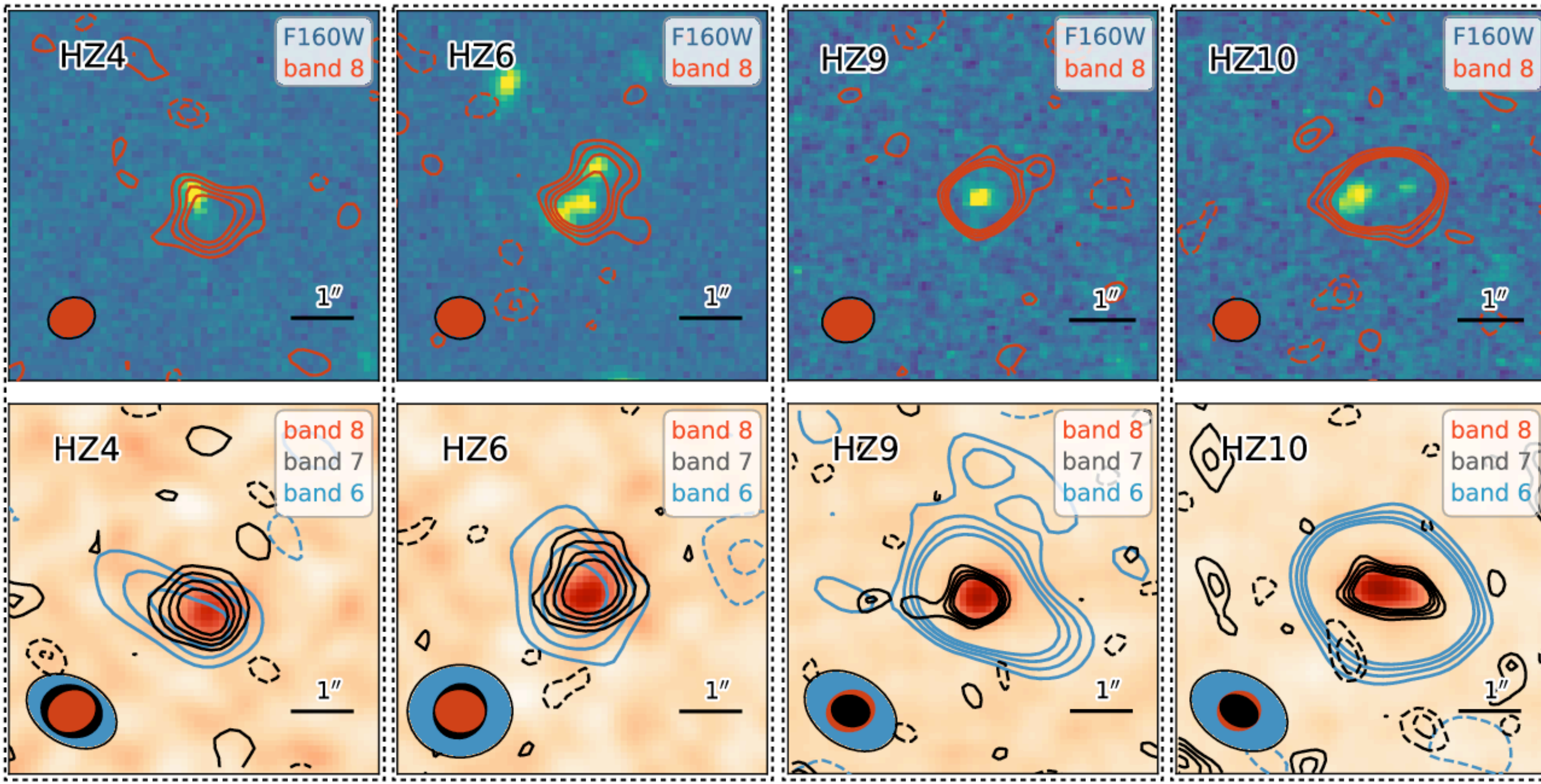

A. Faisst et a. 2020, MNRAS,

SED Starburst galaxy

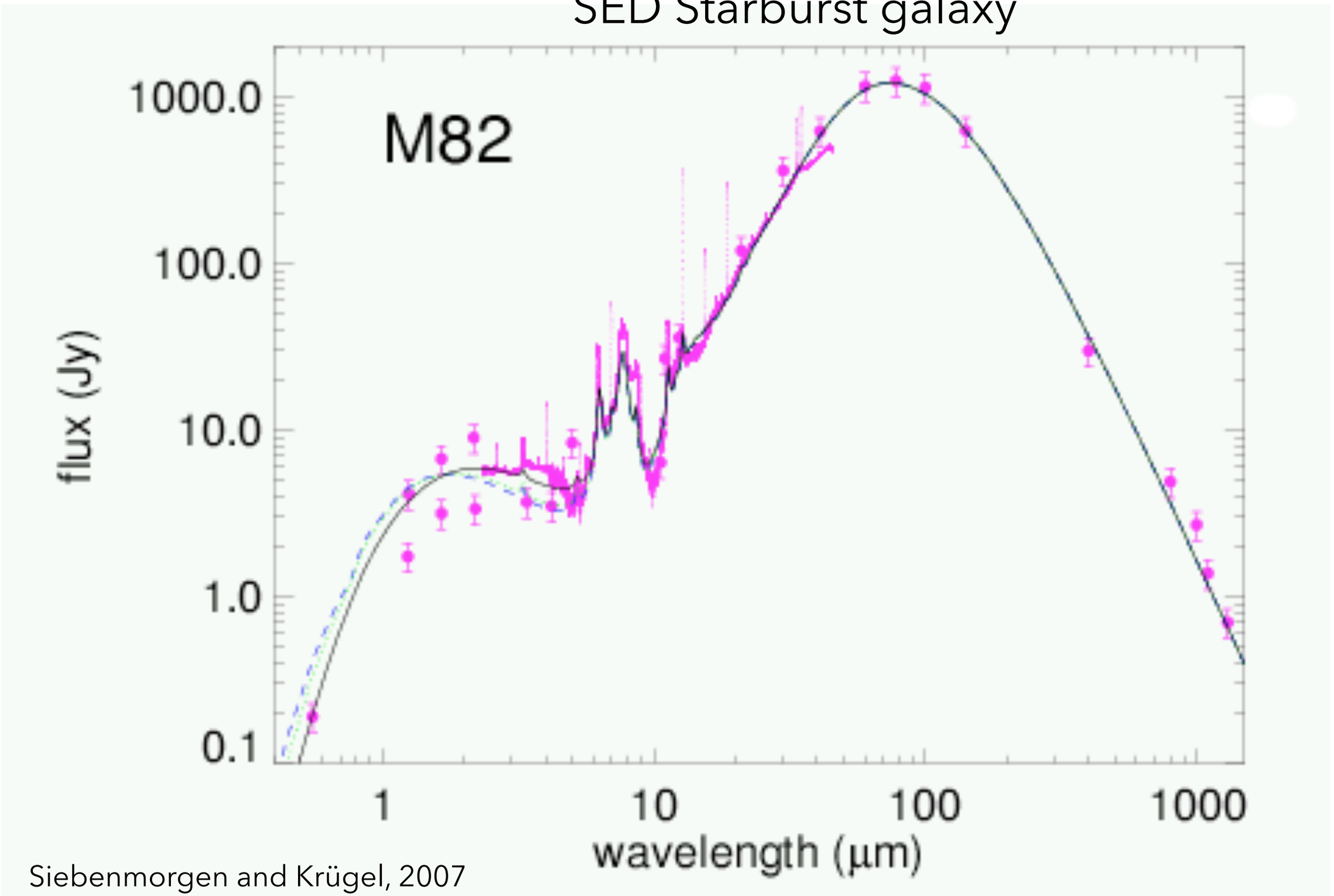

Siebenmorgen and Krügel, 2007

Fig. 1. SED of the central region of M82. The 0.4 – 1500μm wavelength range is given top, a zoom into the 12 – 34μm region bottom.

Evidence of presence of disks around YSO: Spectral Energy Distribution in the IR

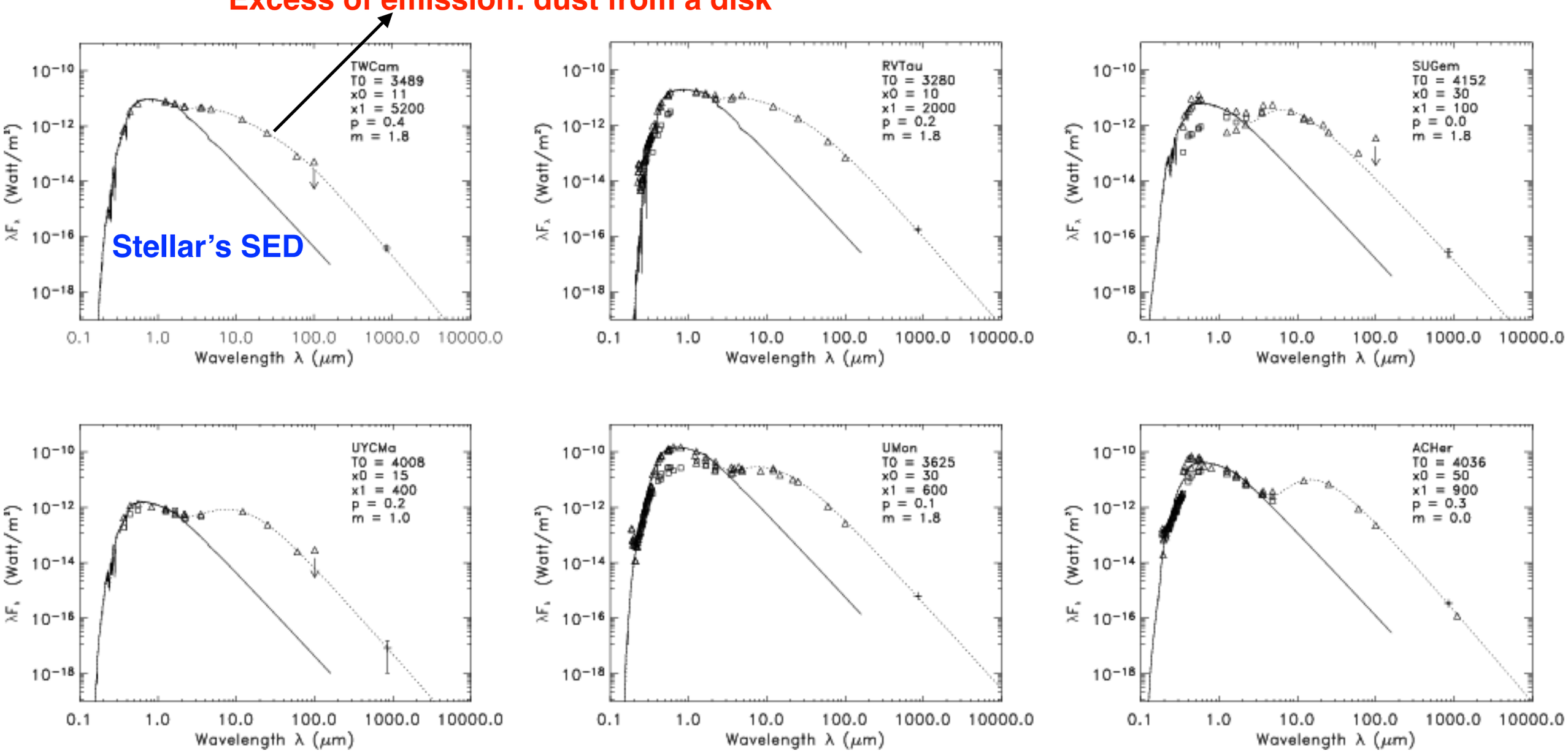

Fig. from De Ruyter et al. Astronomy & Astrophysics, 435, 161-166 (2005)

Spectral Energy Distribution: probe of circumstellar disks

Dust dominates the emission around Young Stellar Objects at near-IR to mm wavelengths.

Multi-wavelength observations from IR to mm are required to constrain the properties of the disk

SED is a necessary observational piece but it may not be enough (inclination strongly affect the SED)

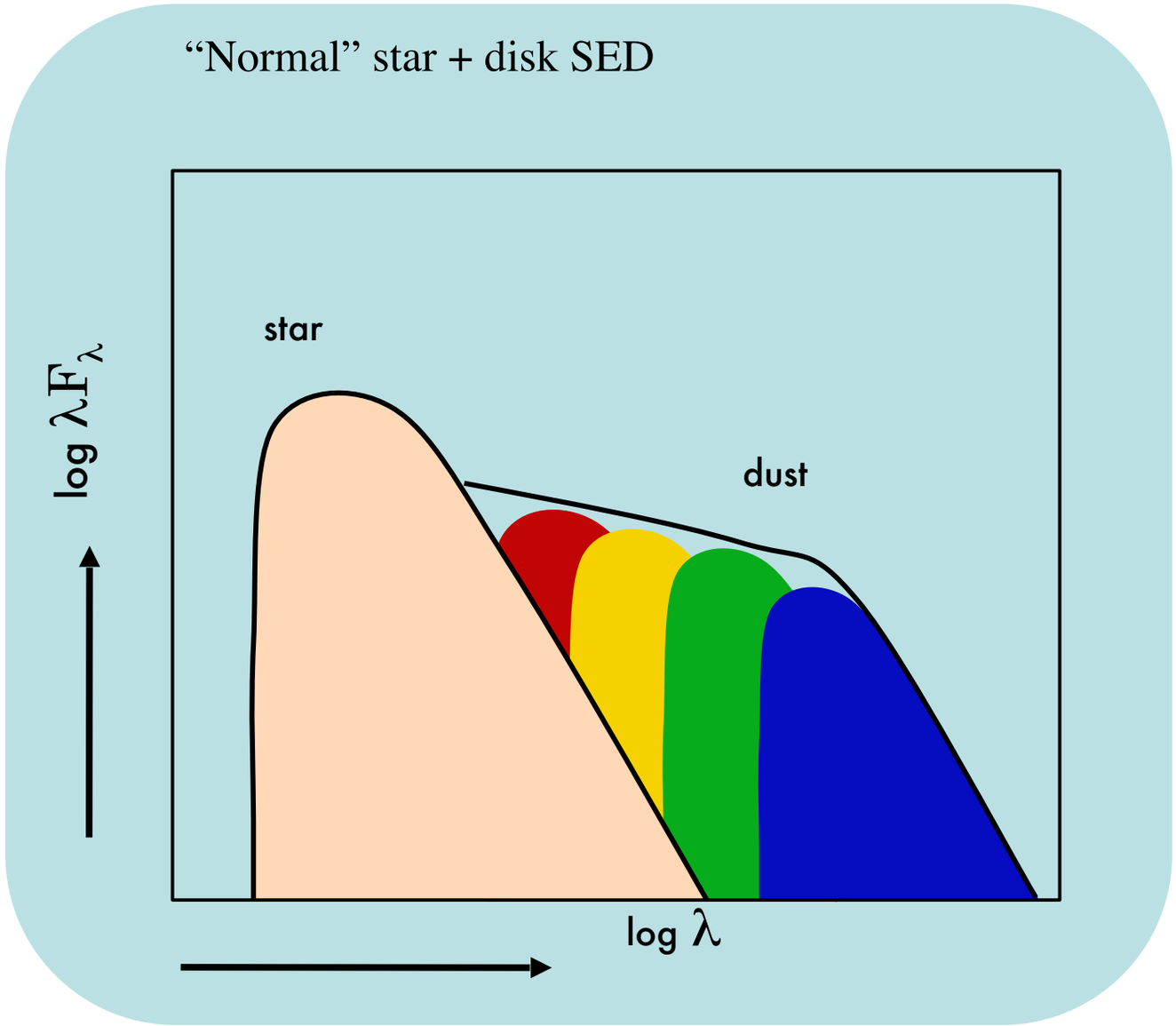

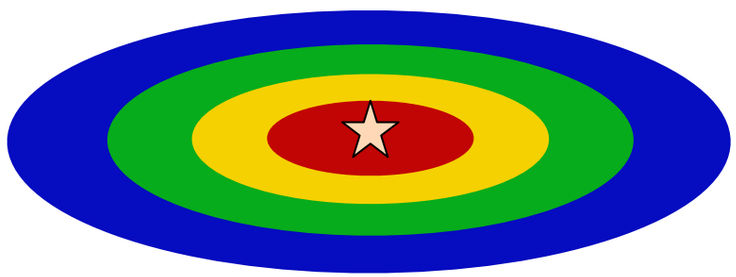

SED and cumulative contributions to Fv at four representative wavelengths

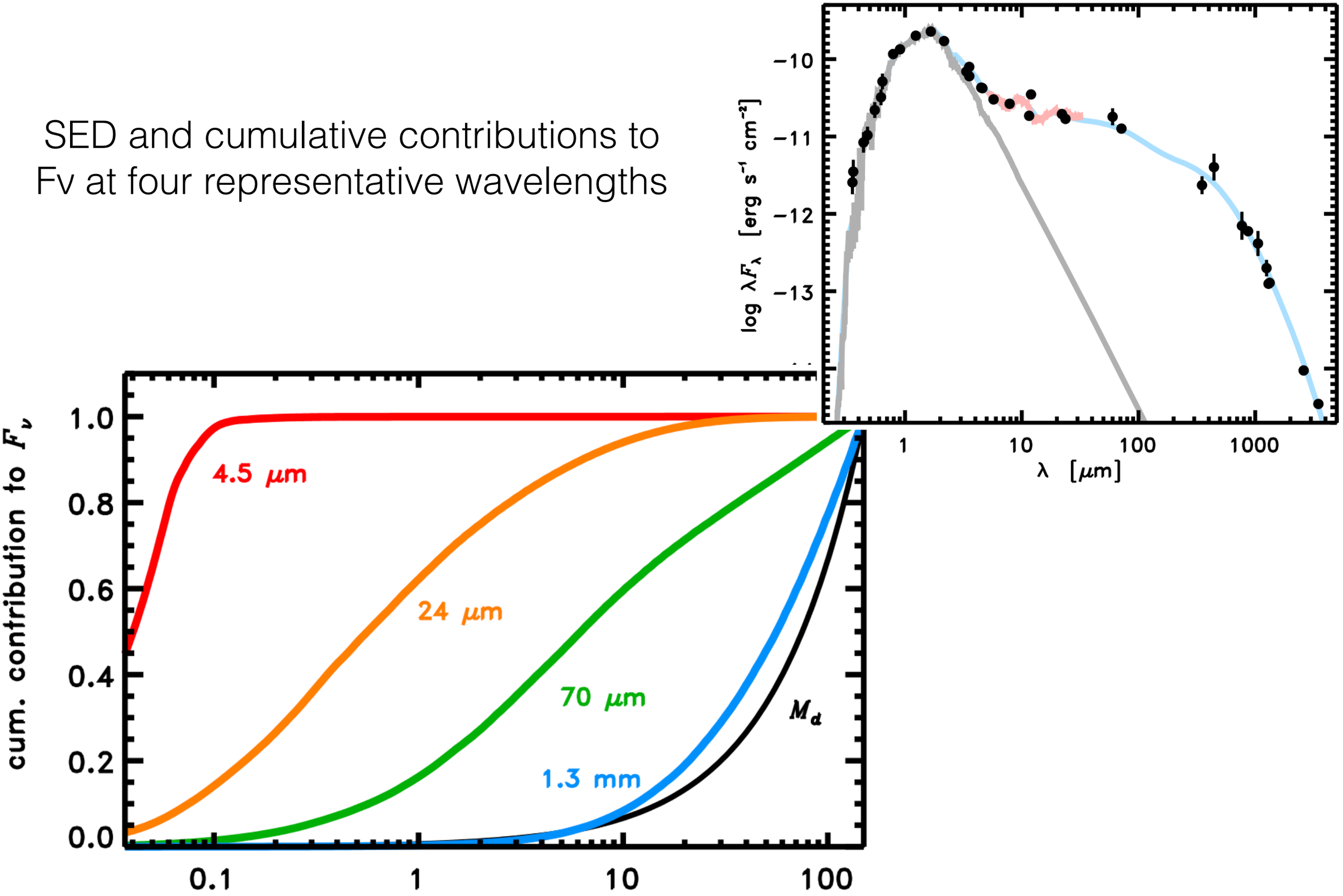

Figs. from Andrews, Publications of the Astronomical Society of the Pacific 127 (956), 961

- Dark clouds in the optical wavelengths: Dust extinction

- Dark clouds in the near-IR wavelengths: Dust extinction

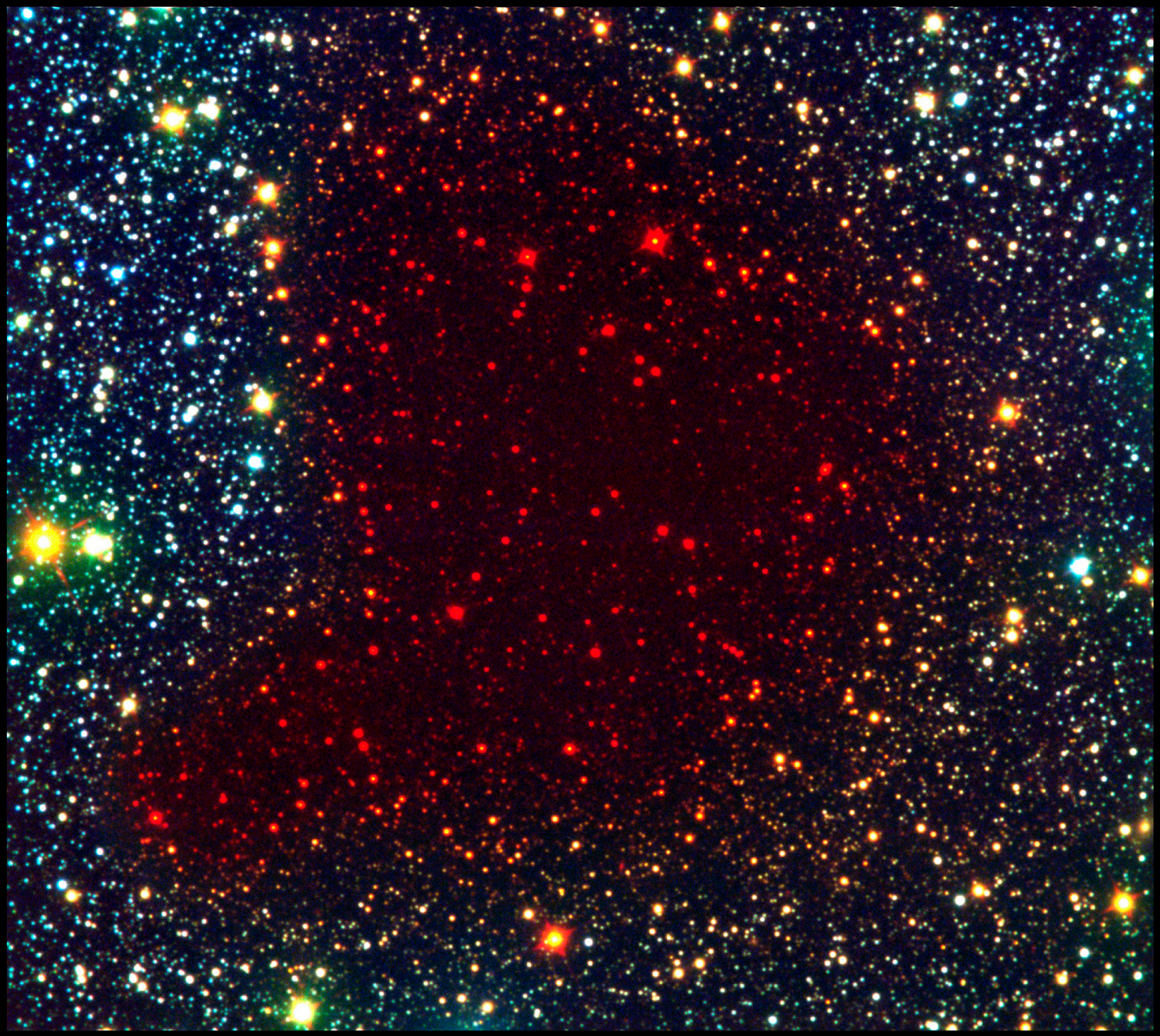

- Dark clouds in the near-IR wavelengths: Dust extinction

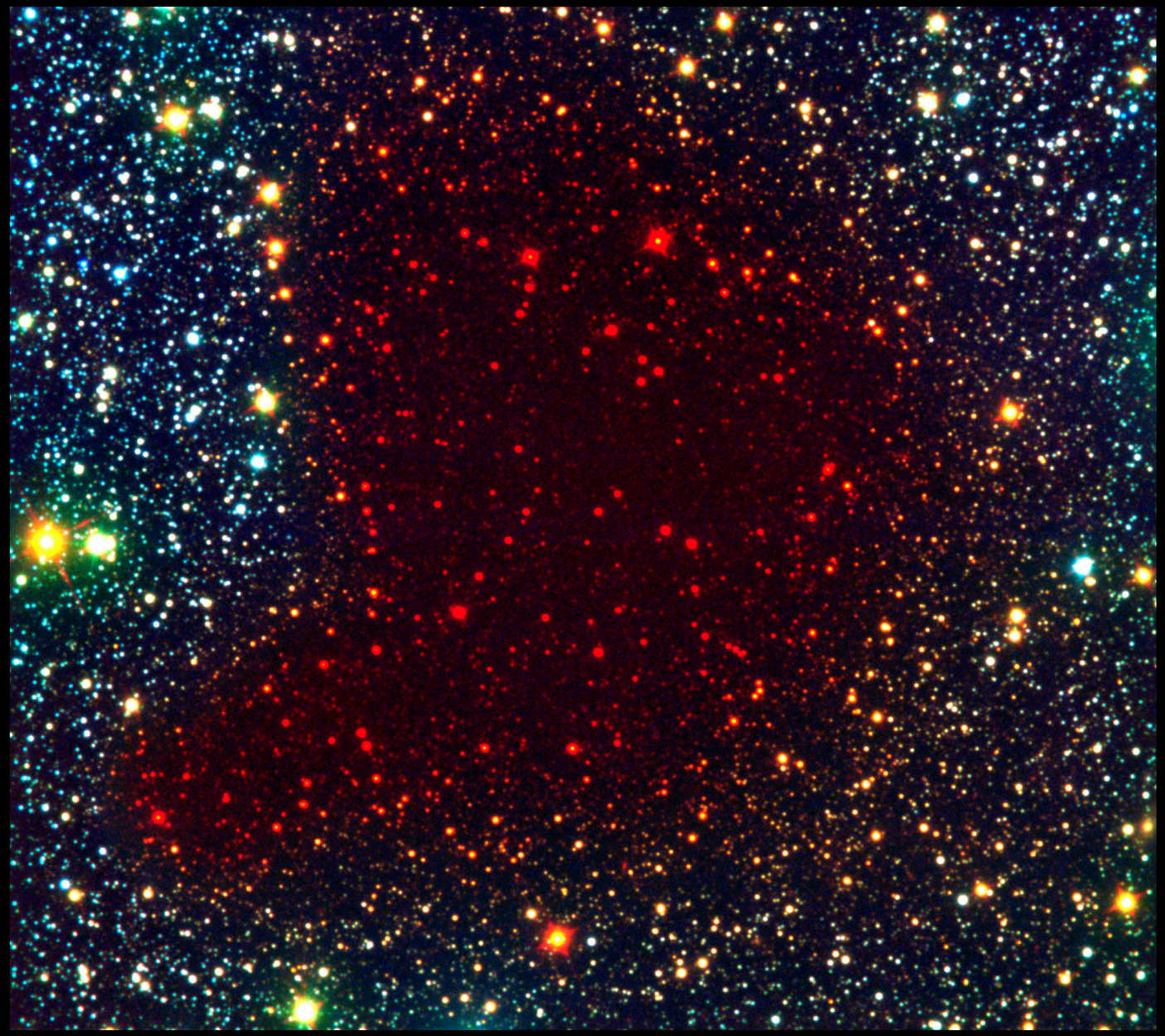

João F. Alves*, Charles J. Lada† & Elizabeth A. Lada‡

2001, Nature, 409, 159

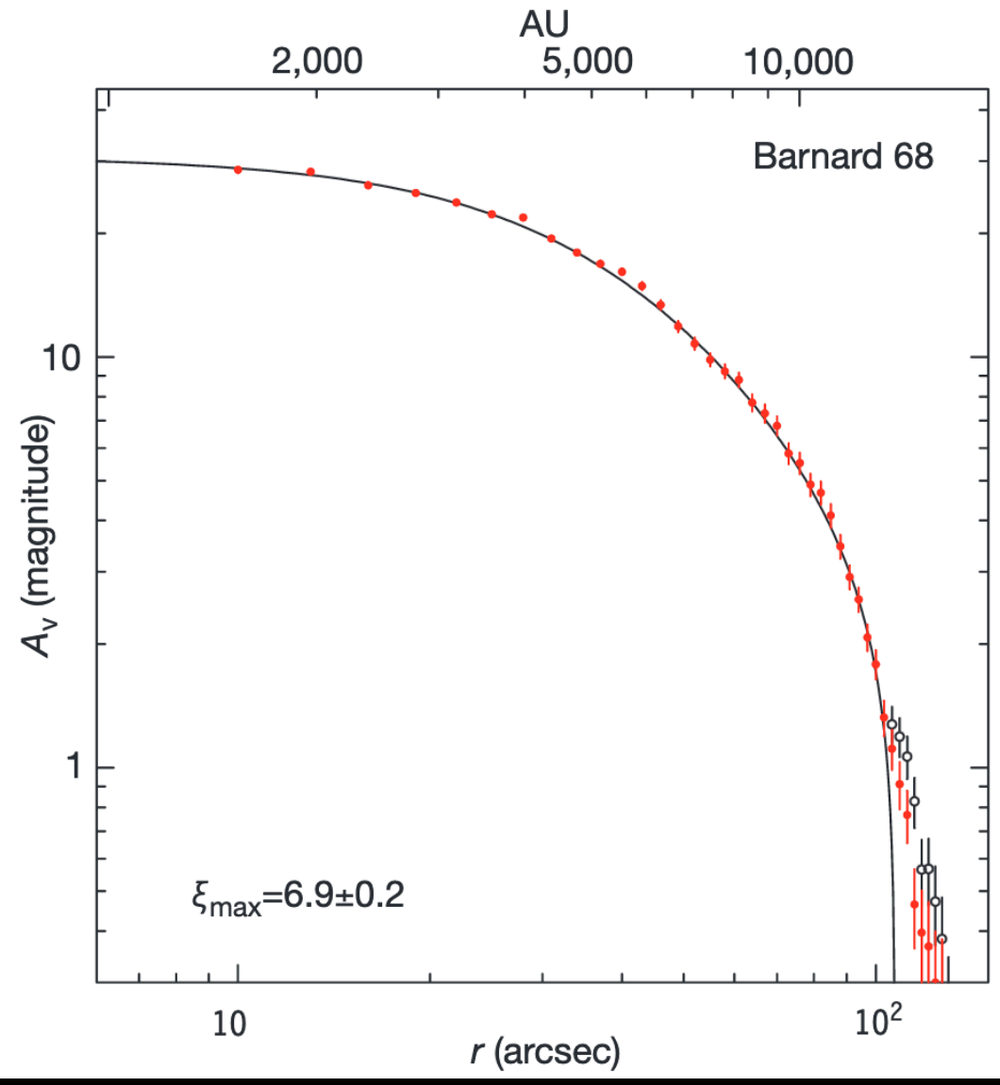

- Dark clouds in the mid-IR wavelengths: Dust extinction

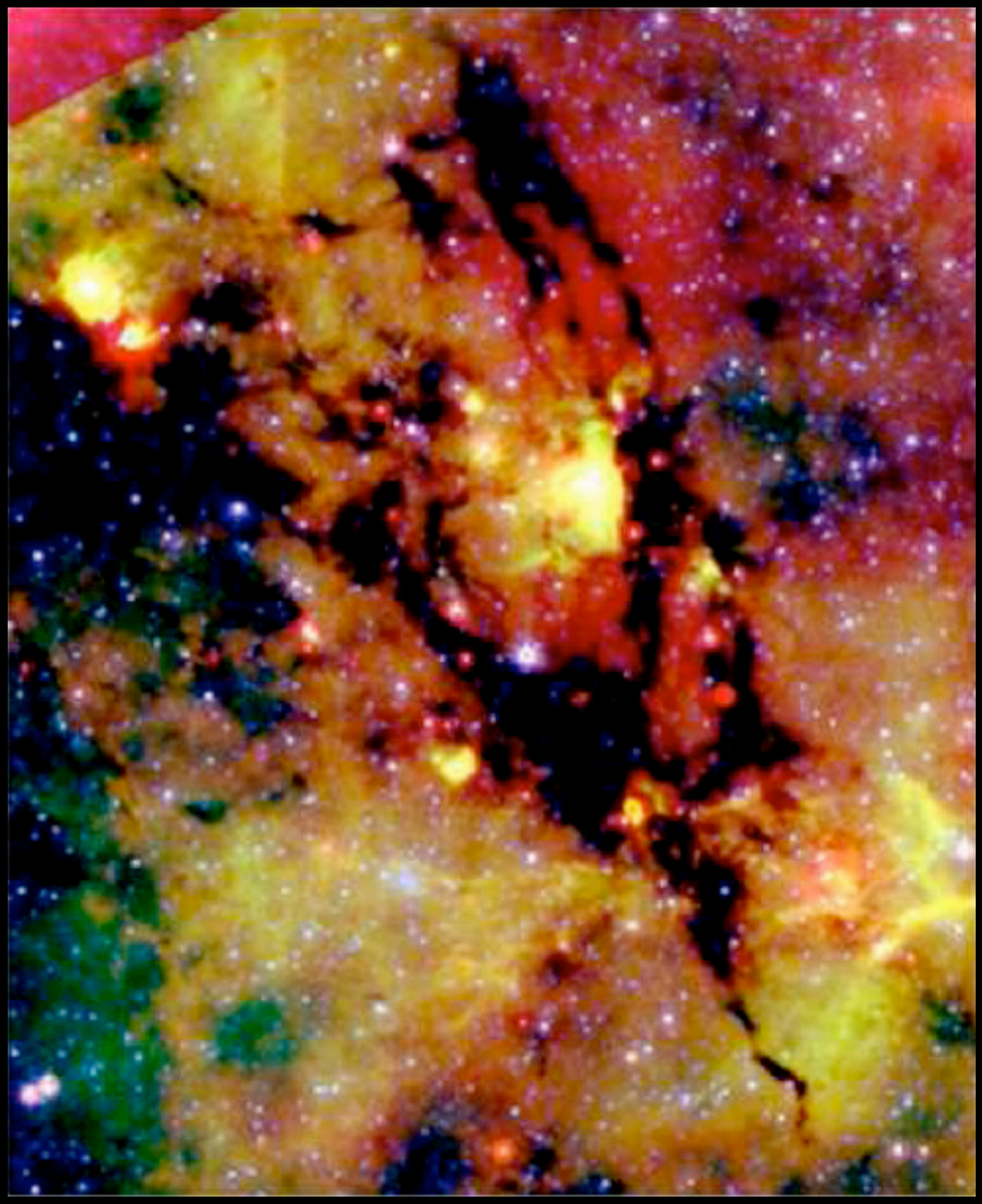

Archival Spitzer 4.5 / 8.0 / 24 μ m (blue / green / red) three-color com- posite image of IRDC G14.225 – 0.506 from Busquet et al. 2012

Dust extinction from (failed?) protoplanetary disks

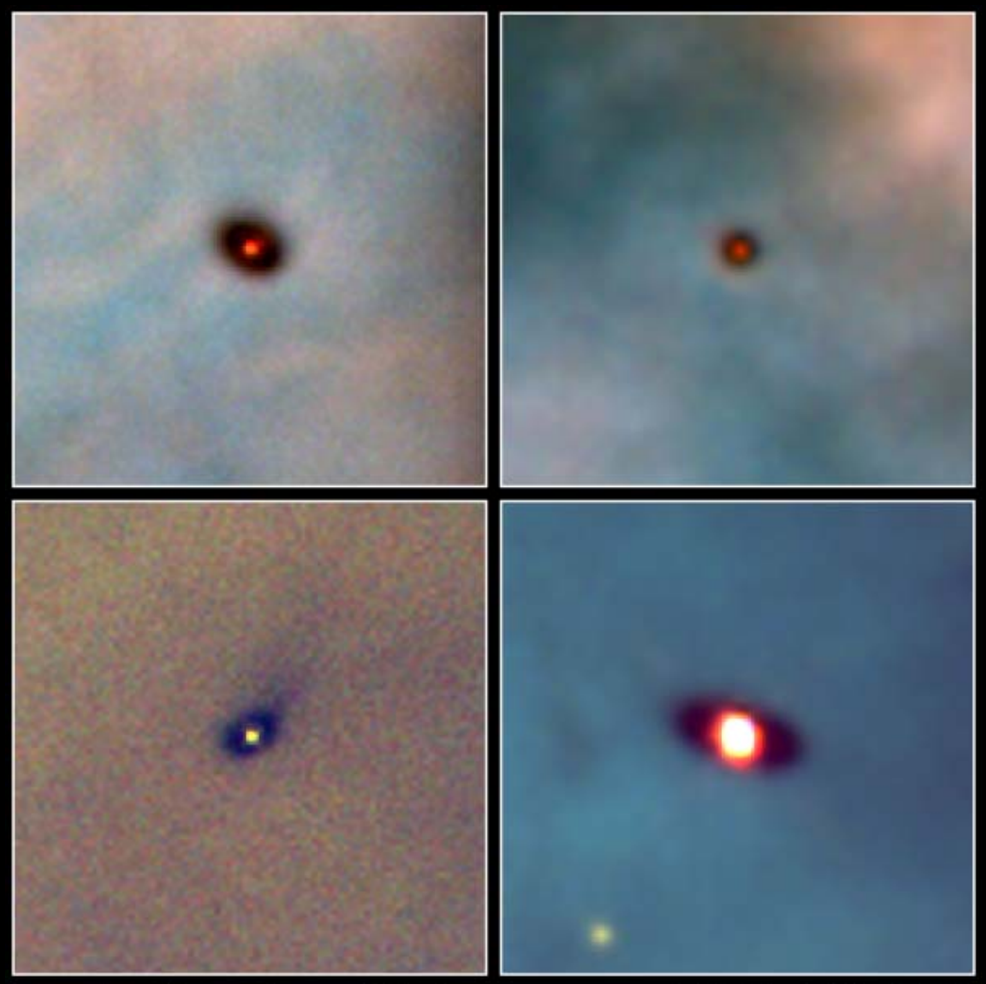

Protoplanetary Disks
Orion Nebula

HST • WFPC2

PRC95-45b · ST ScI OPO · November 20, 1995
M. J. McCaughrean (MPIA), C. R. O'Dell (Rice University), NASA

near-IR Dust Scattering

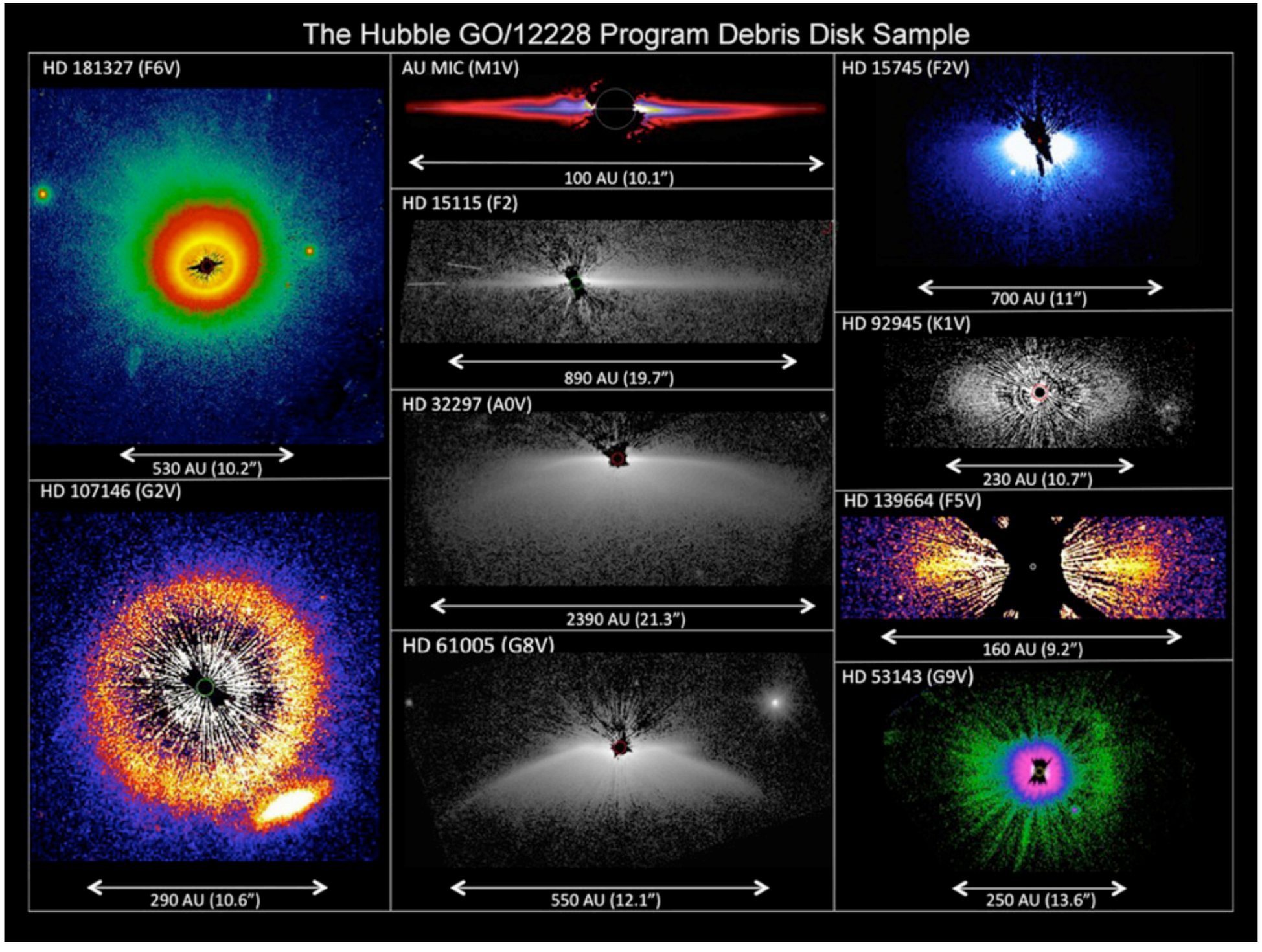

Dust Scatter in the near-IR

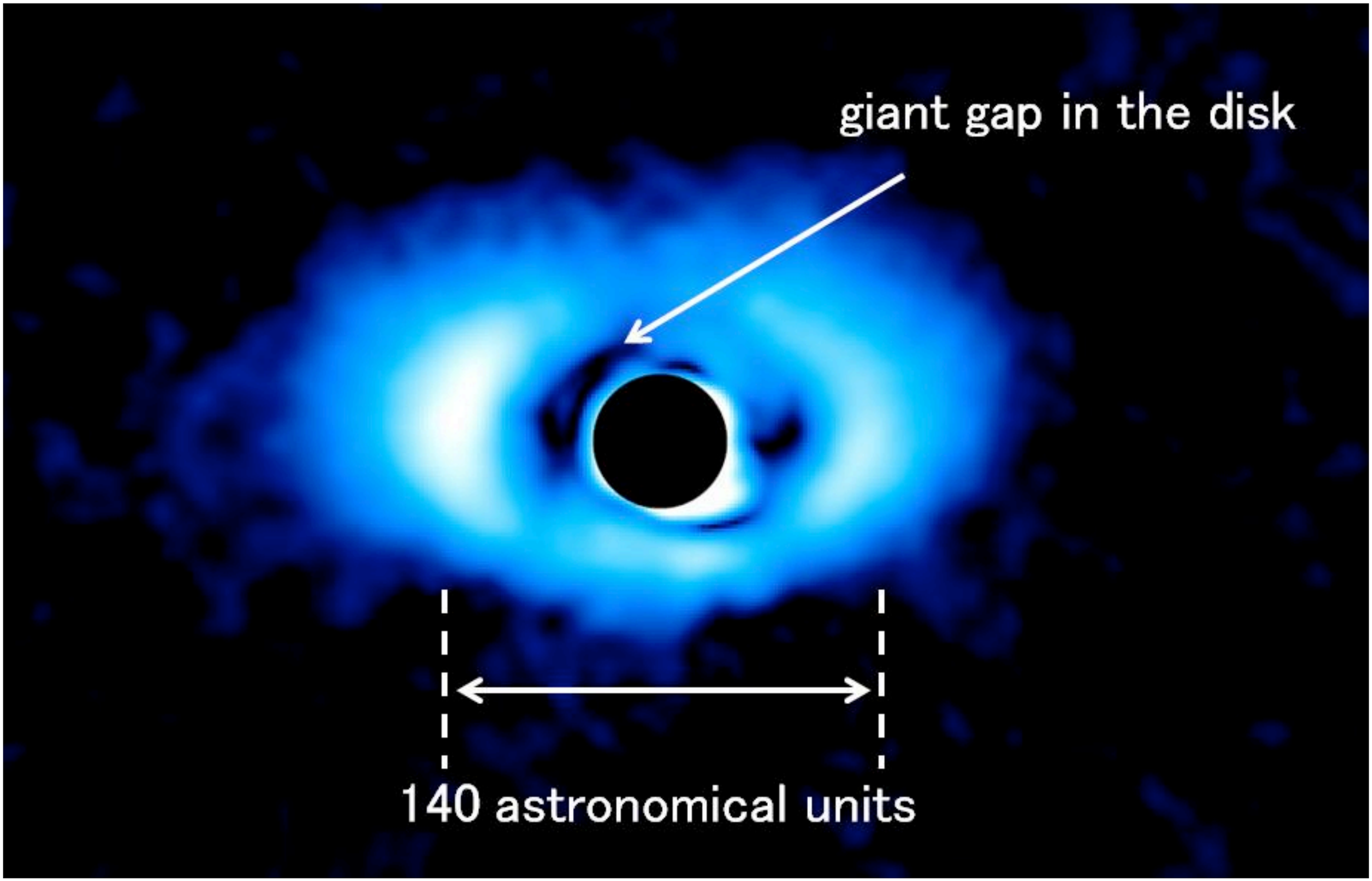

Dust polarization: scatter in the near-IR

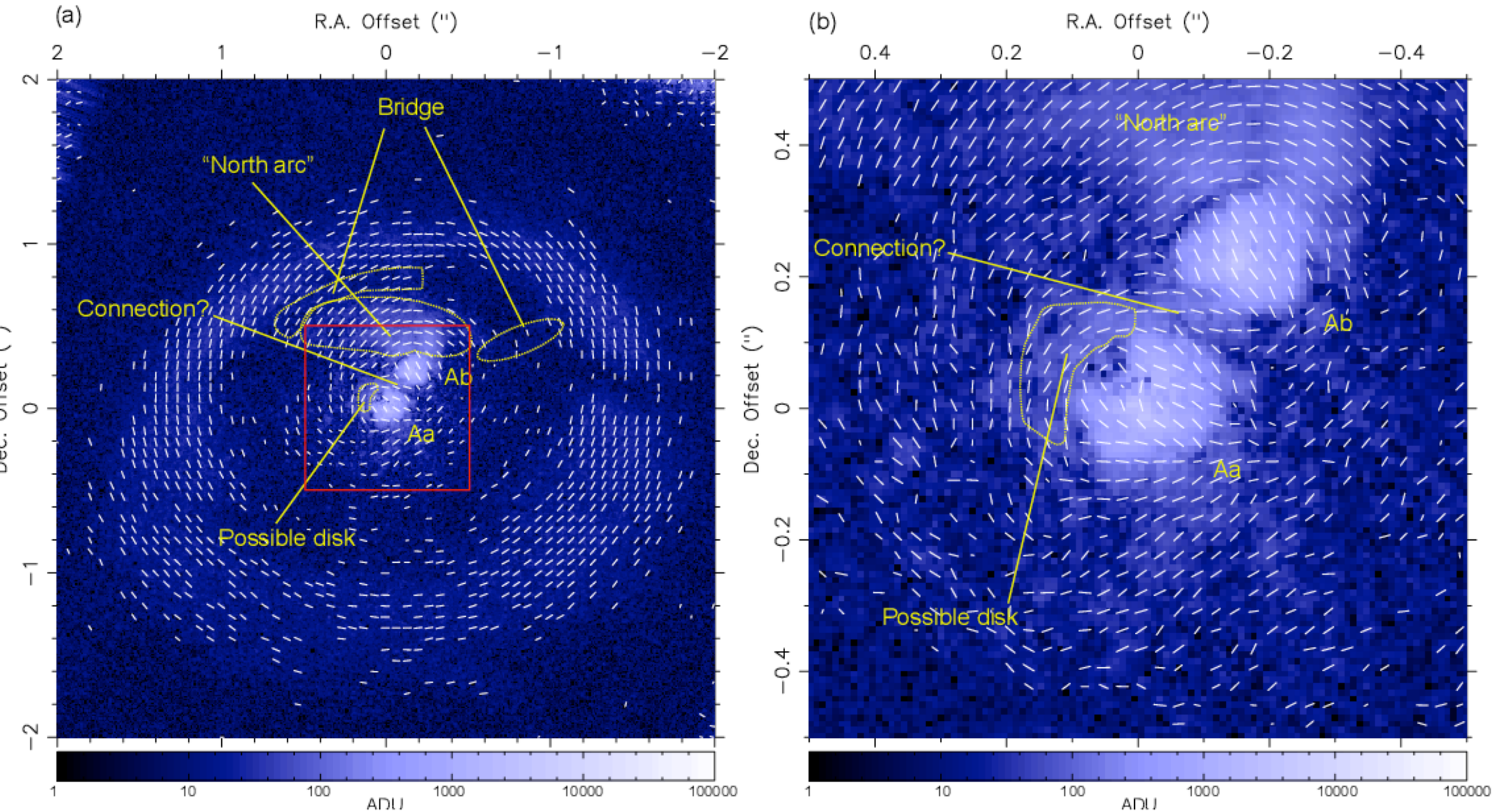

Figure 2: Polarization vector maps of GG Tau A near the central region for the PI image with fields of view of (a) 4′′ × 4′′ and (b) 1′′ × 1′′ centered on GG Tau A. (b) is an enlarged view of the area outlined by a red square in (a). From Yang et al. 2016, AJ,

Dust polarization. emission in the submm

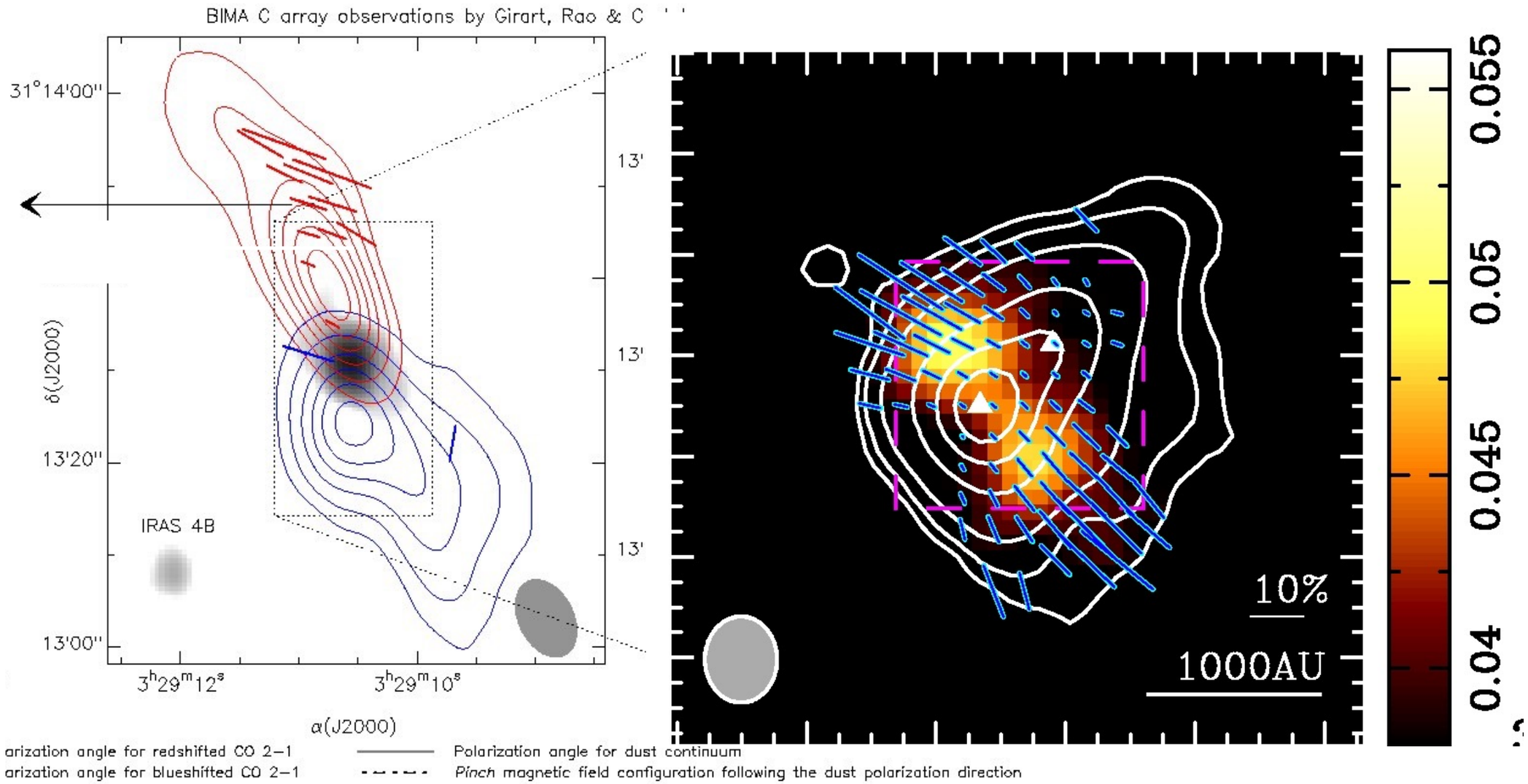

IRAS 4A is a dense molecular core at 235 pc Luminosity ~ 10 L◉:

Girart, Crutcher & Rao1999, Lai 2001, Girart et al. 2006, Attard et al. 2009

Anomalous Microwave Emission

The spectrum of G160.26–18.62 in the Perseus molecular cloud (top) and the residual spectrum showing the spinning dust component (bottom)

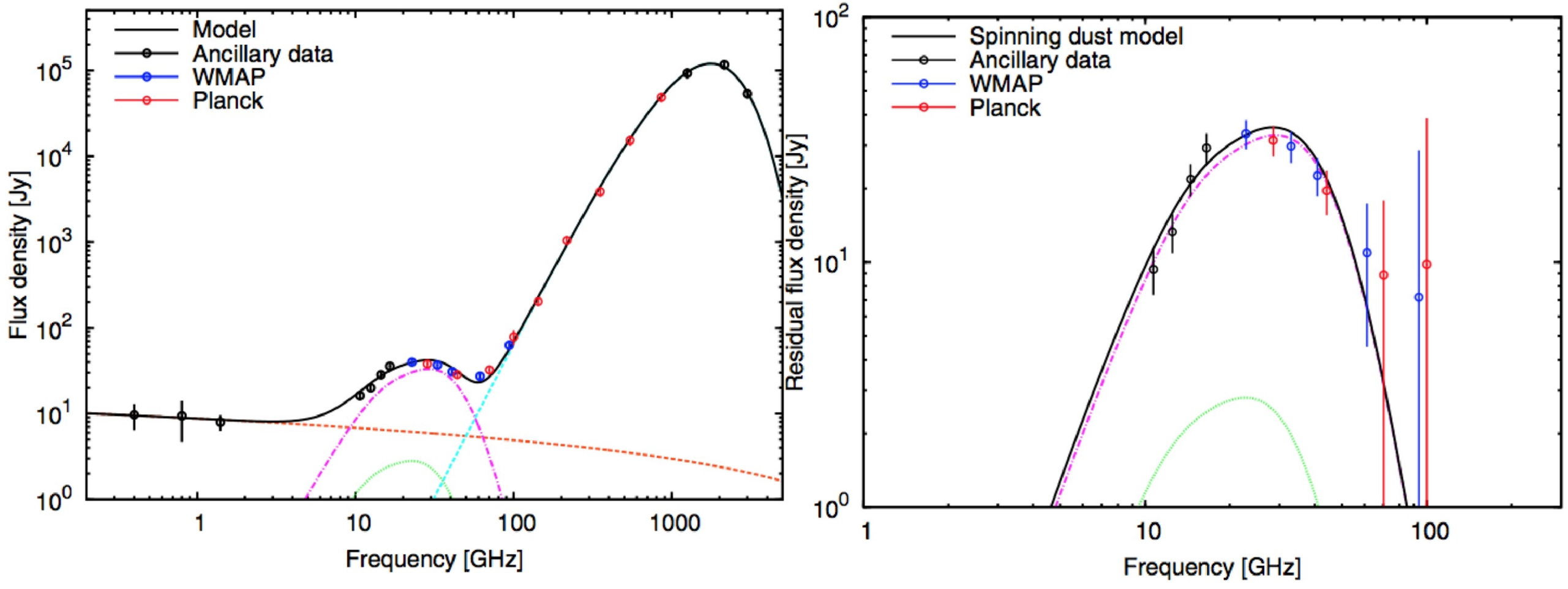

Figs. from Dickinson, C. et al. 2018, New Astronomy Reviews

Anomalous Microwave Emission

Multi-frequency maps of the ρ Oph W molecular cloud region centred at . From the left to right, from the top row: 28.5, 44.1, 70.3, 100, 143 and 857 GHz from Planck, 1.4 GHz and Hα.

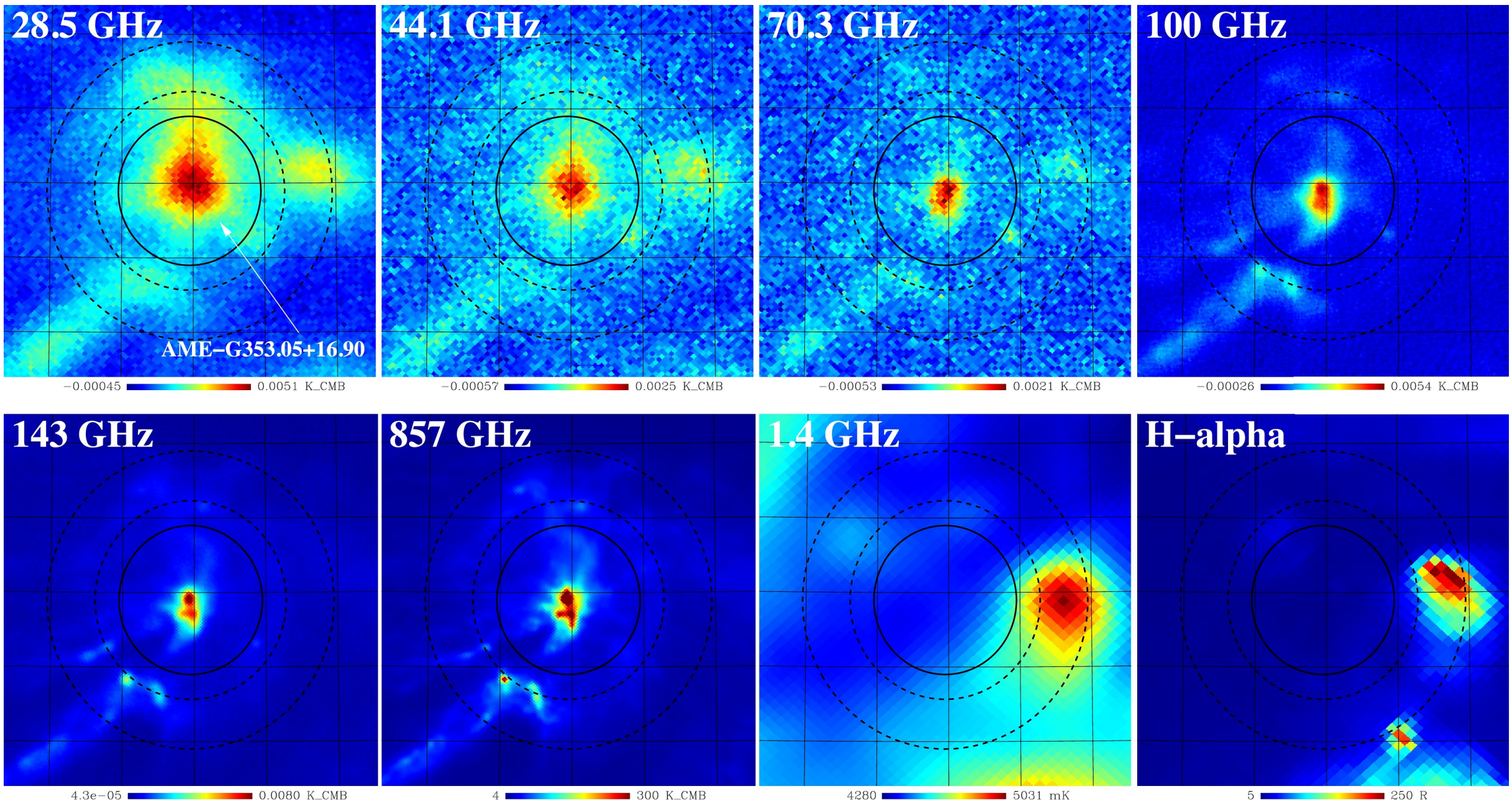

Figs. from Dickinson, C. et al. 2018, New Astronomy Reviews

Dust Spectral features in cool stars

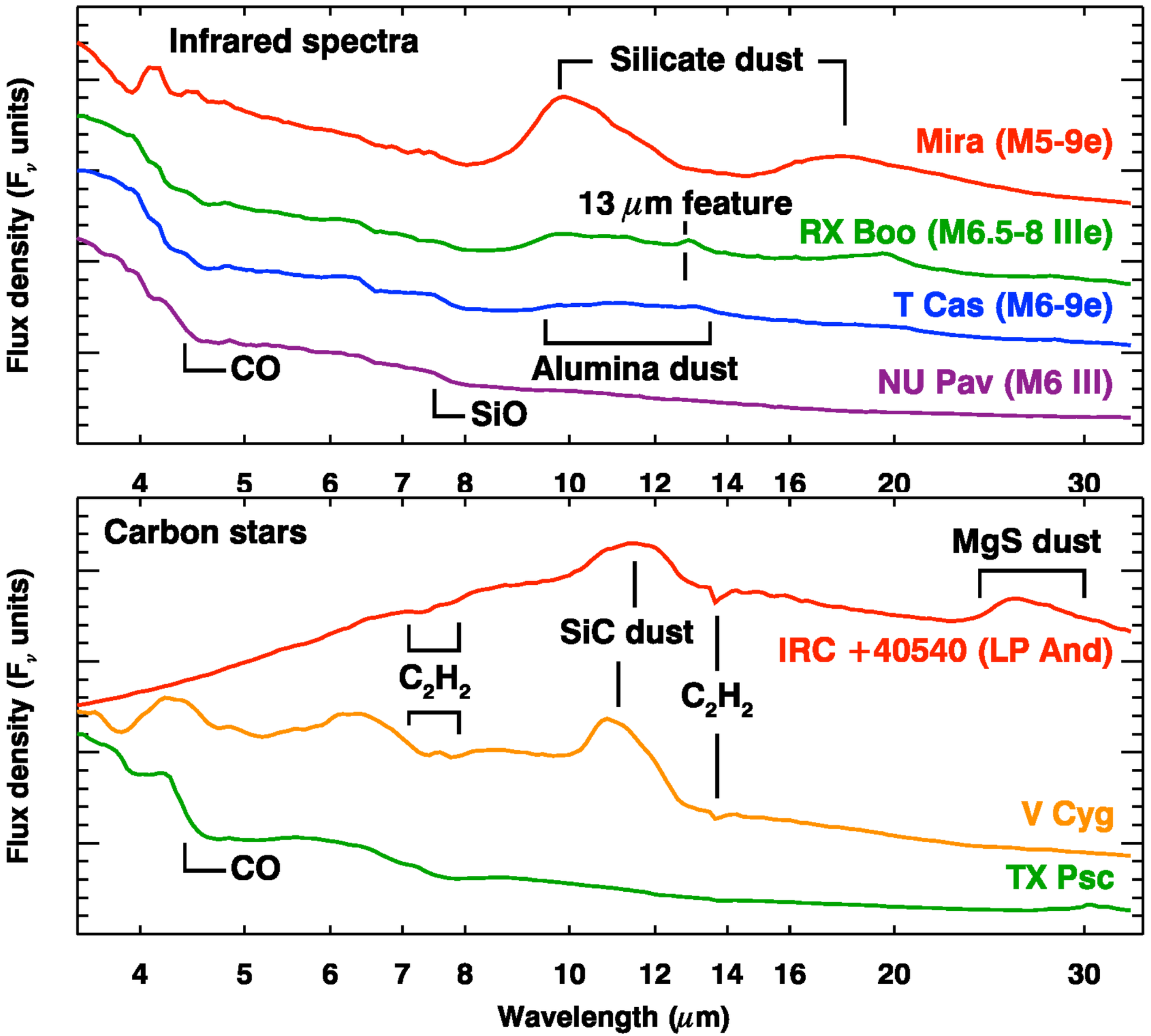

Dust Spectral features in protostars

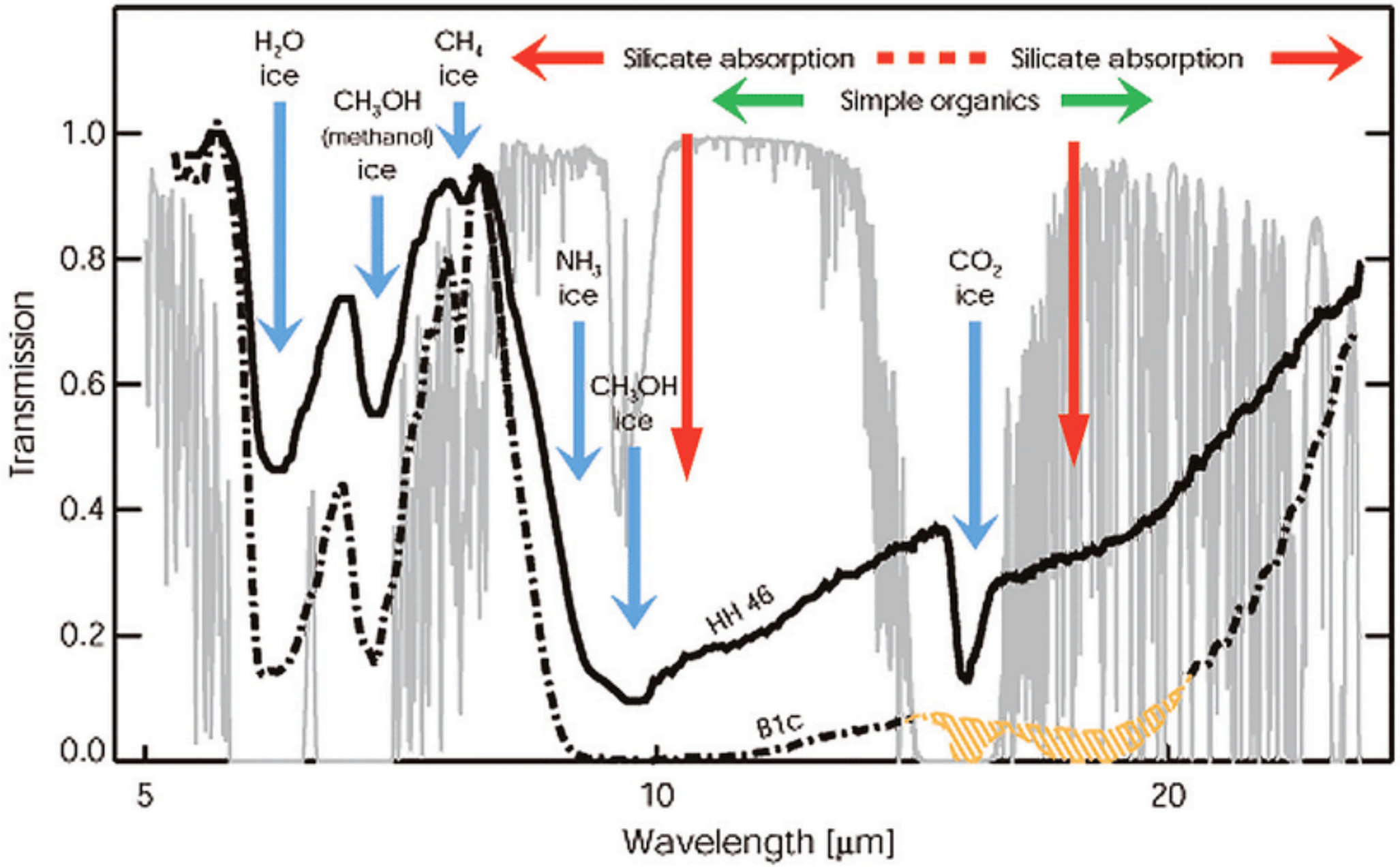

Figs. from Rieke, G. et al. 2015, PASP

JWST: Dust Spectral features in a protostar

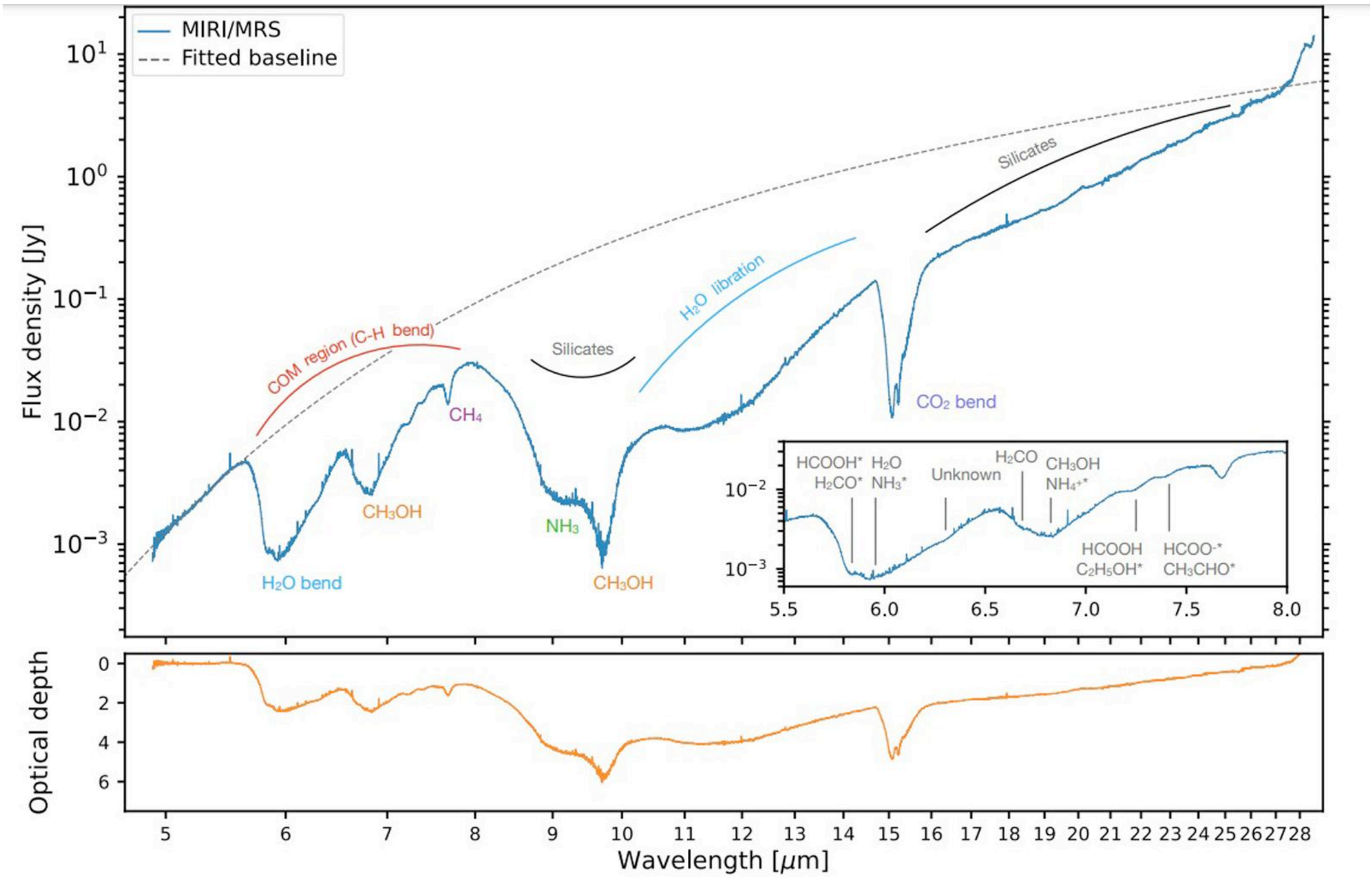

Figure 1. Top: Extracted MIRI MRS spectrum of the IRAS 15398−3359 point source, with major solid-state features indicated. The wavelength axis is in logarithmic scale. The dashed line illustrates the fitted continuum. **Top (inset)**: Detail of the 5.5–8 μm region from same spectrum with secure and possible identifications labeled (see Table 3.1). **Bottom**: The optical depth spectrum derived using the continuum shown in the top panel.

Figs. from Yang, Y-L, et al. 2022, ApJL

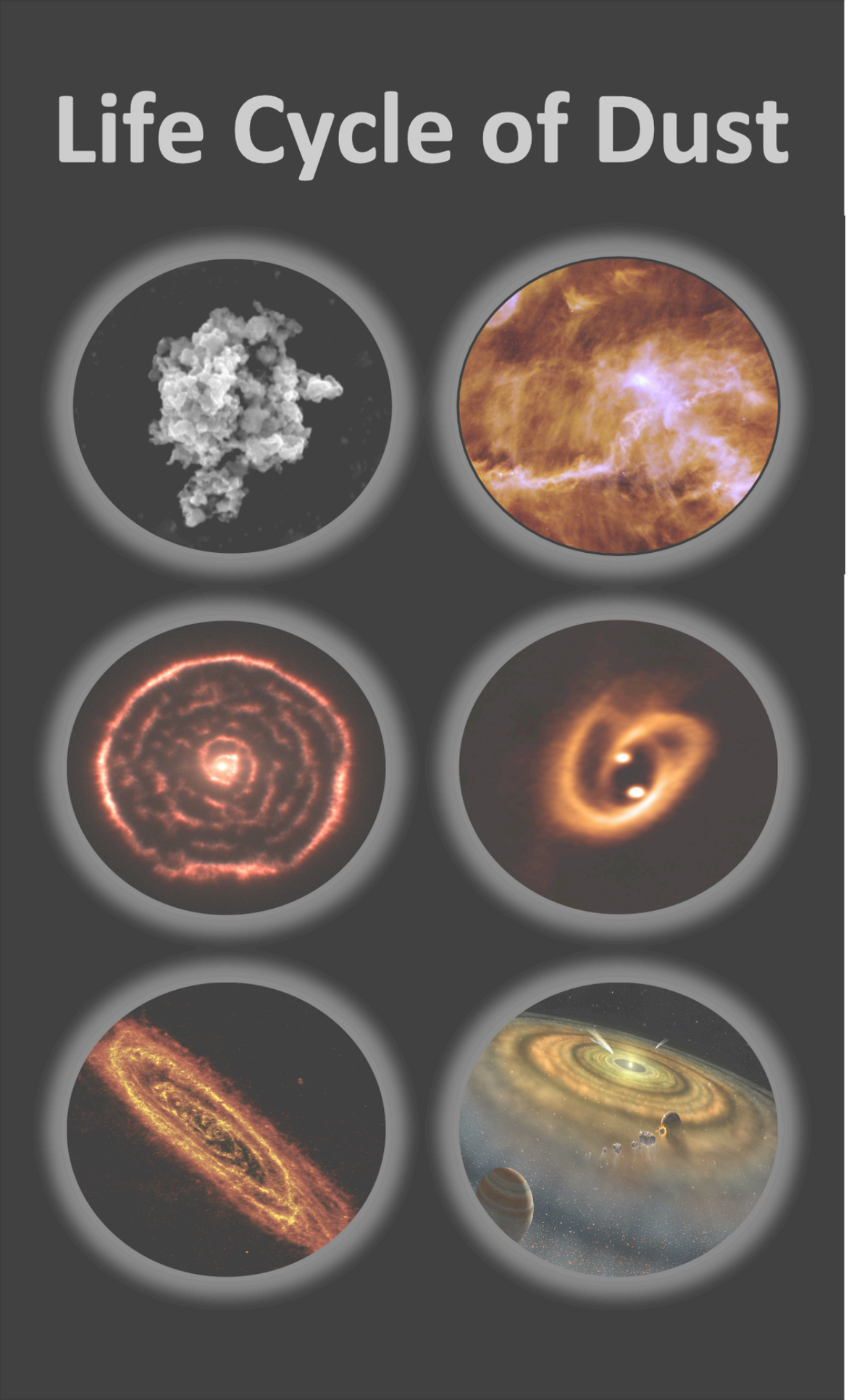

★ Telescope Basics

- Fundamental parameters
- Antenna types
- Detectors
- Aperture Synthesis Basics

Where to build and observatory

- Ground-based observatories
- Atmospheric observatories: aircrafts and balloons
- Space-based observatories

Ground-based observatories

- Lowest cost
- Familiar environment, but gravity → limitations on size
- Access for construction, correction, repairs, and technology upgrading
- Good locations also for small projects
- Short term observations
- Atmospheric constraints
  - Limited spectral window and noise on radio
  - Weather & Light pollution
  - Air stability → limited resolution
- Seismic instability

Observatory sites

- Best astronomical sites on Earth

Mauna Kea (Hawaii)

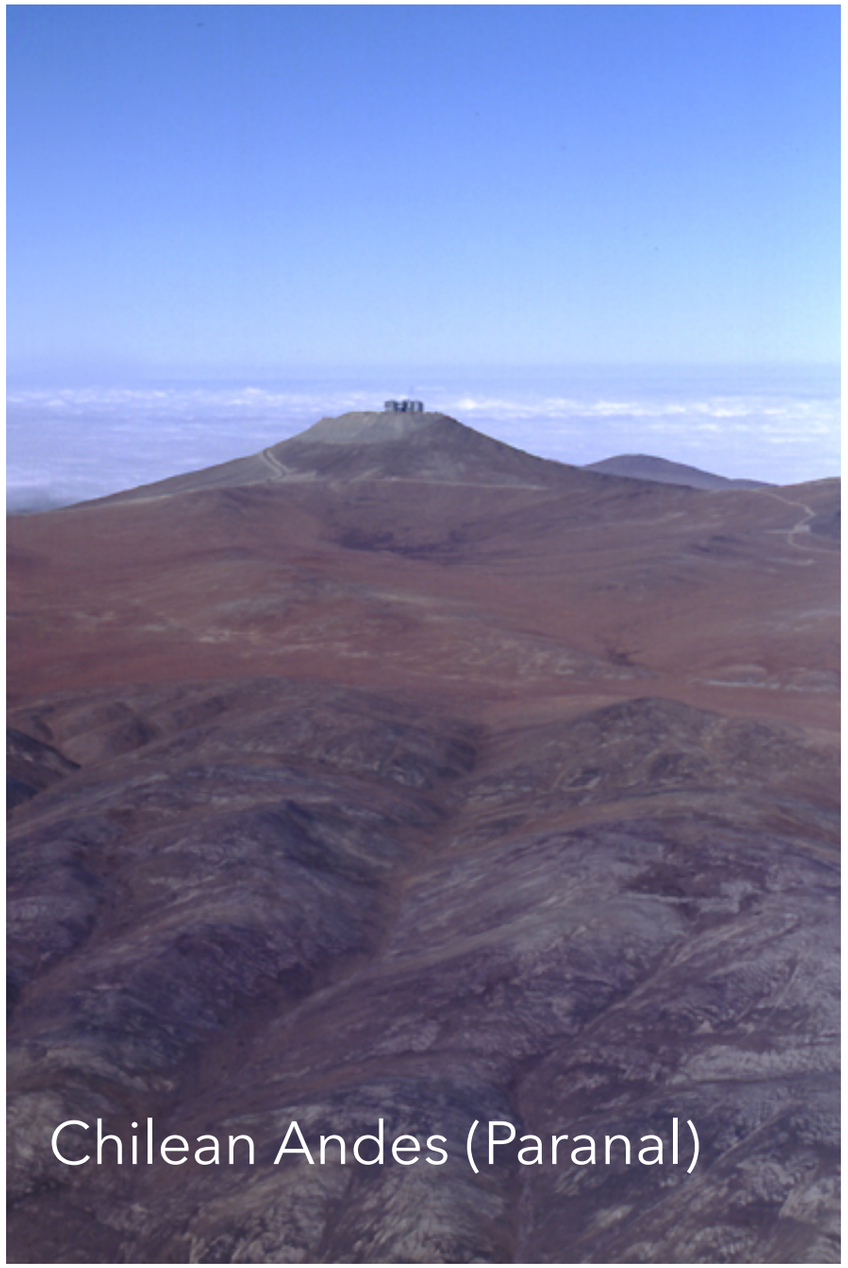
Chilean Andes (Paranal)

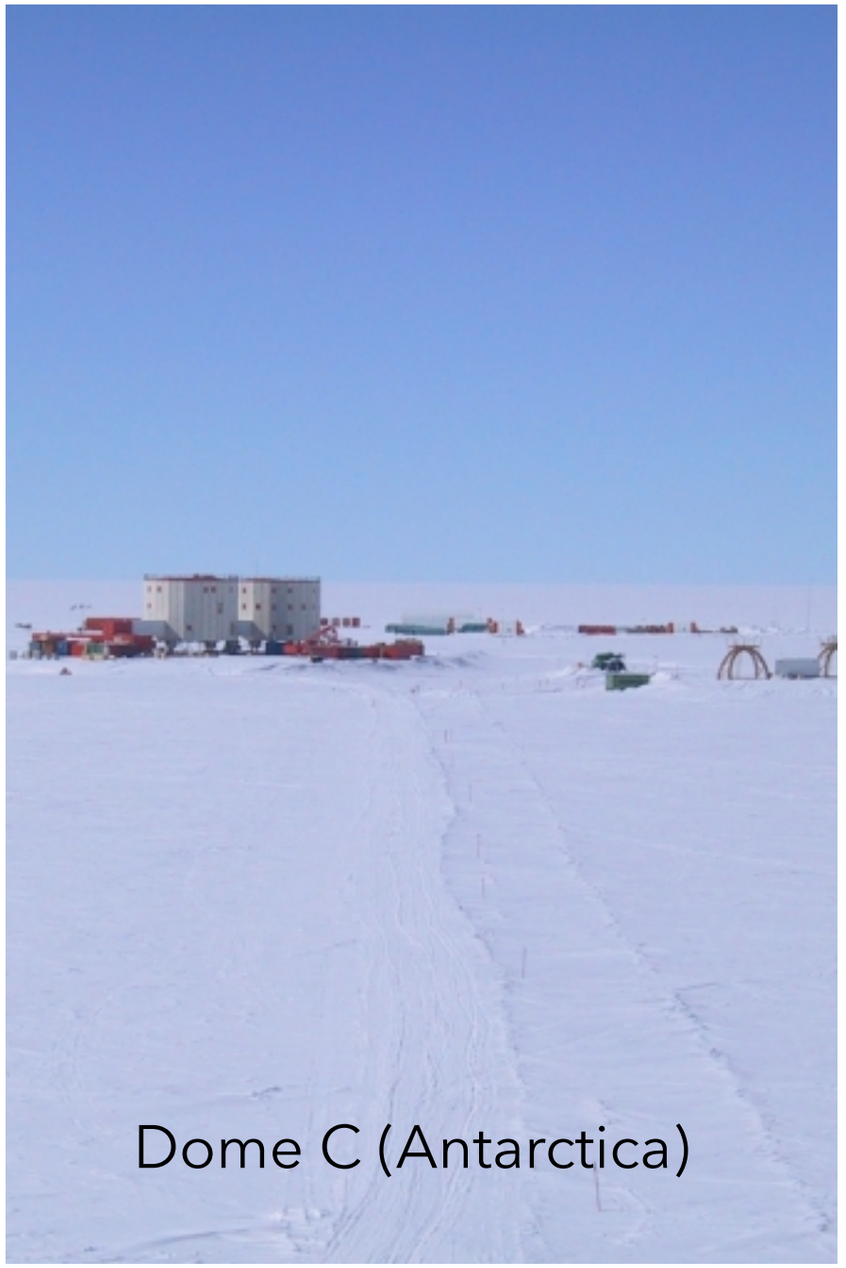
Dome C (Antarctica)

Atmospheric observatories

- Lack of atmospheric turbulence and absorption
- Minimal atmospheric opacity and radiance
- Lower cost than satellites
- Advantageous in the infrared
- Some degradation due to vibration

Atmospheric observatories

- Airplane based:

KAO

SOFIA

- Balloon based:

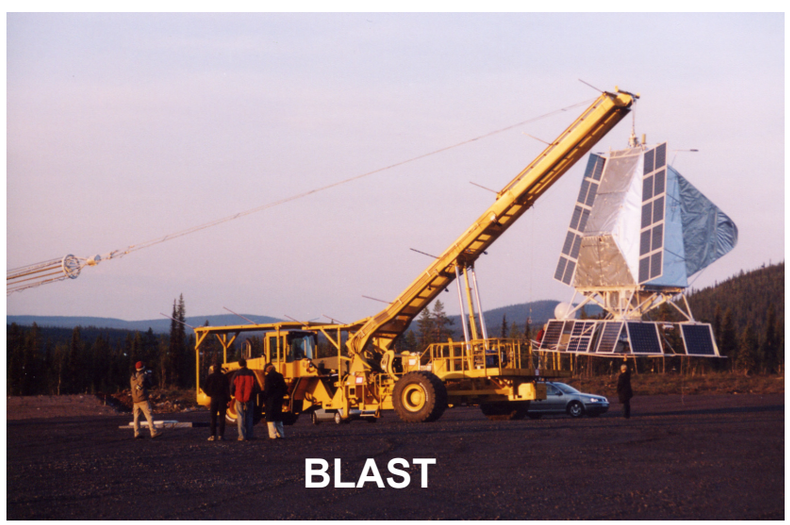
BLAST

Boomerang

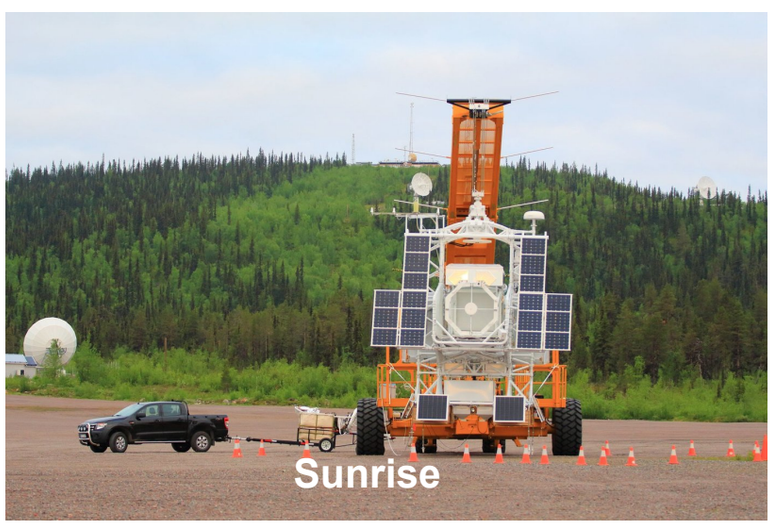
Sunrise

Space-based observatories

- Image quality just conditioned by optics → diffraction limited resolution
- Long term observations
- Access to every wavelength range
- Excellent instrumental stability
- Low levels of mechanical and thermal disturbances and weak gravity → engineering advantages
- Cost 10 to 100 times higher than Earth-based
- Relatively short lifetimes and no instrument upgrading
-

Popular observatory orbits

- Earth orbits:
  - Low Earth orbit (LEO)
  - Geostationary and Geosynchronous orbit (GEO)
  - High Earth Orbits (HEO)

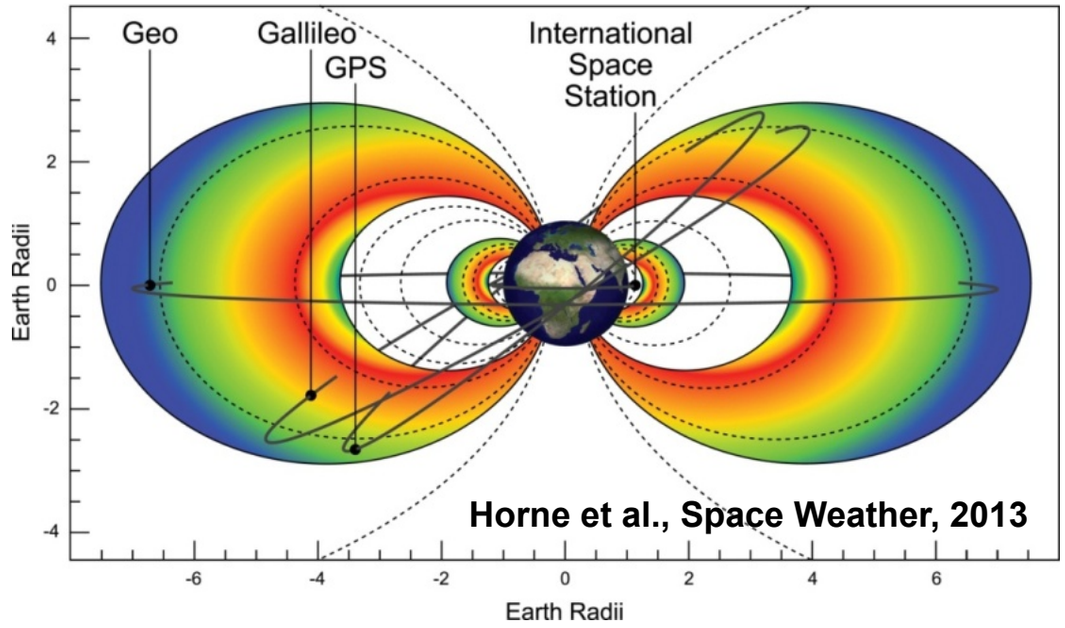

$$P = \frac{2 \cdot \pi}{\sqrt{GM_{\oplus}}} \cdot a^{\frac{3}{2}}$$

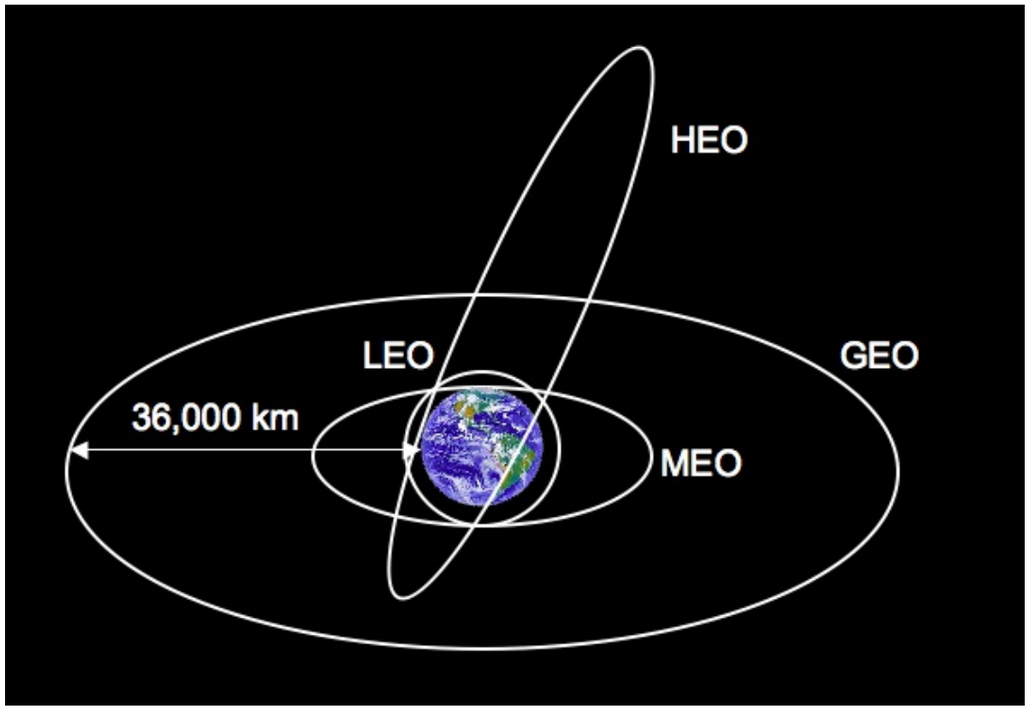

Popular observatory orbits

- Lagrange points at 1.5 million km
  - Sun-Earth Lagrangian point L1: SOHO
  - Sun-Earth Lagrangian point L2: Herschel, Planck, Gaia, JWST, PLATO, ARIEL, etc

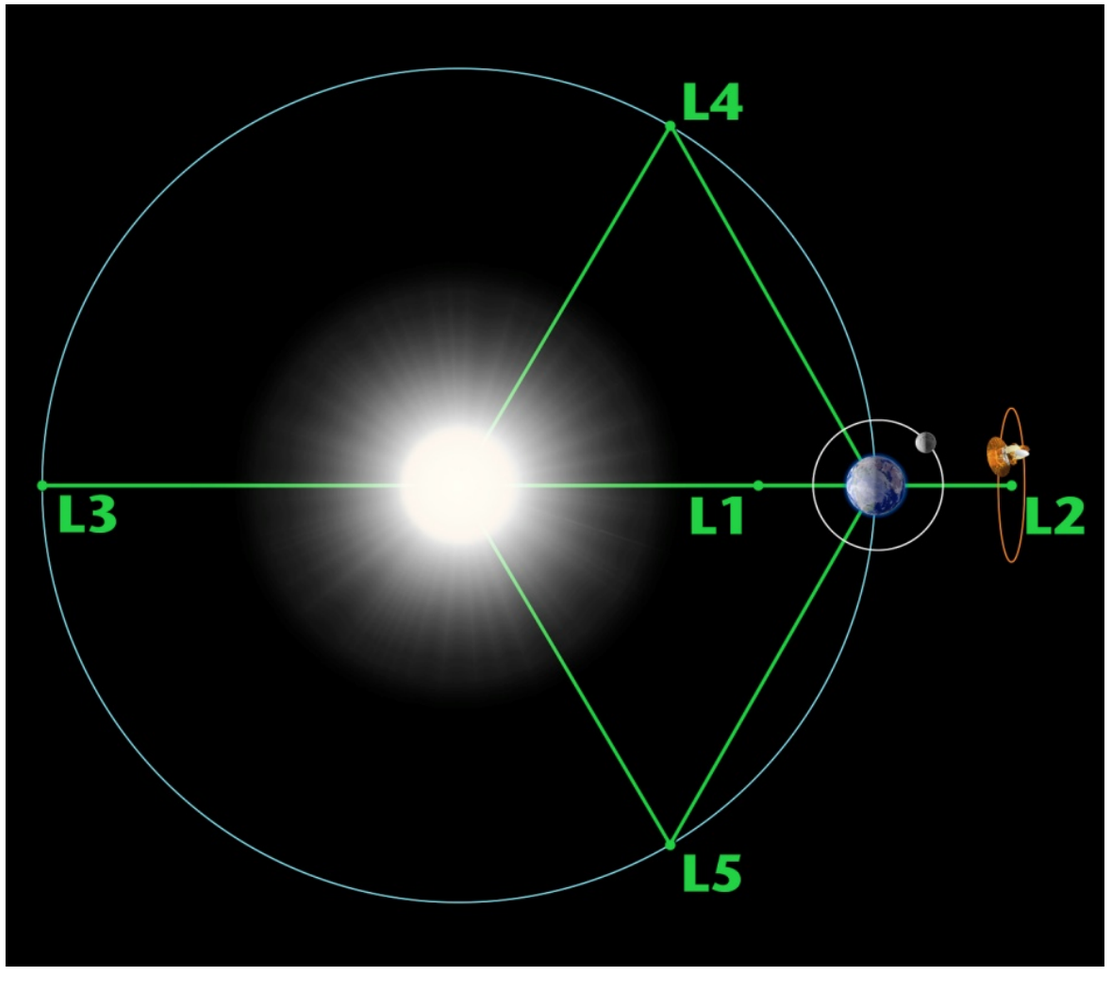

Optical Astronomy: Optics in Astronomy

- **Telescope**: Optical instrument to observe very distant objects
- **Types**: refractor & reflector (& catadioptrics)
- **Rays trace**
- **Basic concepts**

  Aperture: D

  Focal length: f

  Focal ratio: f-number = n = f/D

  Fast telecope (small n), Slow telesco

  Field of view & vigneting

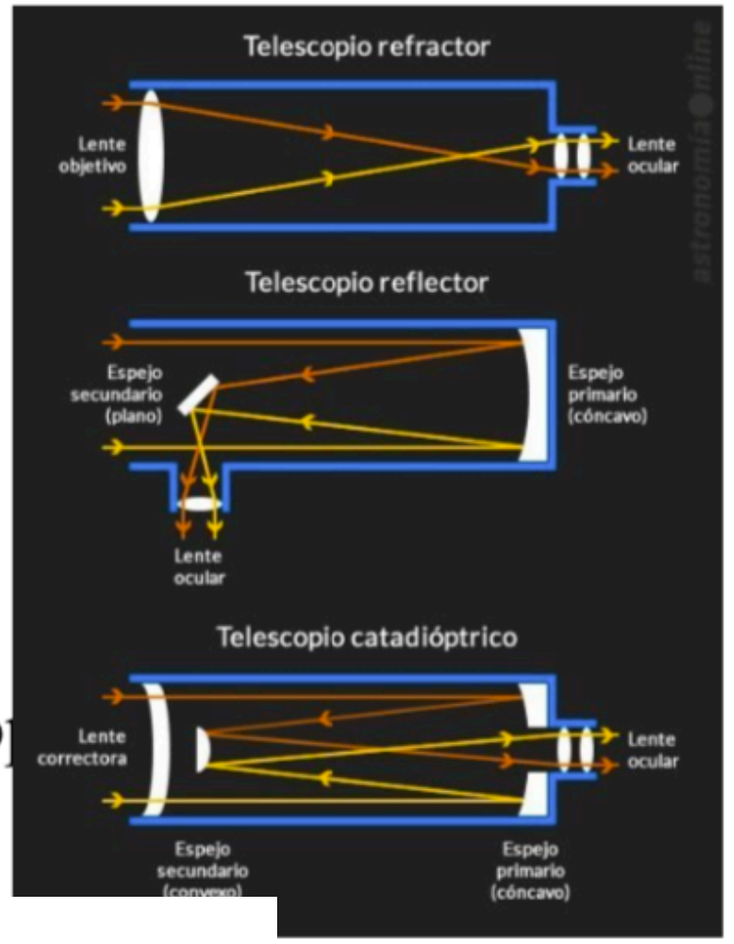

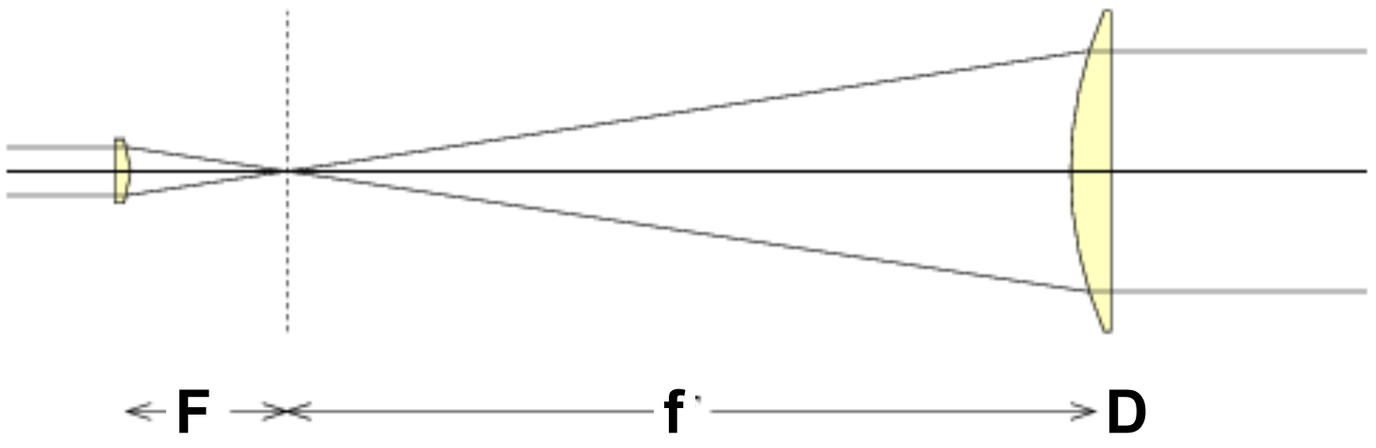

Telescope structure and mechanisms

- Mounts for ground-based telescopes
  - The purpose of a “telescope mount” is to support the telescope tube and allow for its rotation during pointing and tracking.

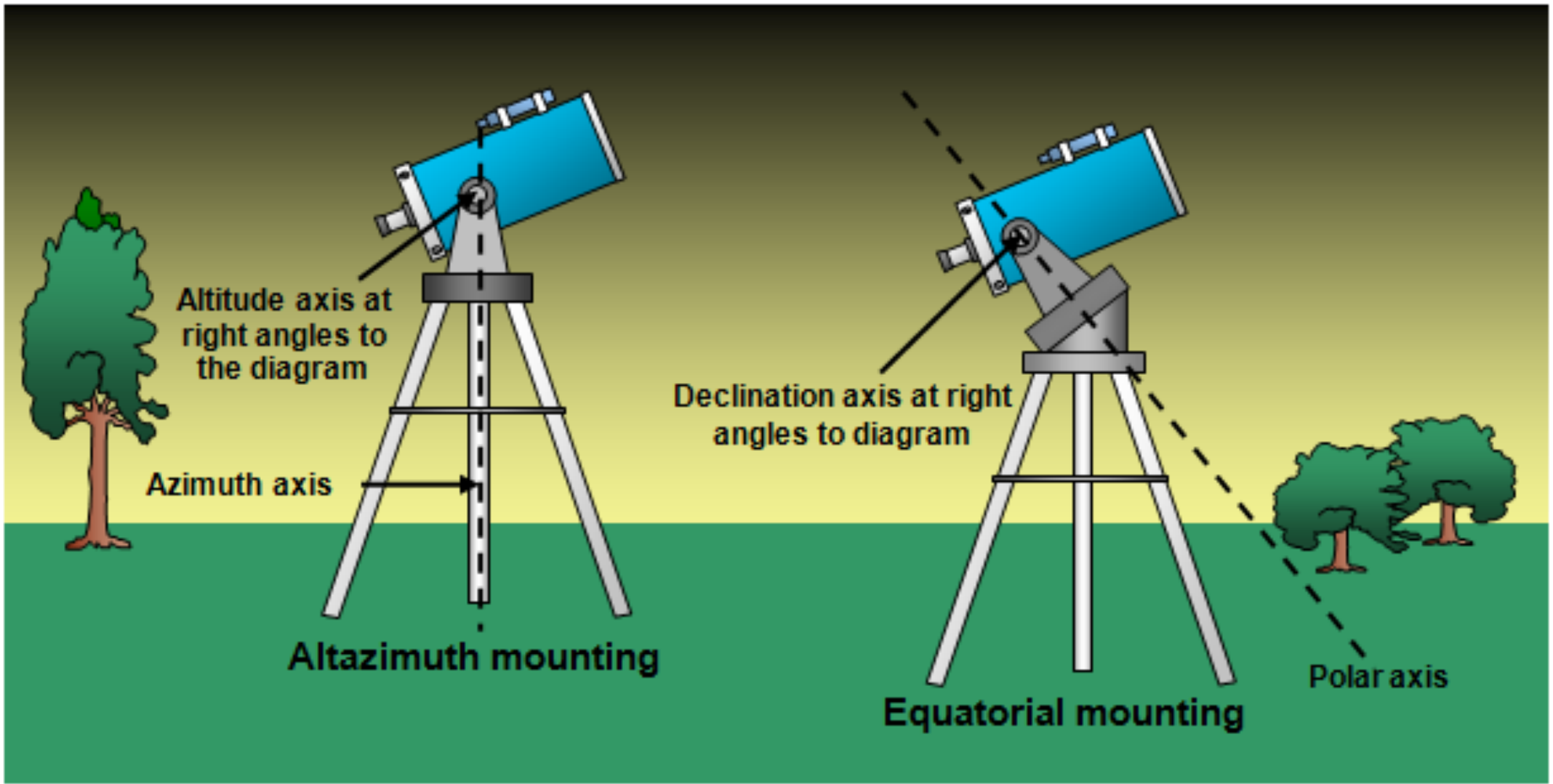

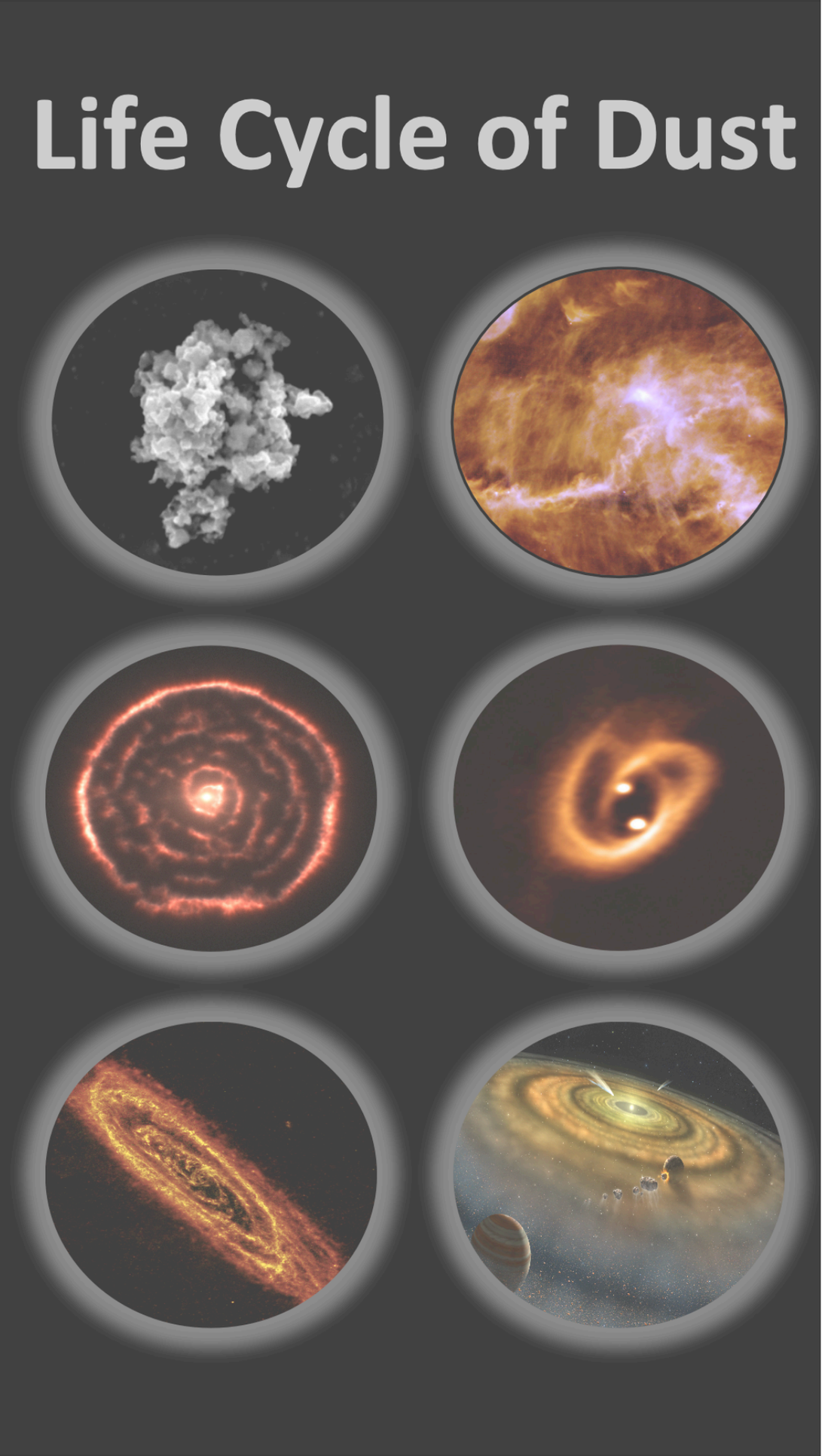

- Fundamental parameters

★ **Wavelength coverage**: $\lambda_{min} - \lambda_{max}$

★ **D: Aperture** (diameter of the main dish / mirrow / lens)

★ **θ: Angular resolution** (in radians):

$$\theta = 1.22 \frac{\lambda}{D}$$

★ **PSF: Point Spread function**

★ **FoV: Field of view**

★ **R: Resolving power (spectral resolution)** $R = \lambda / \Delta\lambda$

$$\Delta v = \frac{300{,}000}{R} \text{ km/s}$$

ALMA Receiver Bands

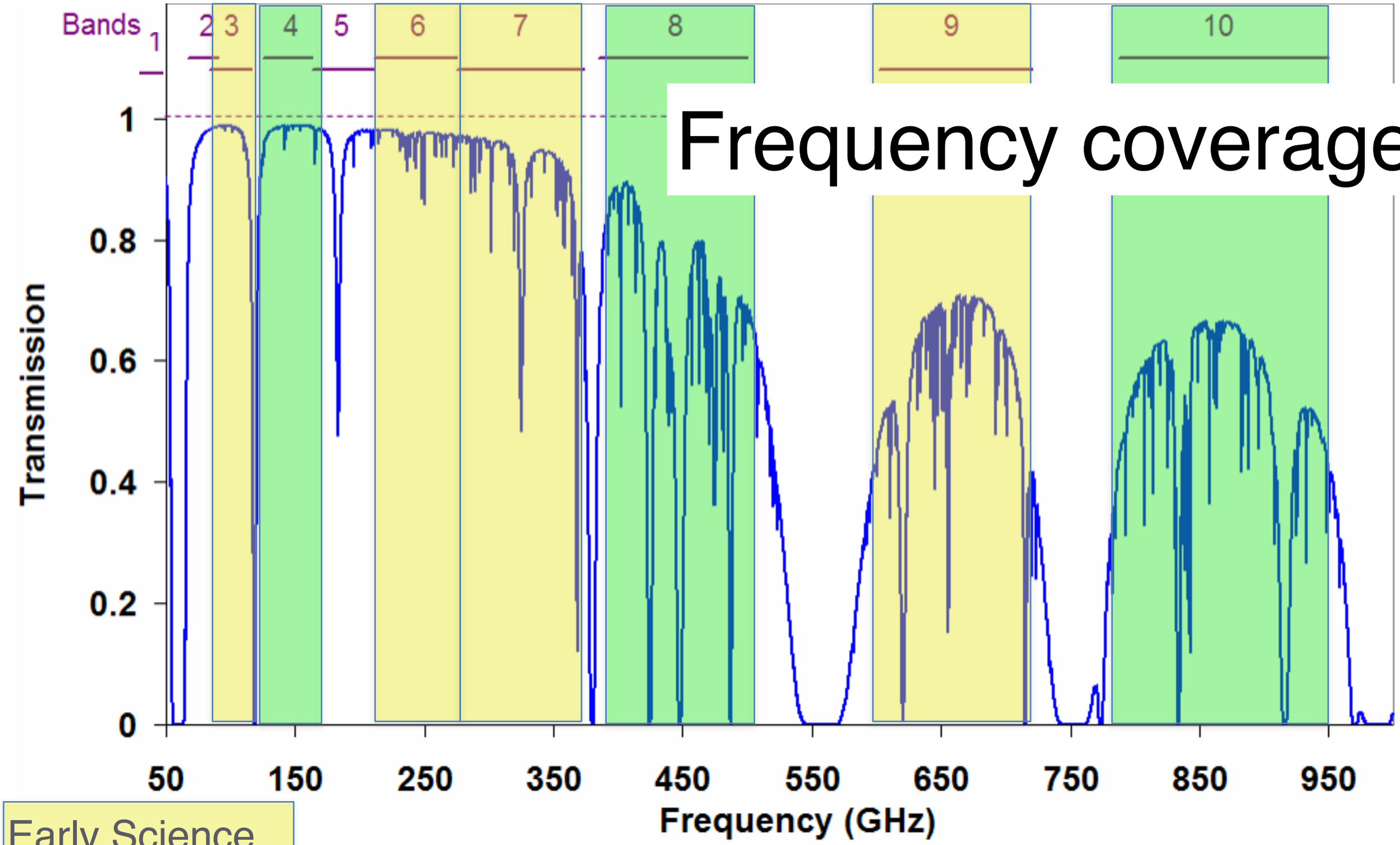

Early Science

Full Operations

Great Paris Exhibition Telescope
(lens at the same scale)
Paris, France (1900)

Yerkes Observatory
(40" refractor
lens at the same scale)
Williams Bay,
Wisconsin (1893)

Hooker (100")
Mt Wilson,
California
(1917)

Hale (200")
Mt Palomar,
California
(1948)

(1979-1998) (1999-)
Multi Mirror Telescope
Mount Hopkins, Arizona

BTA-6 (Large Altazimuth Telescope)
Zelenchuksky, Russia
(1975)

Large Zenith Telescope
British Columbia, Canada
(2003)

Gaia
Earth-Sun L2 point
(2014)

Kepler
Earth-trailing
solar orbit
(2009)

James Webb Space Telescope
Earth-Sun L2 point
(planned 2018)

Hubble Space Telescope
Low Earth
Orbit
(1990)

Tennis court at the same scale

Large Sky Area Multi-Object Fiber Spectroscopic Telescope
Hebei, China
(2009)

Hobby-Eberly Telescope
Davis
Mountains,
Texas (1996)

Large Binocular Telescope
Mount Graham,
Arizona (2005)

Very Large Telescope
Cerro Paranal, Chile
(1998-2000)

Magellan Telescopes
Las Campanas,
Chile (2000/2002)

Gran Telescopio Canarias
La Palma,
Canary Islands,
Spain (2007)

Southern African Large Telescope
Sutherland,
South Africa
(2005)

Keck Telescope
Mauna Kea, Hawaii
(1993/1996)

Gemini North
Mauna Kea,
Hawaii (1999)

Subaru Telescope
Mauna Kea,
Hawaii (1999)

Gemini South
Cerro Pachón,
Chile (2000)

Large Synoptic Survey Telescope
El Peñón, Chile
(planned 2020)

Giant Magellan Telescope
Las Campanas Observatory,
Chile (planned 2020)

Thirty Meter Telescope
Mauna Kea, Hawaii (planned 2022)

European Extremely Large Telescope
Cerro Armazones,
Chile (planned 2022)

Human
at the
same scale

0 5 10 m
0 10 20 30 ft

Overwhelmingly Large Telescope
(cancelled)
Arecibo radio telescope at the same scale

Basketball court at the same scale

Angular resolution

✓Optical: to get θ~0.5 arcsec, λ=500nm ⇒ **D~50 cm**

✓Radio: to get θ~0.5 arcsec, λ=5cm ⇒ **d~50 km**

GBT 100m:

Antenna off-axis 100×110m

Receivers: 0.58 → 100 cm

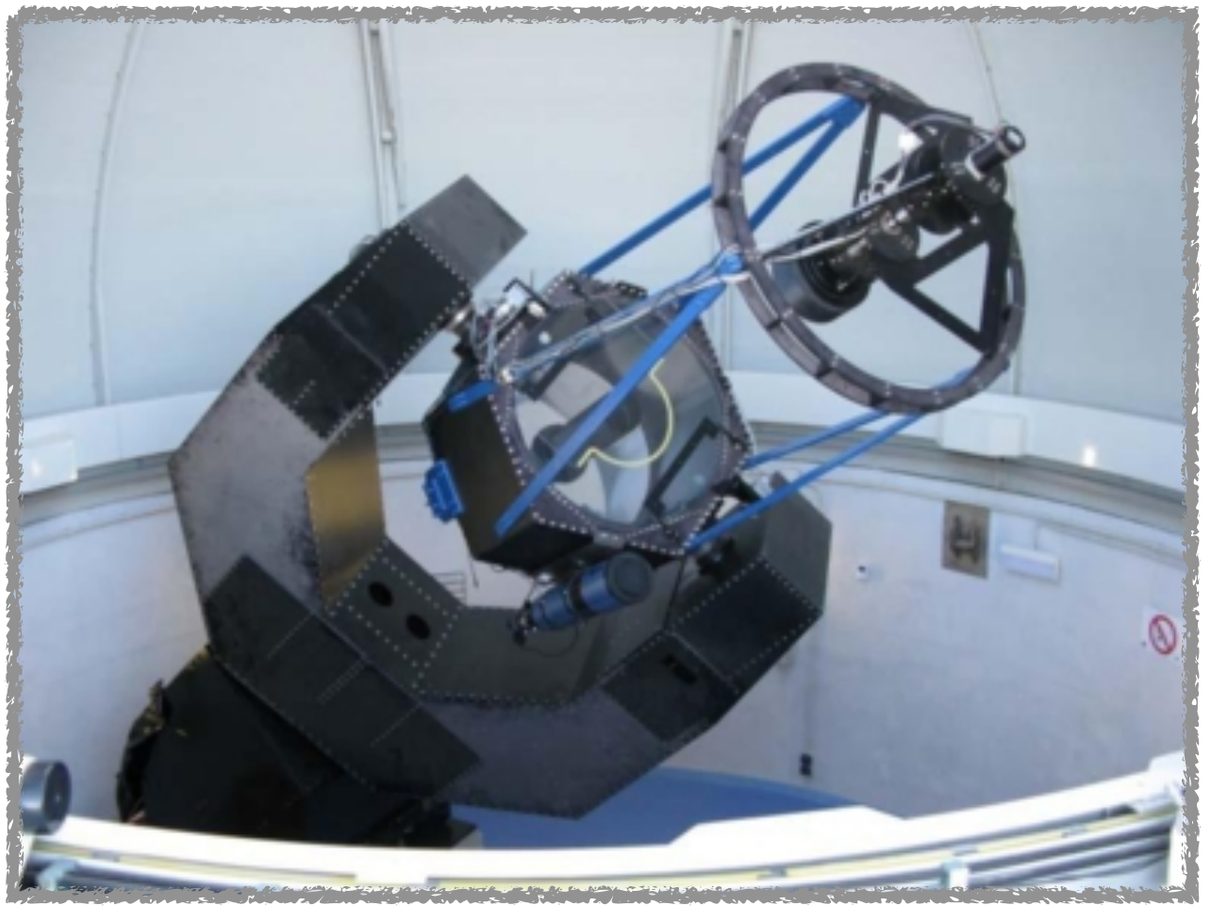

Joan Oró 0.8m:

Antenna 0.8m

Receivers: 350 → 1100 nm

Diffraction: PSF

- ✓ The PSF of the image of a point source at infinity is proportional to the two-dimensional Fourier transform of the complex pupil function
- ✓ Degradation factors: dust and mirror surface defects

Aperture

PSF

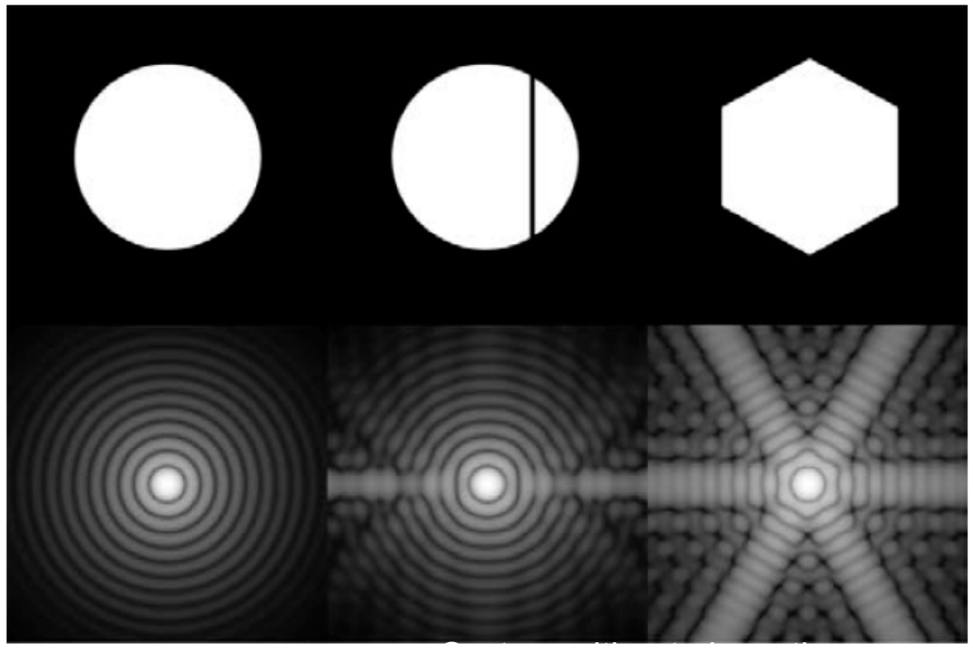

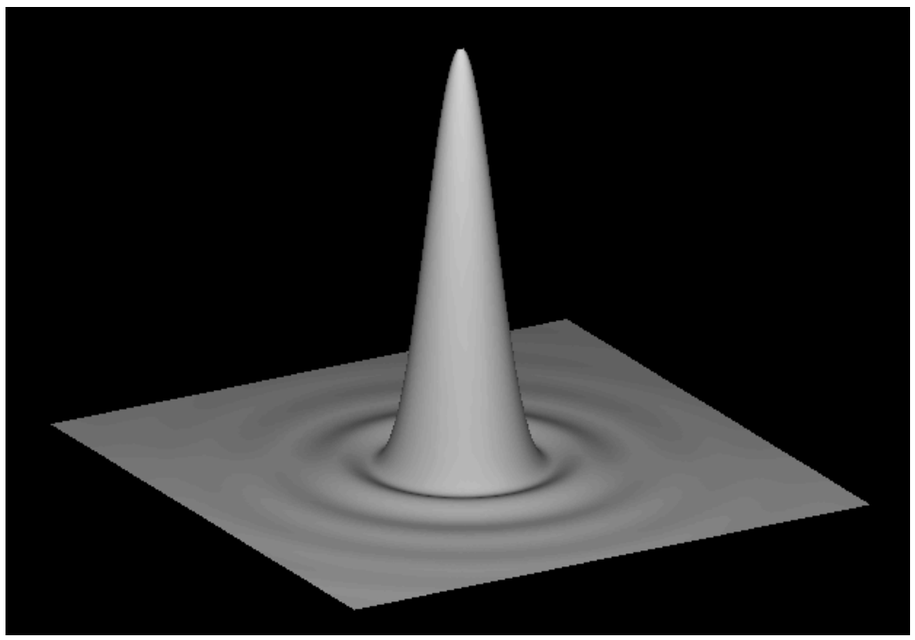

Diffraction: PSF

- ✓ The PSF of the image of a point source at infinity is proportional to the two-dimensional Fourier transform of the complex pupil function
- ✓ Degradation factors: dust and mirror surface defects

Aperture

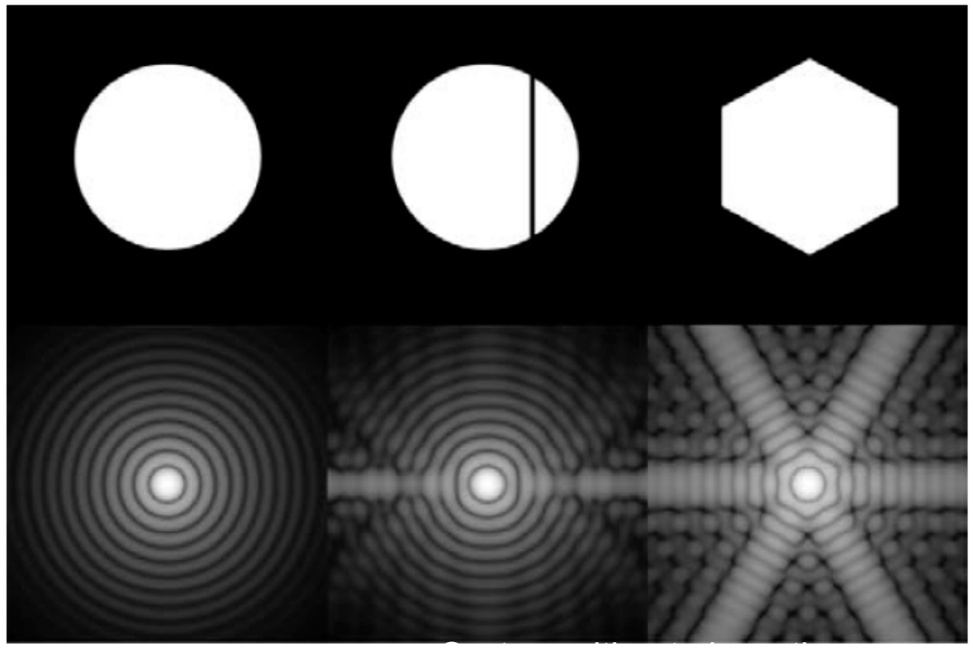

PSF

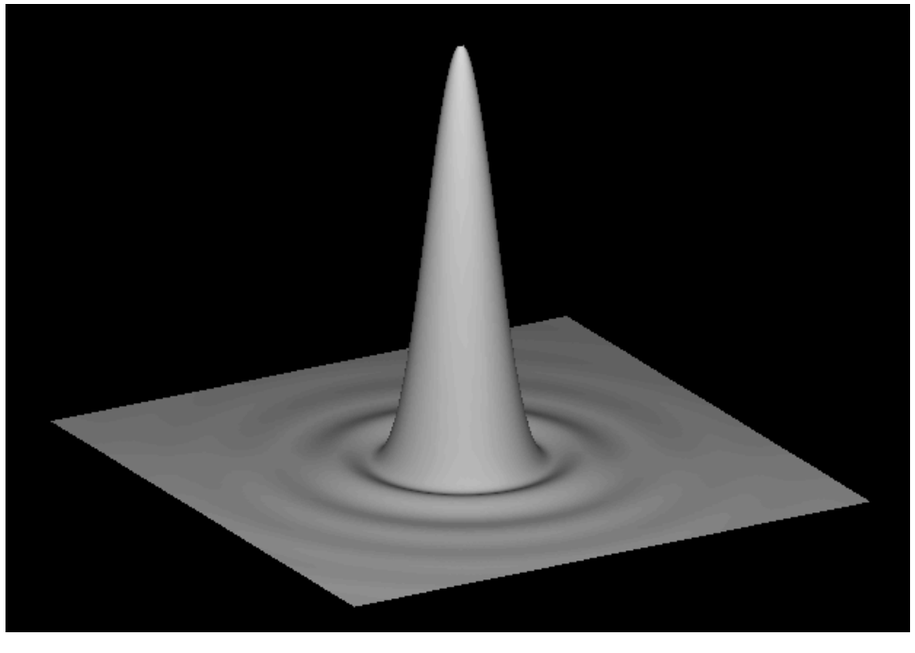

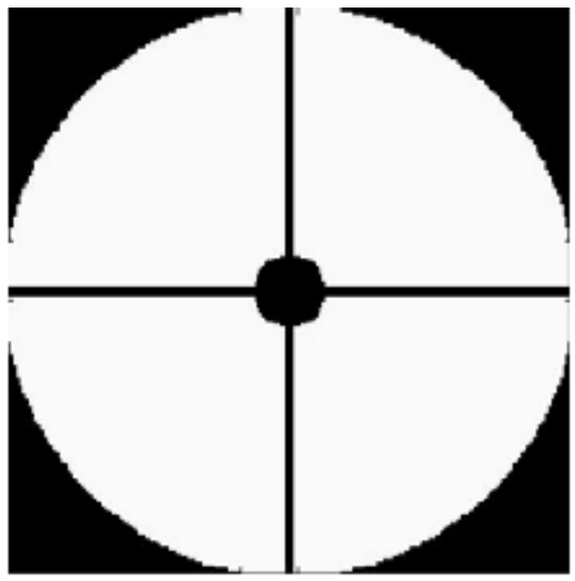

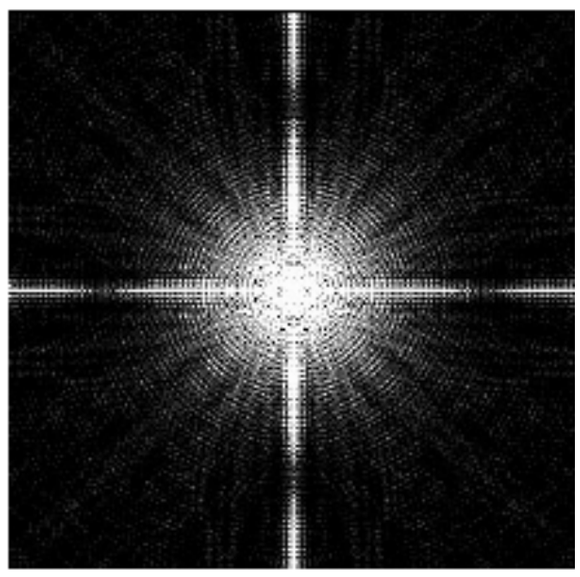

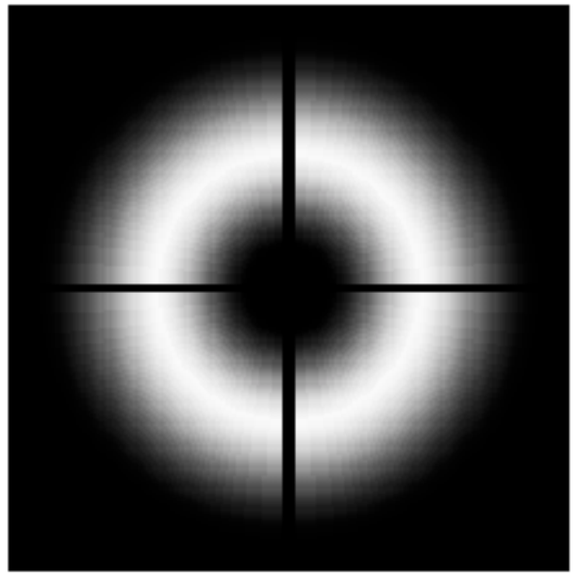

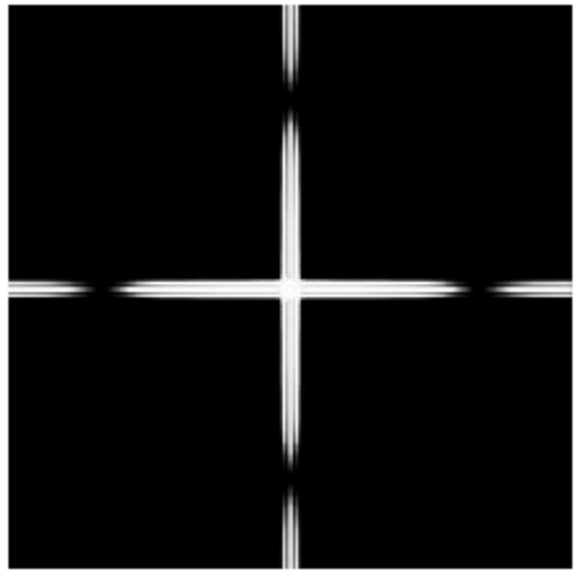

Diffraction: PSF

Modelled PSF MIRI JSWT

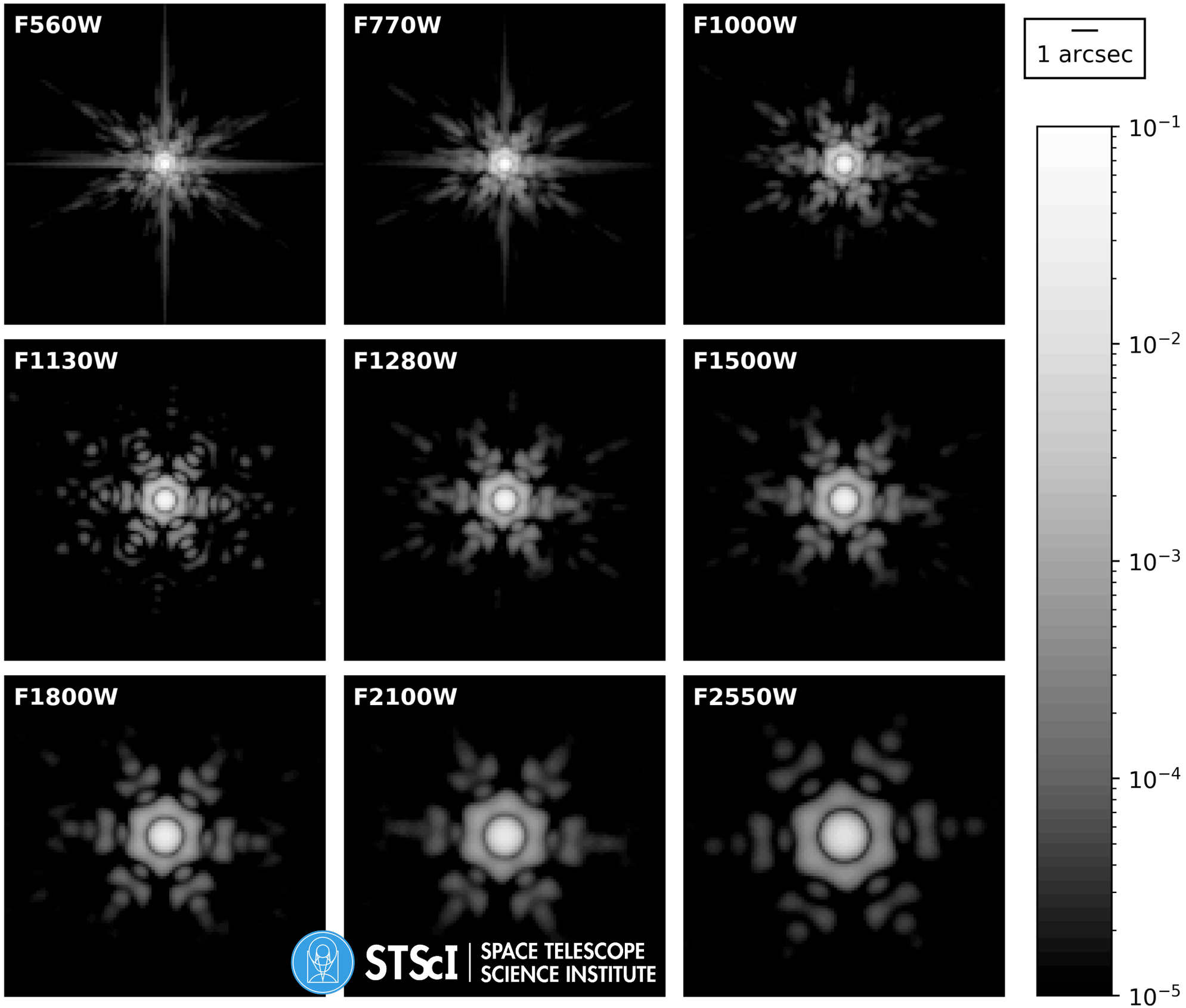

Angular resolution: PSF and seeing

PSF:

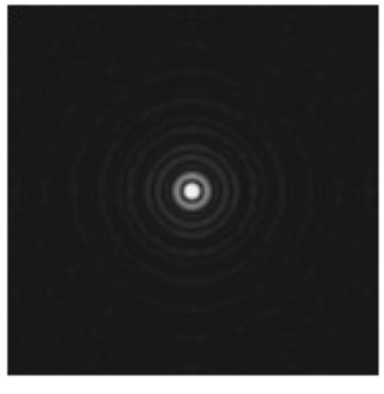

Real exposure images, seeing limits the effective angular resolution:

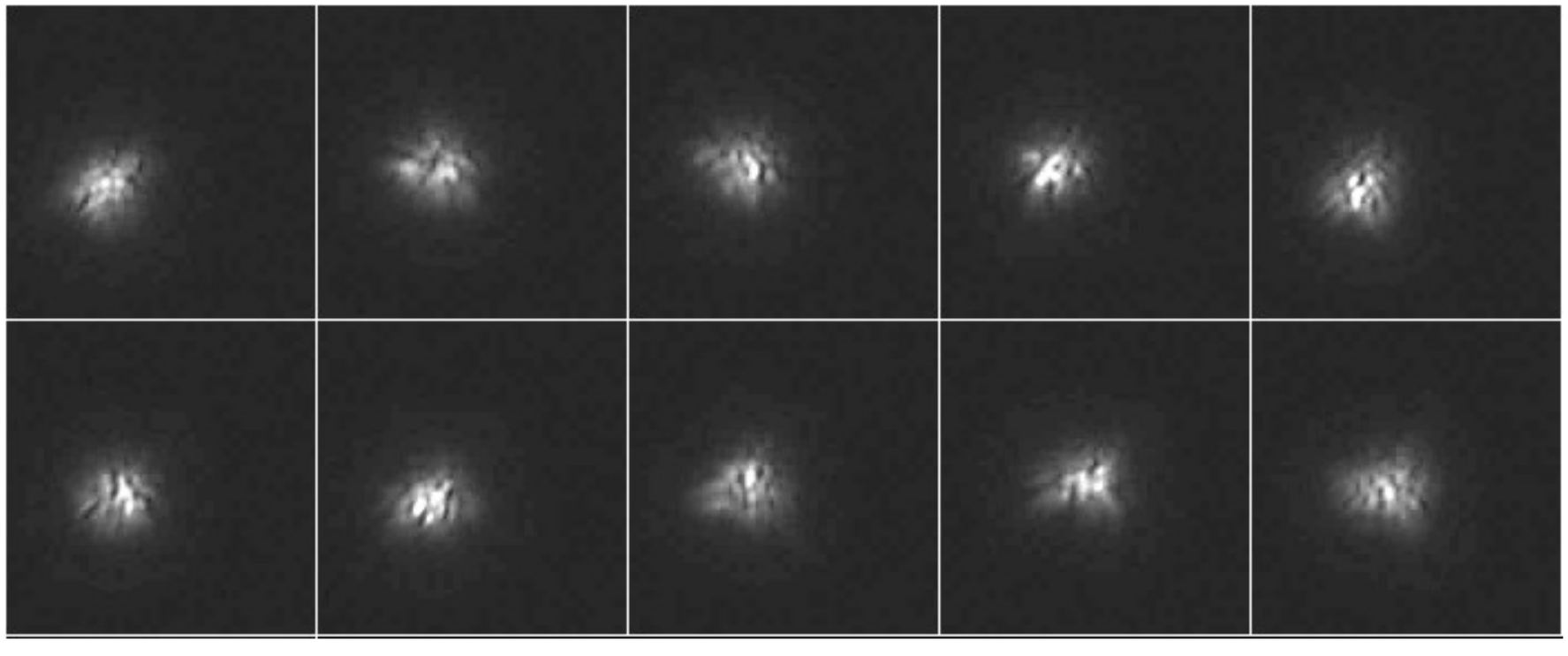

- Adaptive optics

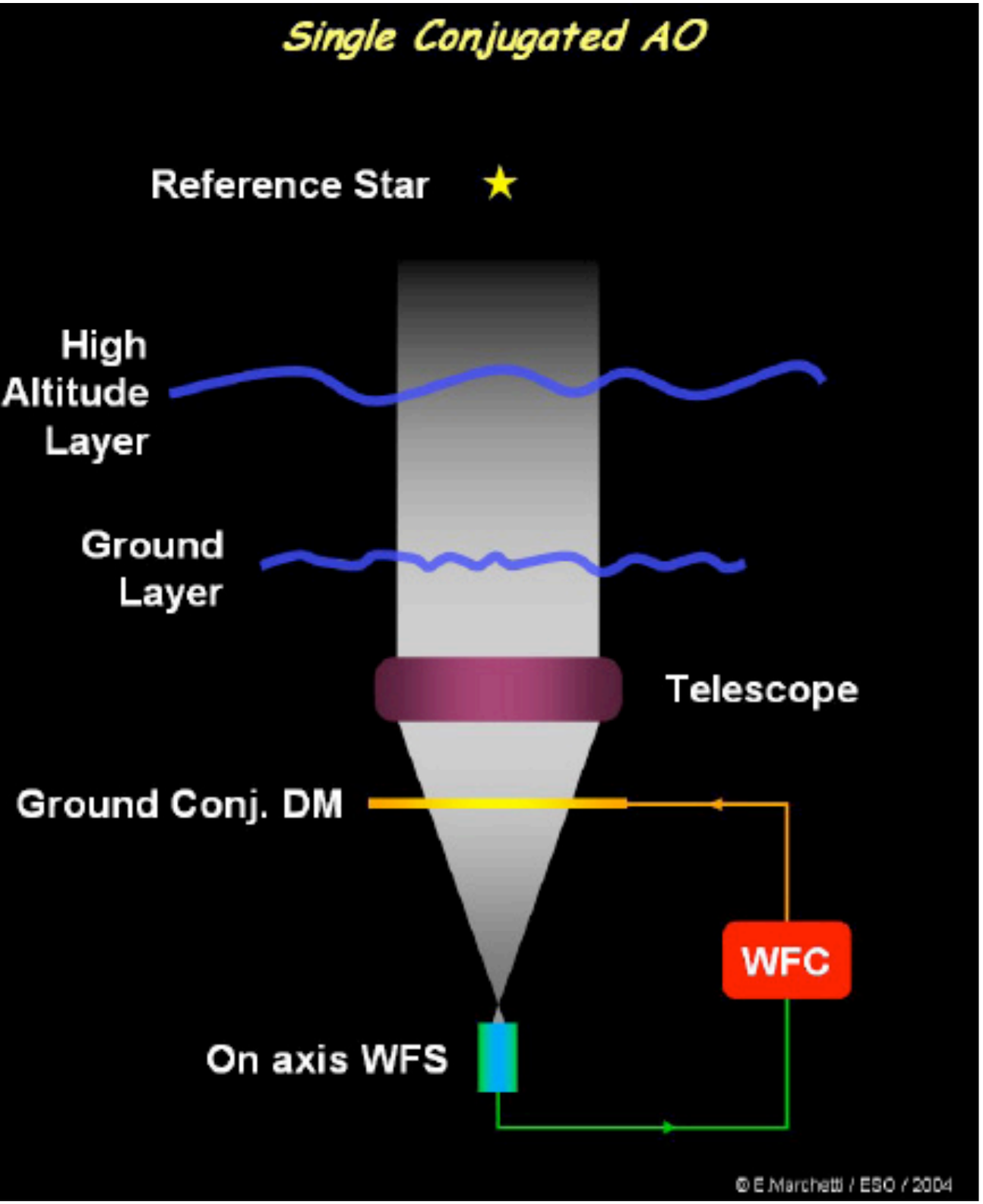

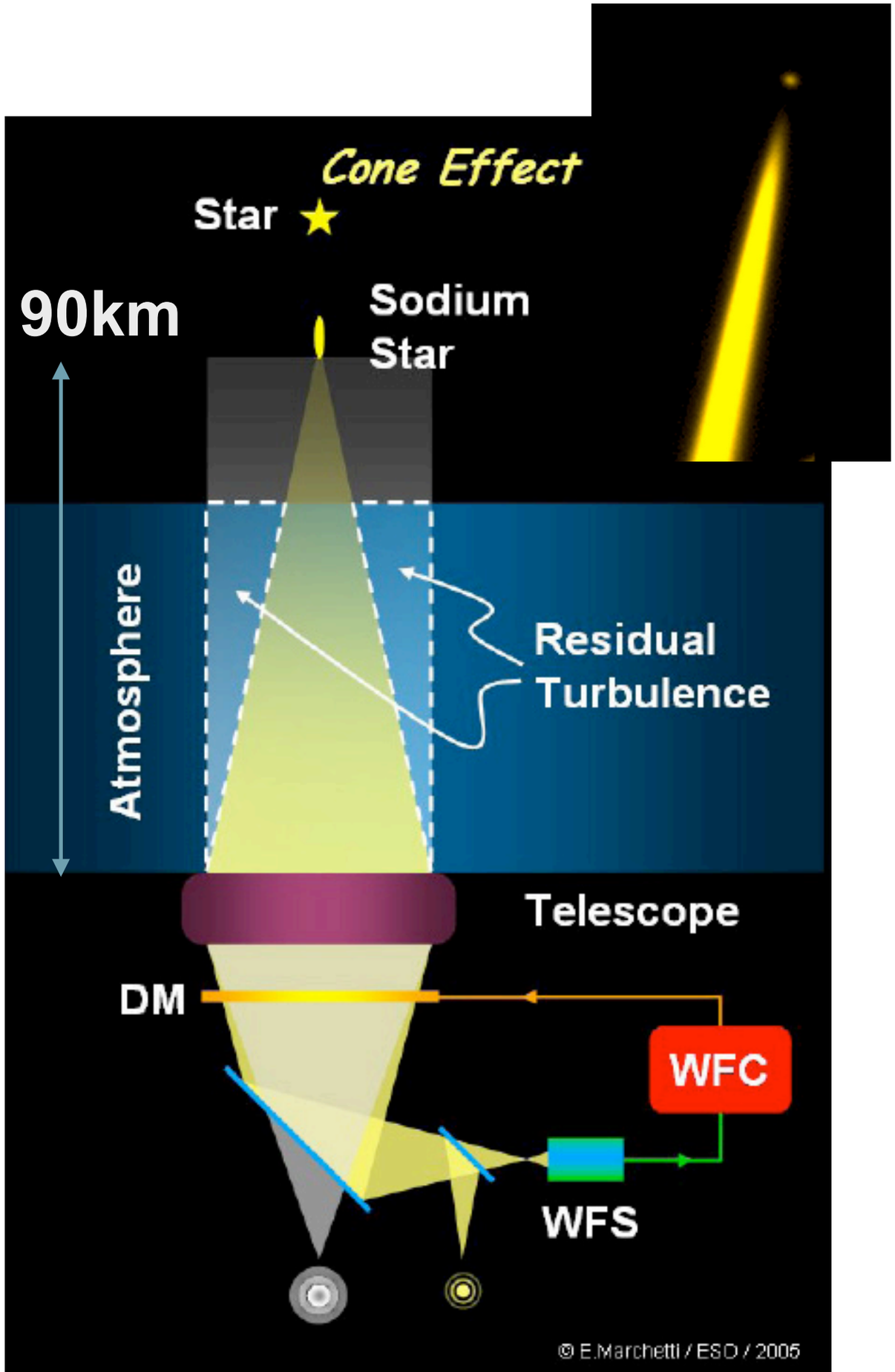

- Adaptive optics:

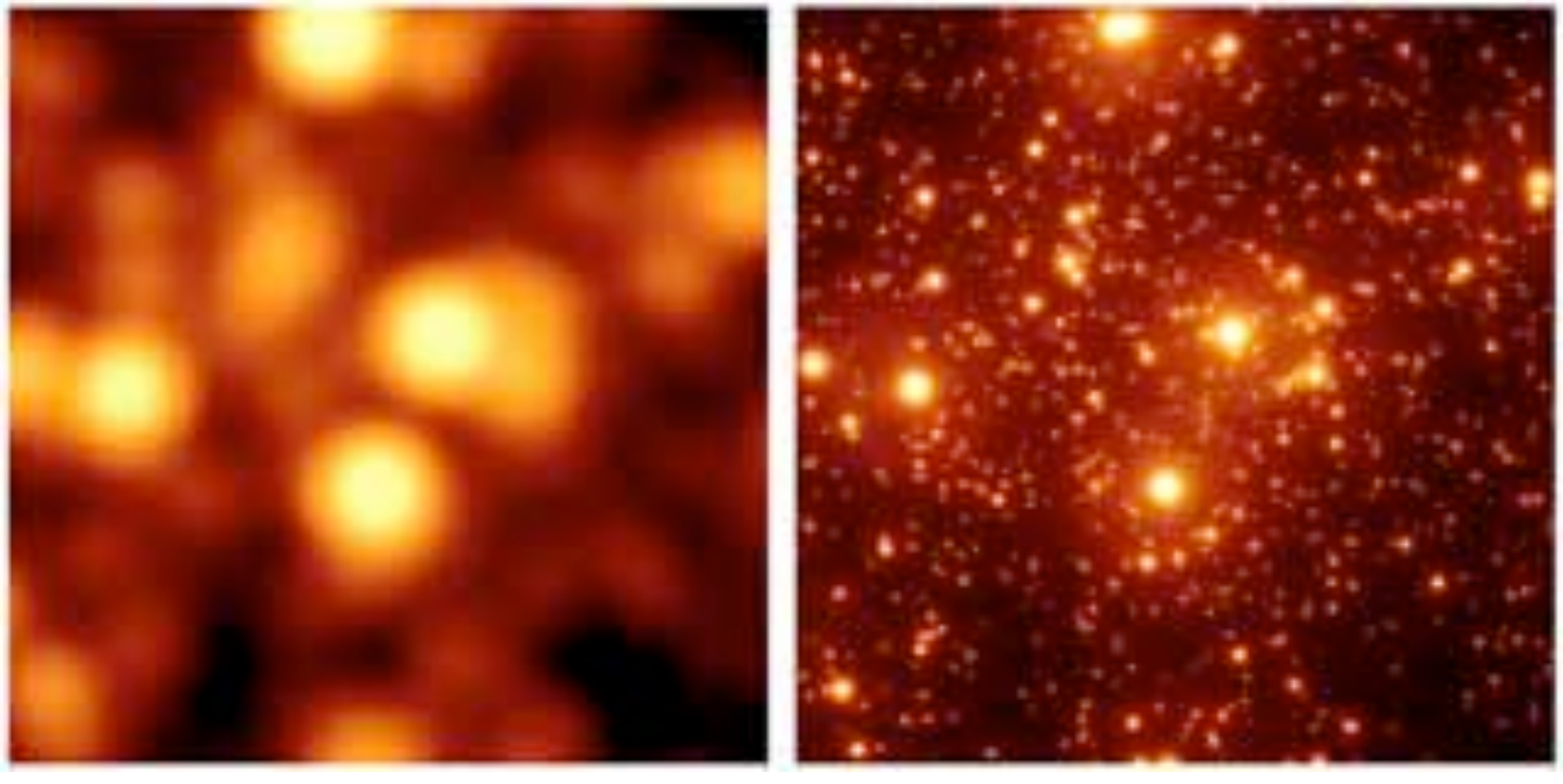

The Galactic center in the near-IR

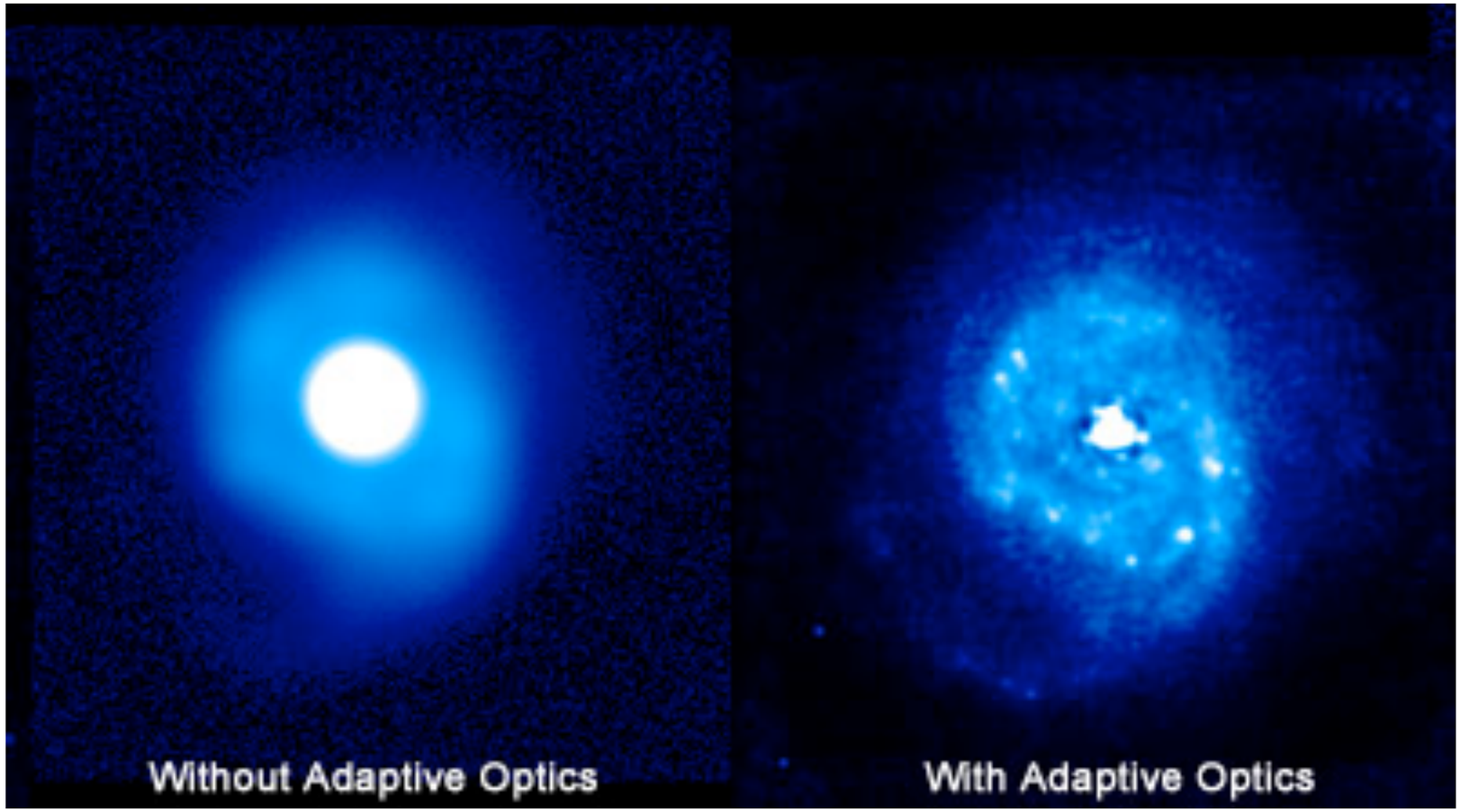

FoV: Field of view

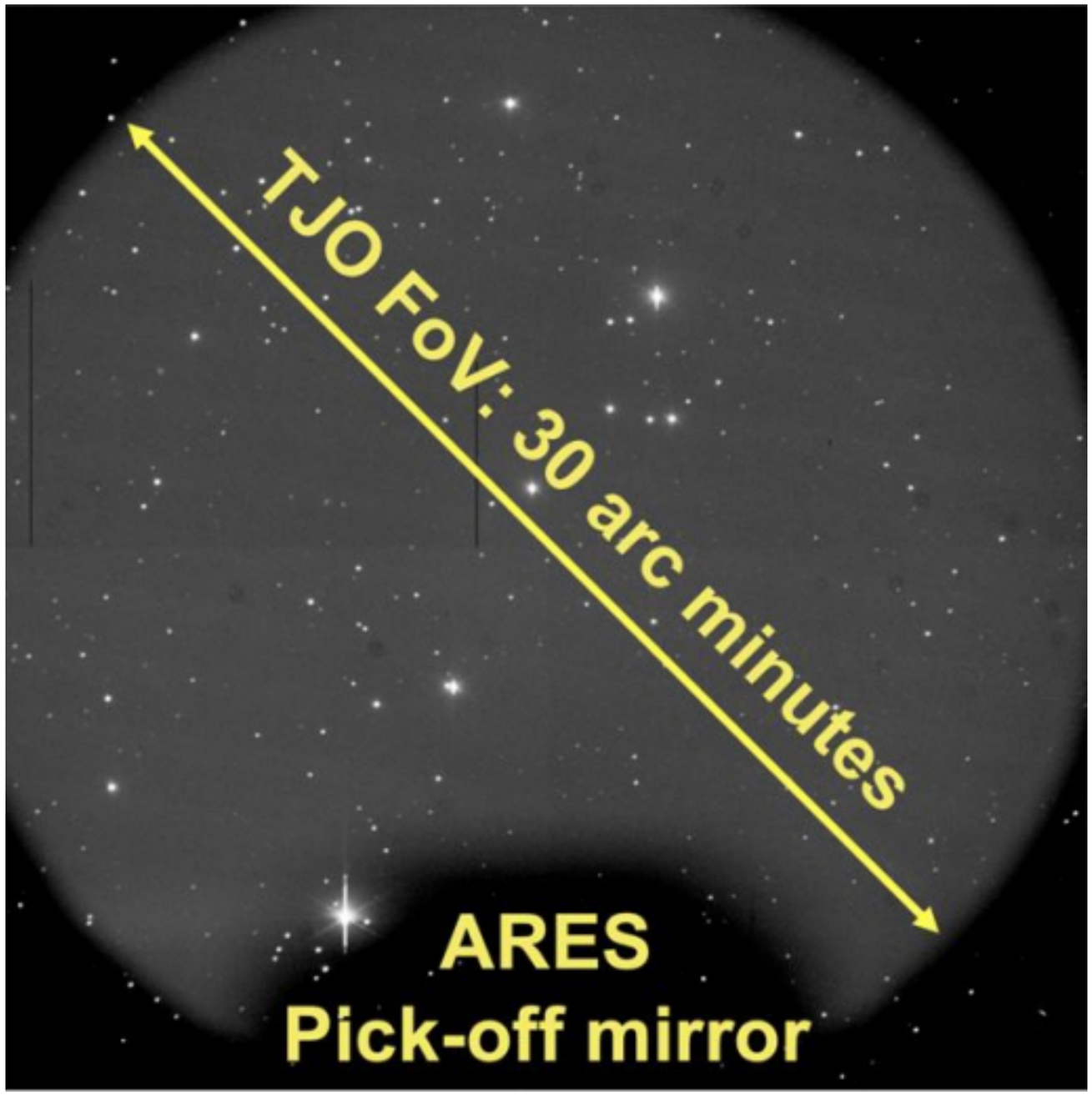

R: spectral resolution

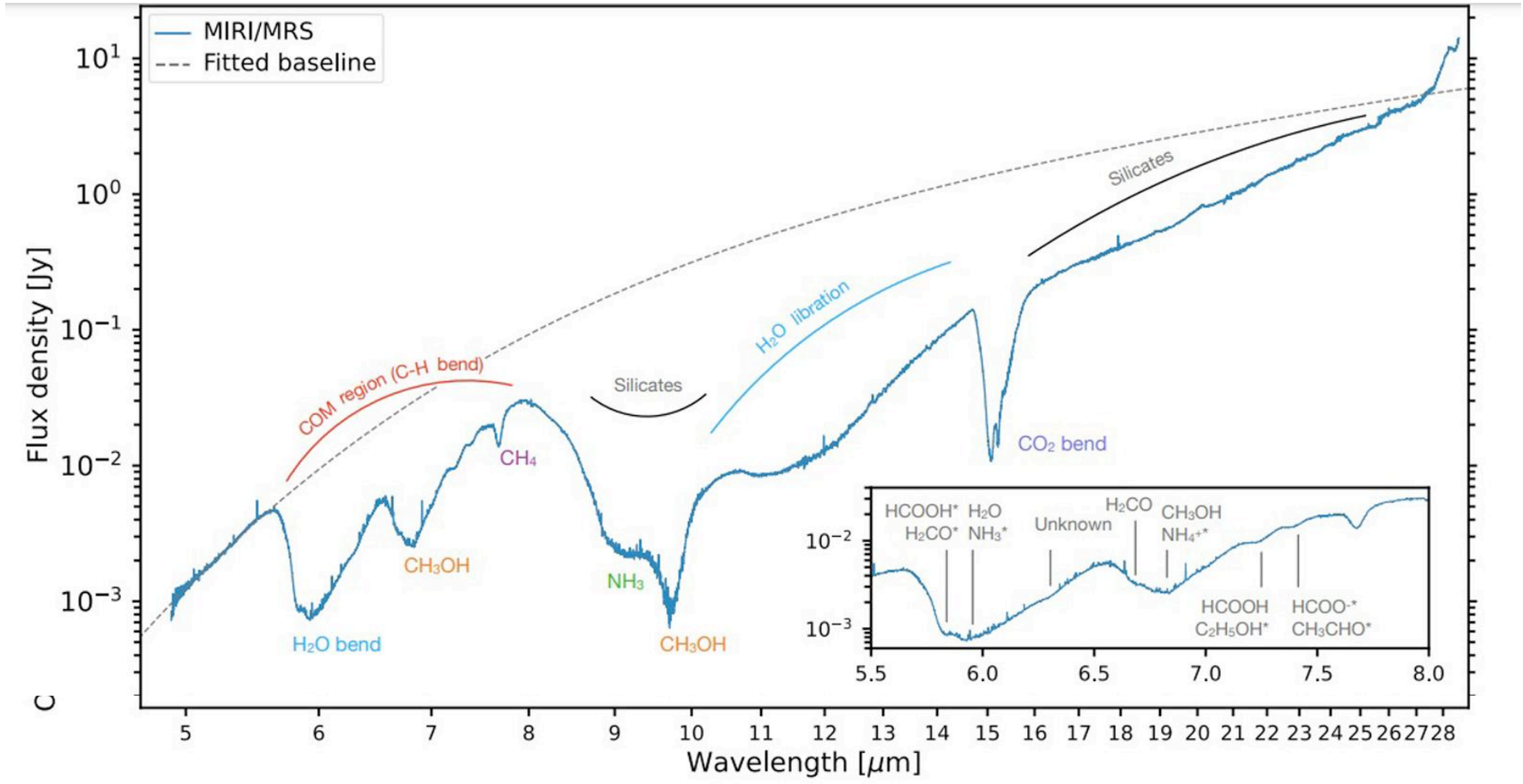

JWST

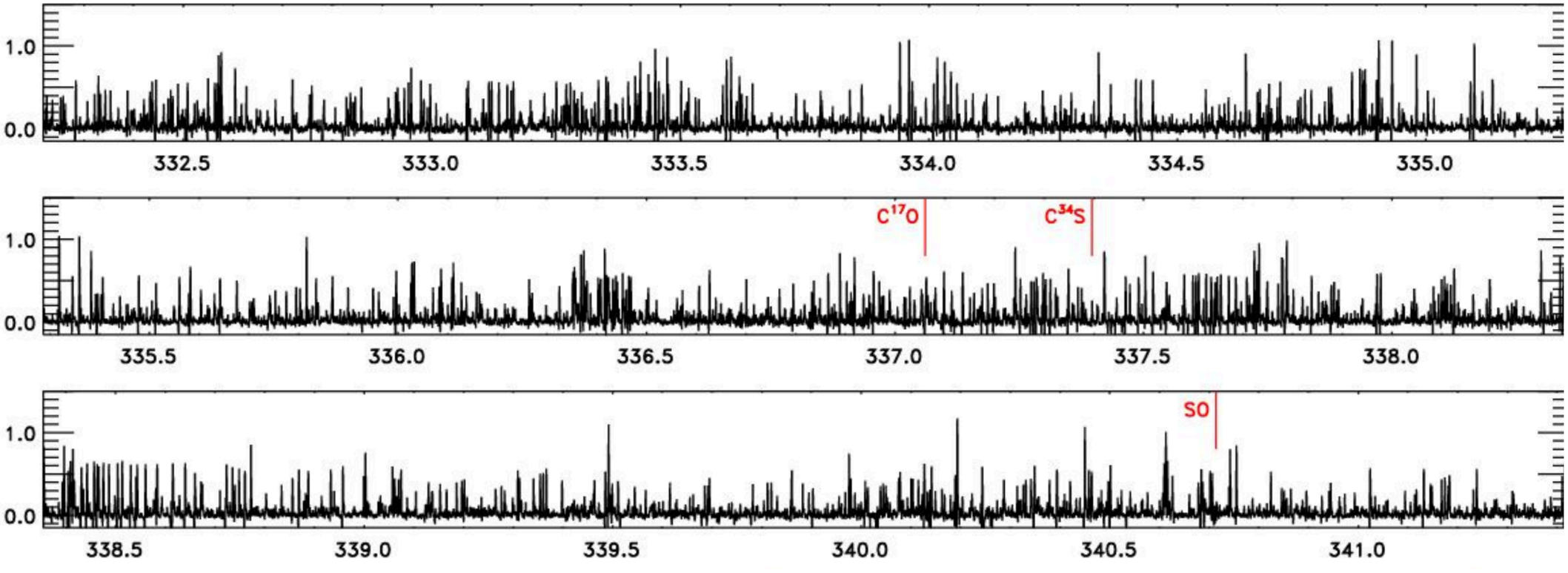

ALMA

Reflector types

Prime focus

Offset Cassegrain

Beam Waveguide

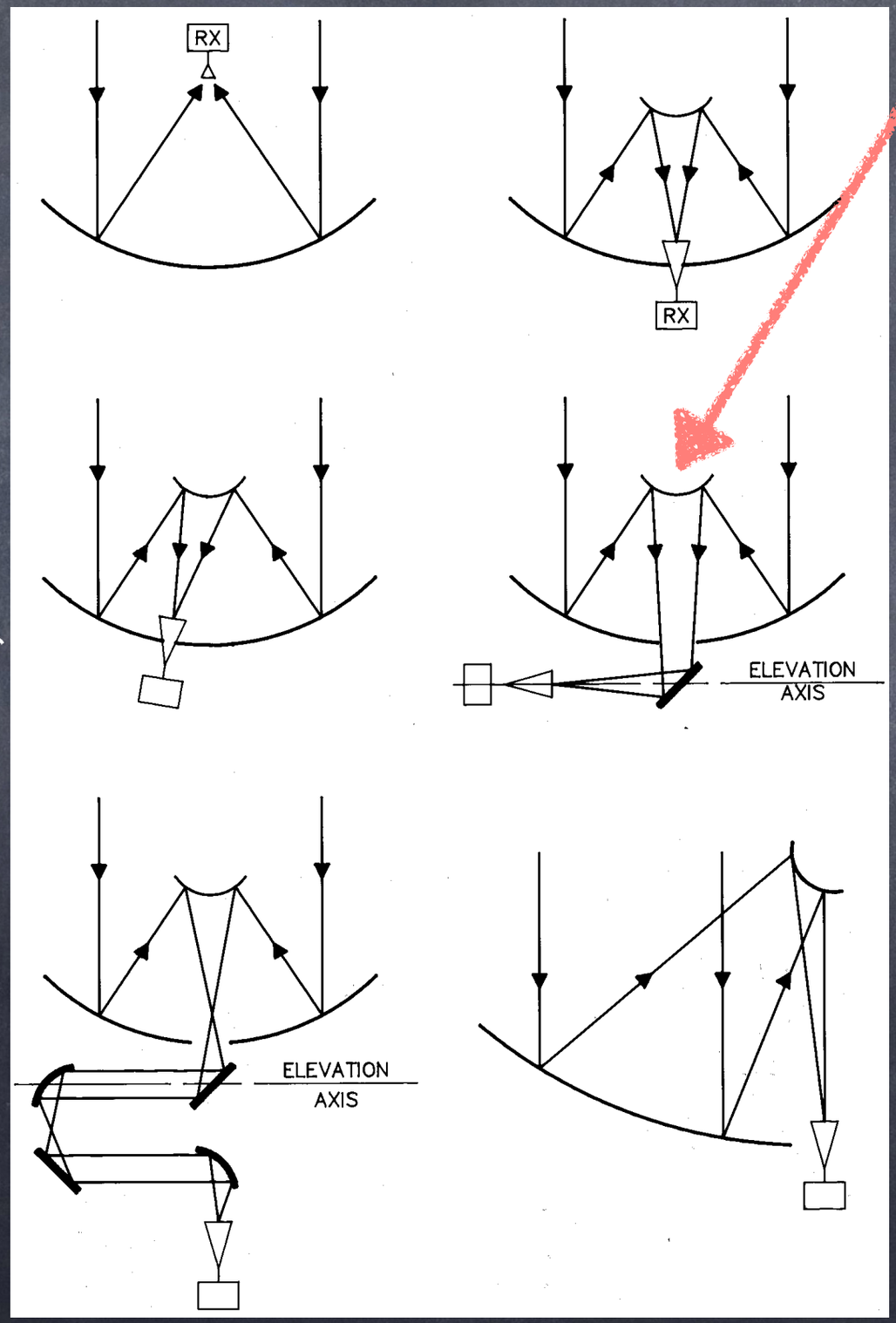

subreflector

Cassegrain focus

Naysmith

Dual Offset

Reflector types

Prime focus
(GMRT)

Cassegrain focus
(Mopra)

Offset Cassegrain
(VLA and ALMA)

Naysmith
(OVRO-CARMA)

Beam Waveguide
(NRO)

Dual
Offset
(ATA, GBT, SKA)

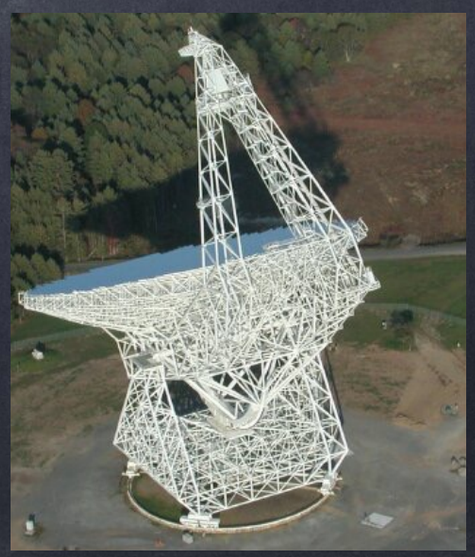

Focus selection

PF: Prime focus

CF: Cassegrain focus

NF: Nasmyth focus

FCF: Folded-Cassegrain focus

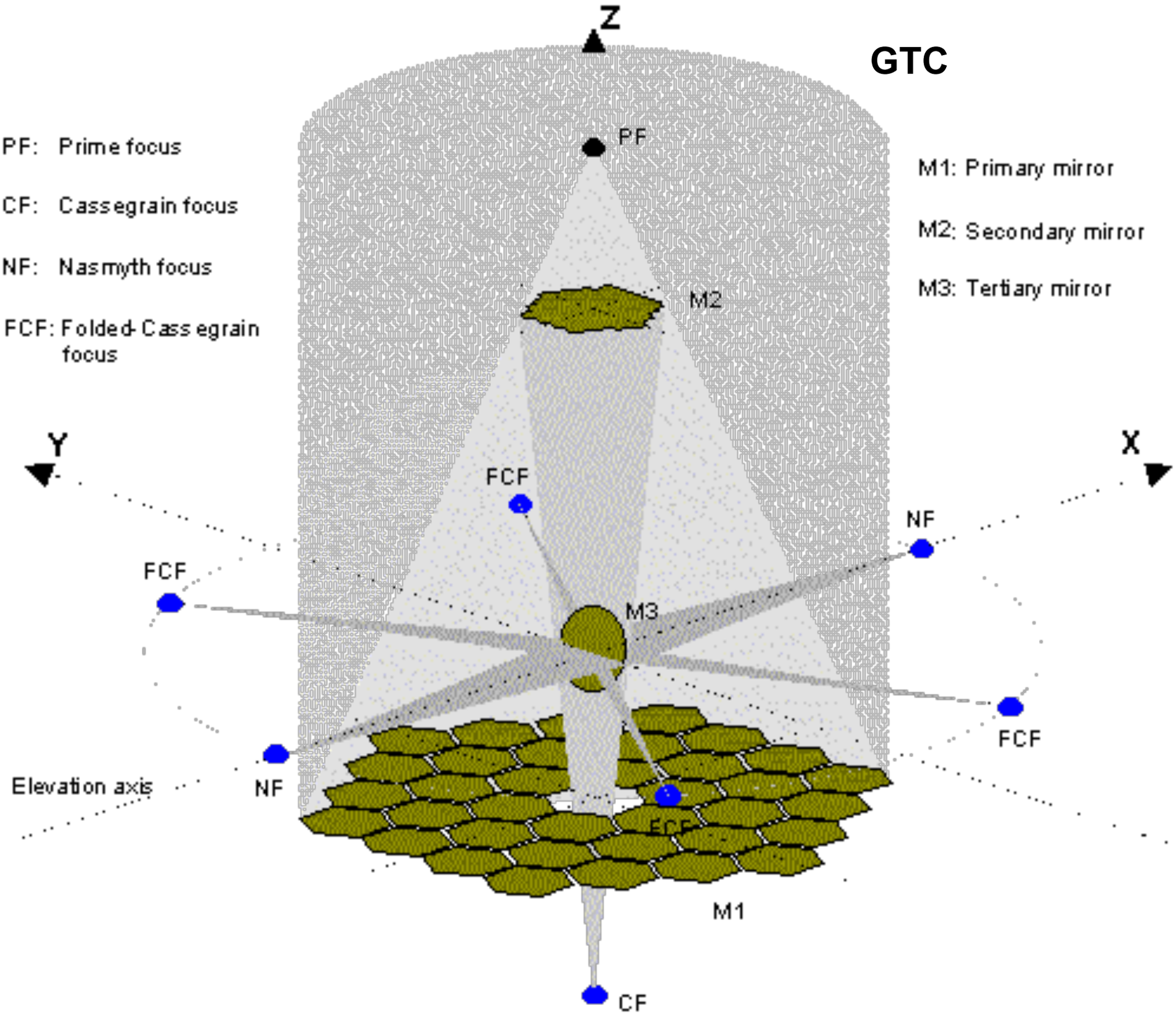

CCD: detectors in the optical & IR

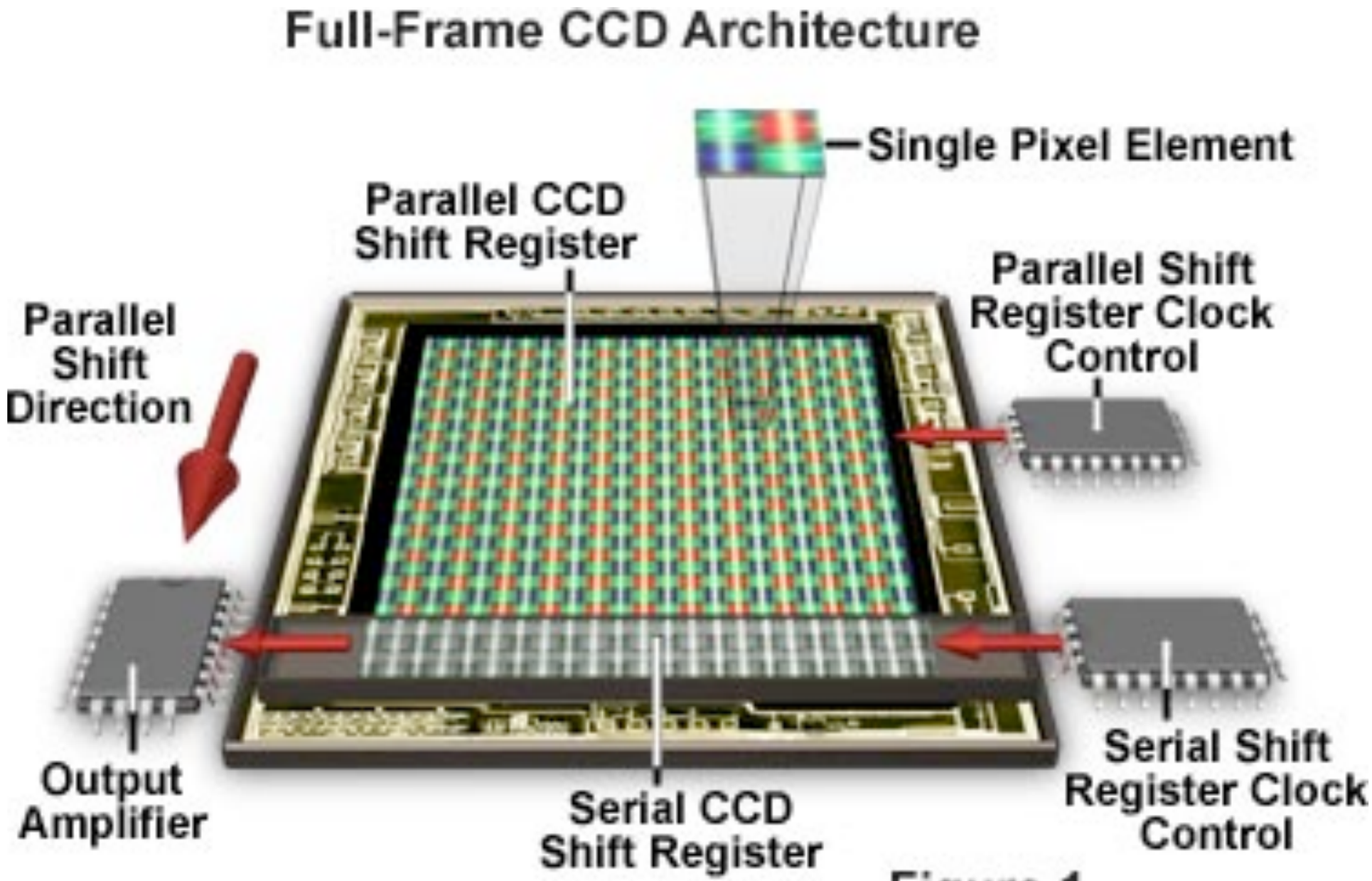

Figure 1

Detectors: radio

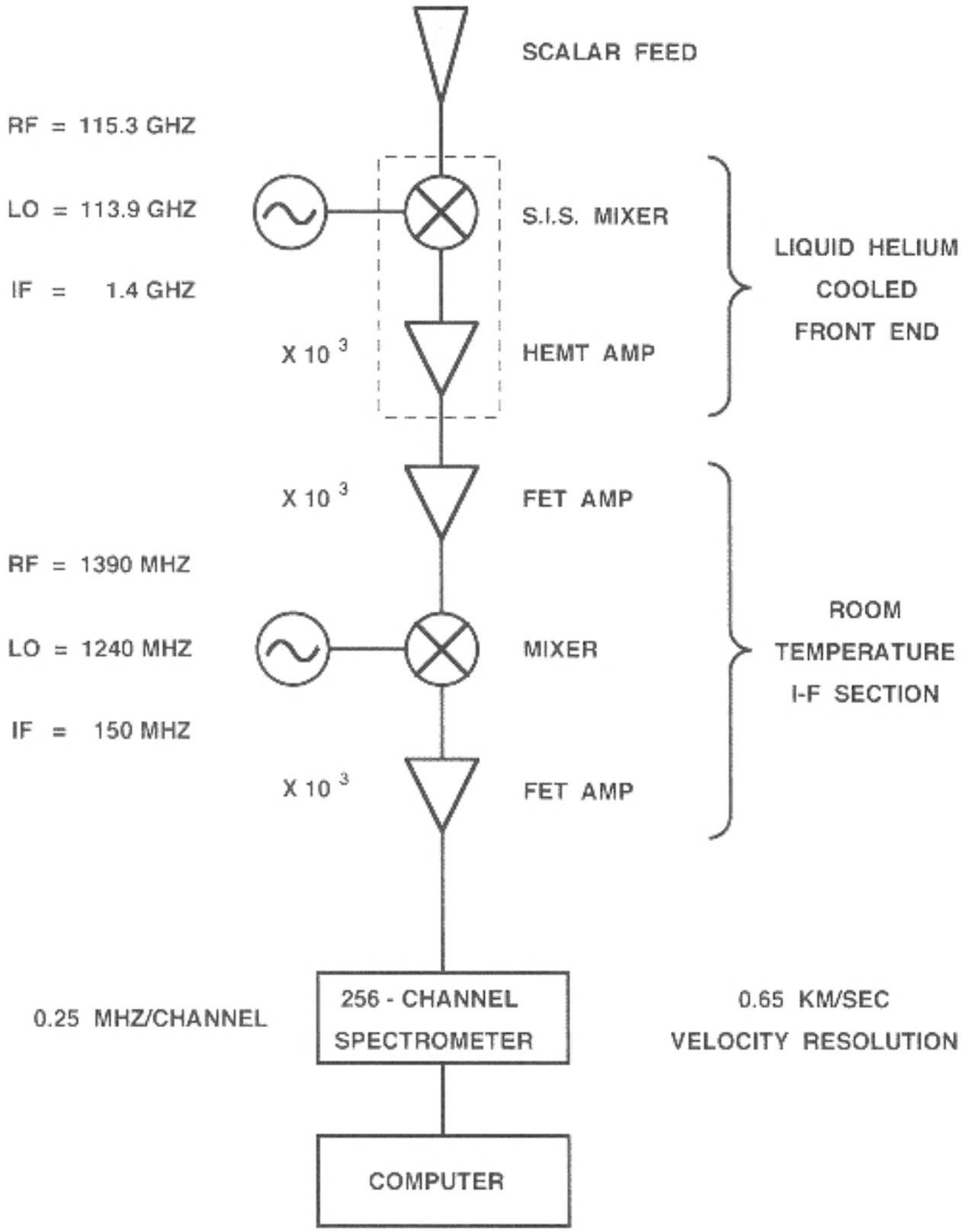

Detectors

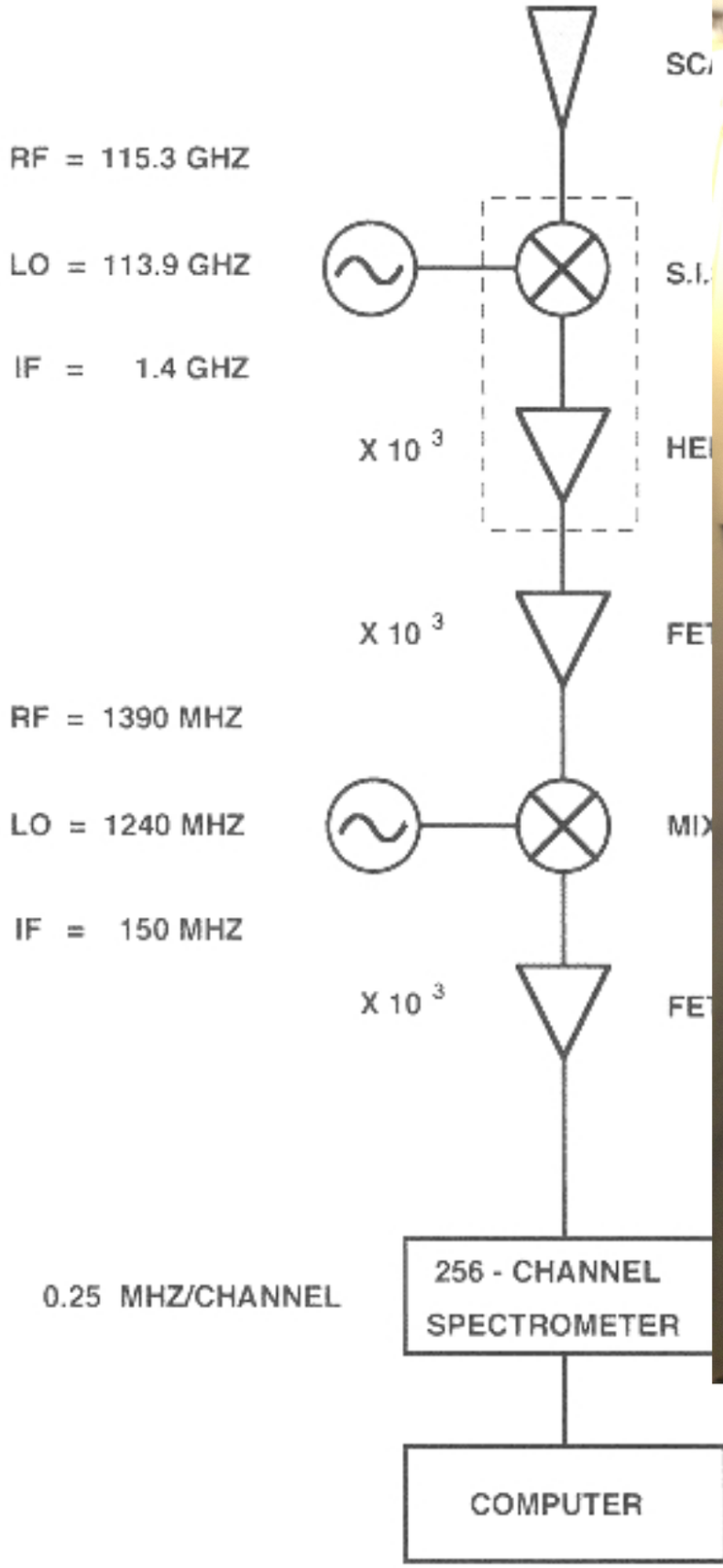
RF = 115.3 GHZ
LO = 113.9 GHZ
IF = 1.4 GHZ
X 10 3
X 10 3
RF = 1390 MHZ
LO = 1240 MHZ
IF = 150 MHZ
X 10 3
0.25 MHZ/CHANNEL
256 - CHANNEL SPECTROMETER
COMPUTER

Detectors for a radio single-dish antenna: bolometers

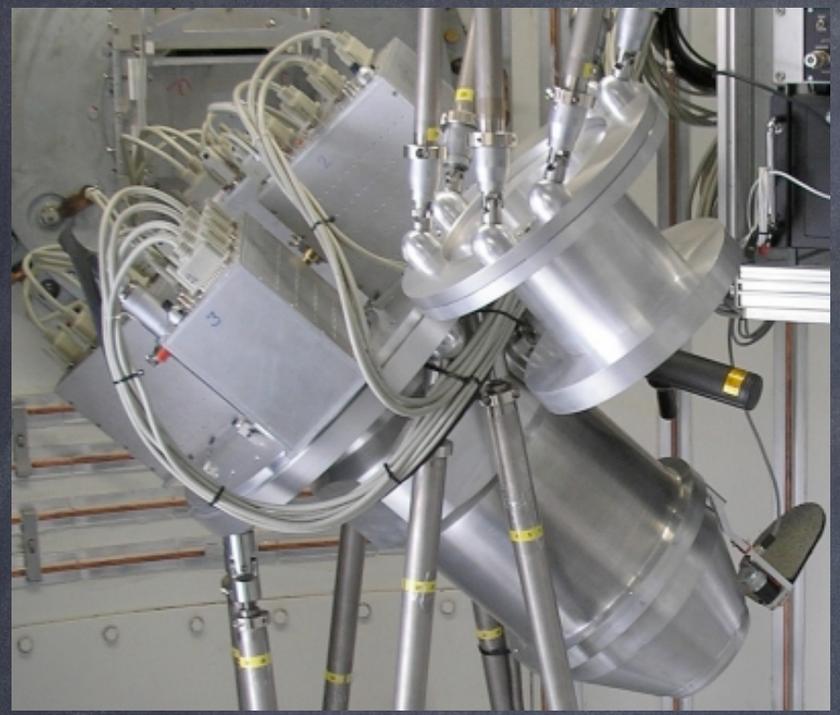

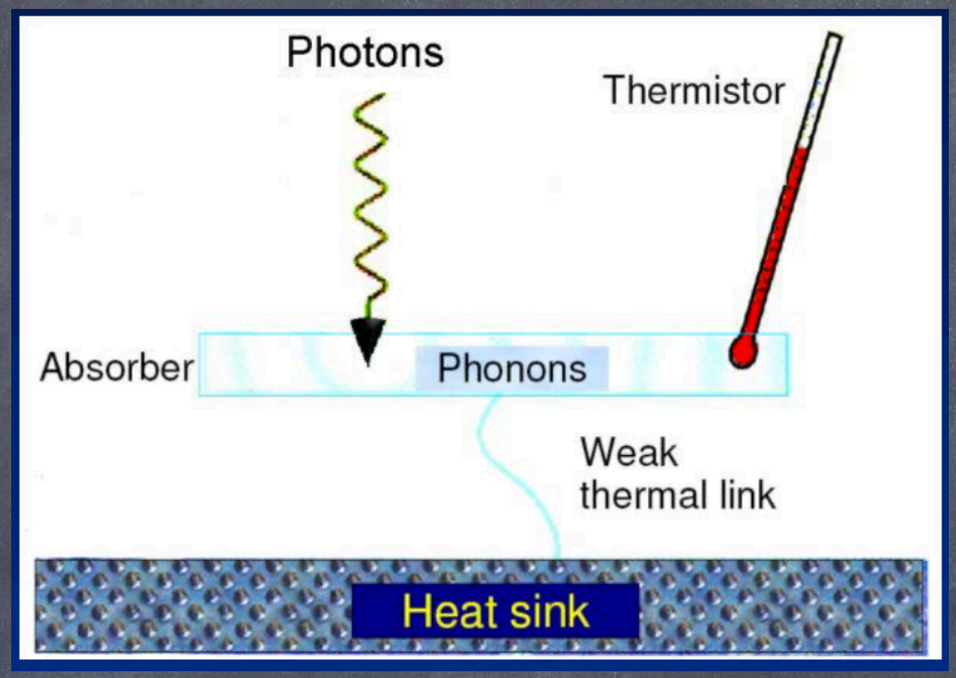

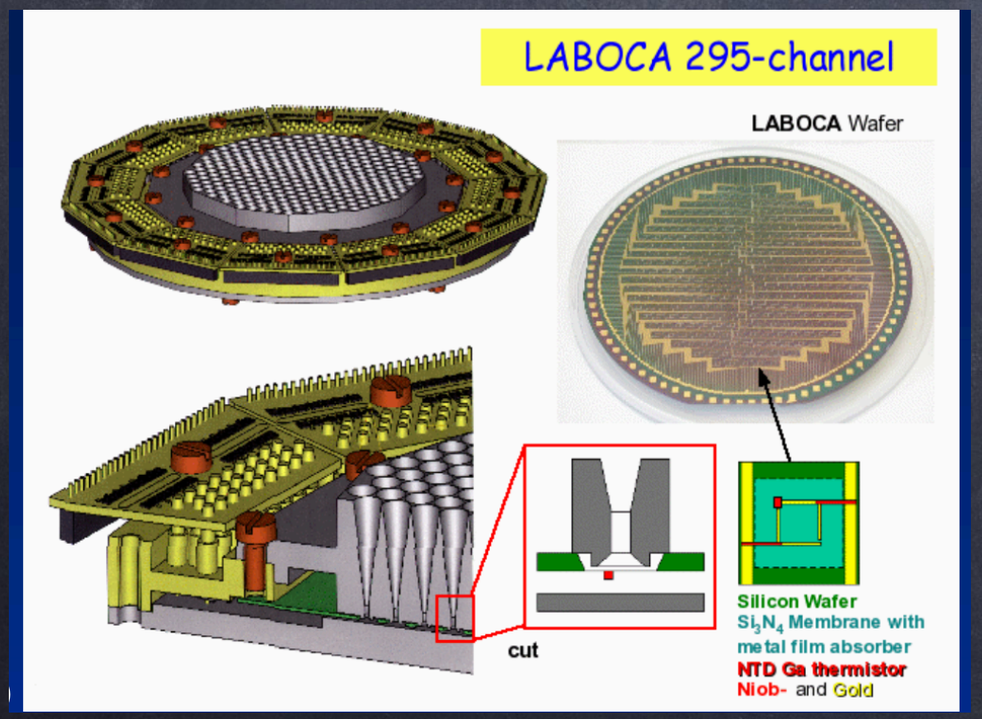

- Bolometers as very sensitive thermometers
- Composite of an absorber and the actual thermometer (thermistor)
- The thermistor transforms the temperature variations of the absorber in electric signals

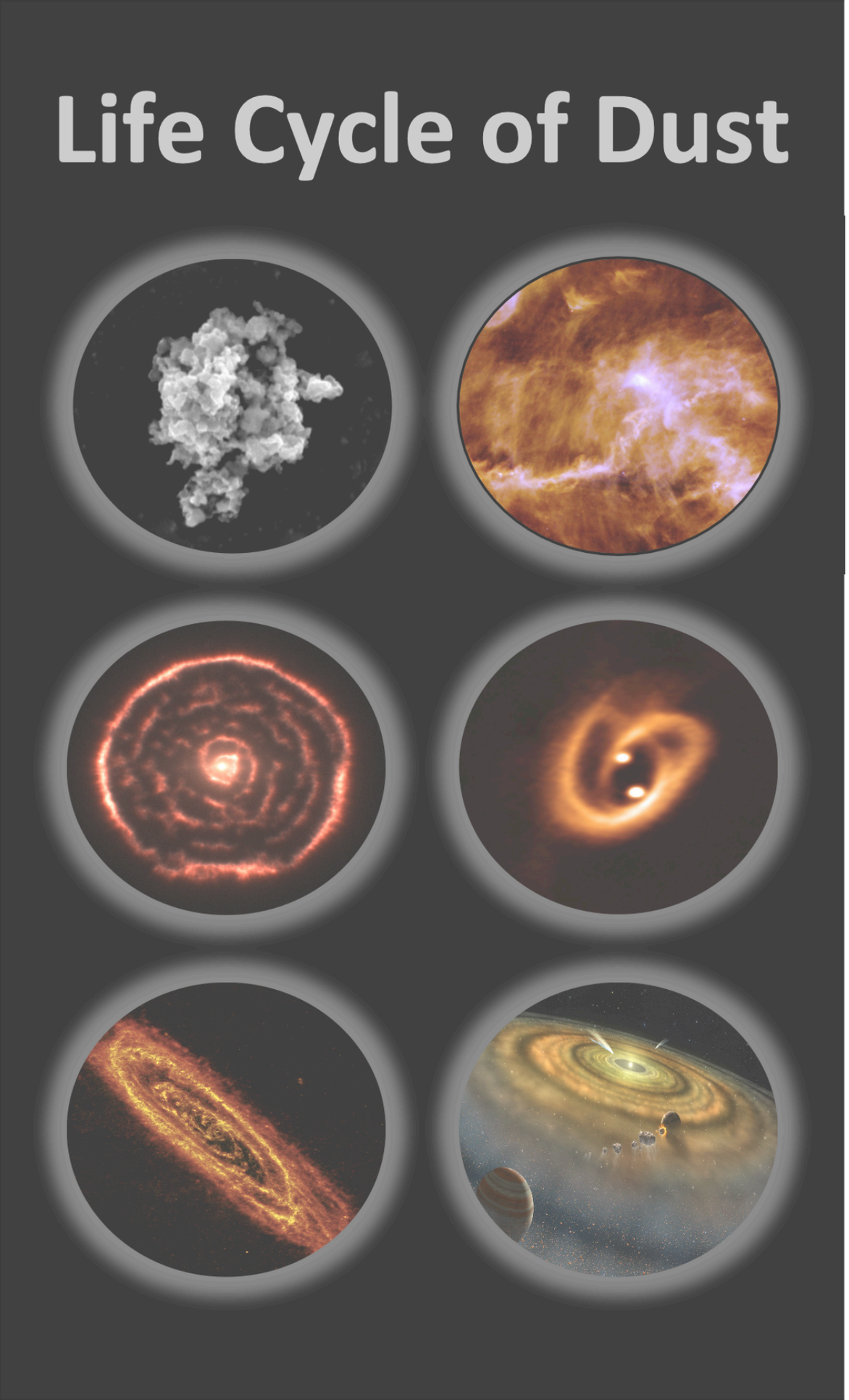

★ Telescope Basics

• Aperture Synthesis Basics

The Stationary, Quasi-Monochromatic Interferometer

- Consider radiation from a small solid angle dΩ, from direction **s**, at frequency ν, within dν :

$$l_{\text{delay}} = b\,sin(\theta)$$

$$\tau_g = b\,sin(\theta)/c$$

Geometric Time Delay

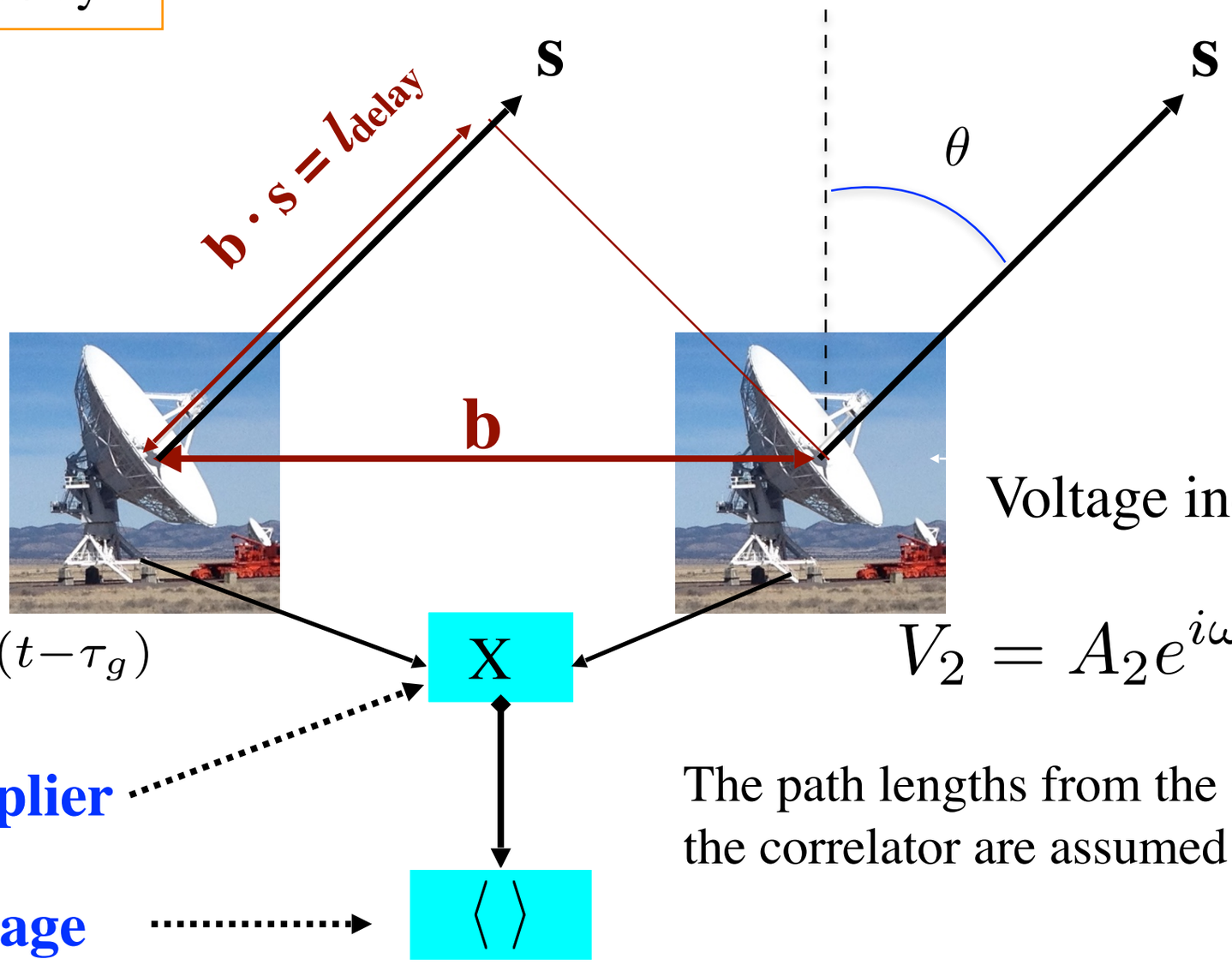

$\omega = 2\pi\nu$

Voltage induced by the signal

$V_1 = A_1 e^{i\omega(t-\tau_g)}$

$V_2 = A_2 e^{i\omega t}$

The path lengths from the antenna to the correlator are assumed equal.

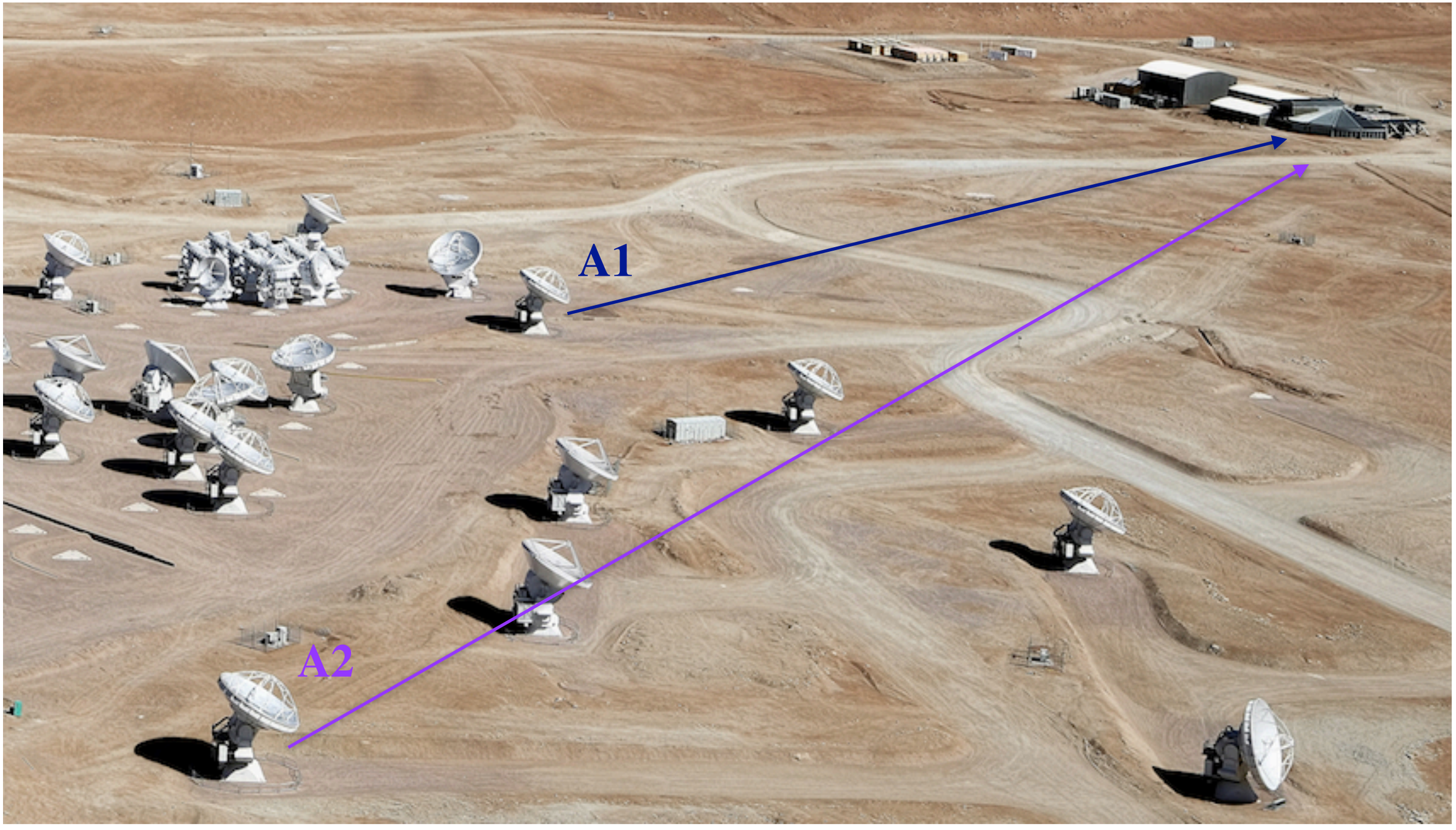

Cable length from A1 and A2 to correlator are different, a time delay correction must be used

The Stationary, Quasi-Monochromatic Interferometer

- Consider radiation from a small solid angle dΩ, from direction **s**, at frequency ν, within dν:

$$l_{\text{delay}} = b\,sin(\theta)$$

$$\tau_g = b\,sin(\theta)/c$$

Geometric Time Delay

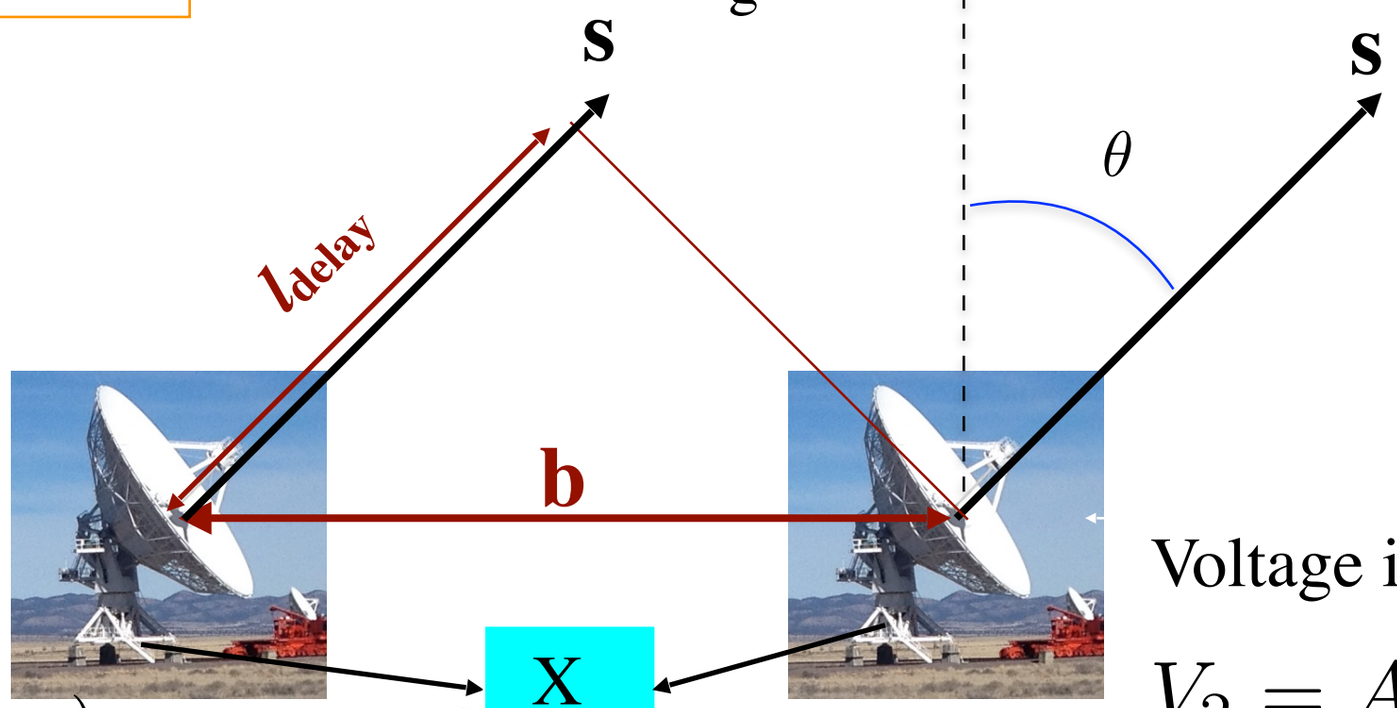

$$V_1 = A_1 e^{i\omega(t-\tau_g)}$$

$$V_2 = A_2 e^{i\omega t}$$

Voltage induced by the signal

multiplier

$$V_1 \cdot V_2^* = A_1 \cdot A_2\, \bar{e}^{i\omega\tau_g}$$

average

$$R_{1,2} = A_1 A_2 \int_{t-T/2}^{t+T/2} \bar{e}^{i\omega\tau_g} dt = A_1 A_2 \frac{\bar{e}^{i\omega\tau_g}}{\omega\tau_g}$$

The path lengths from the antenna to the correlator are assumed equal.

$R_{1,2}=Rc+i\,R_S$

Visibility and Sky Brightness

ALMA

- For small fields of view: the **complex visibility,V(u,v)**, is the **2D Fourier transform** of the brightness on the sky,I(l,m)

$$V(u,v) = \int\int I(l,m) e^{-2\pi i(ul+vm)} dl dm$$

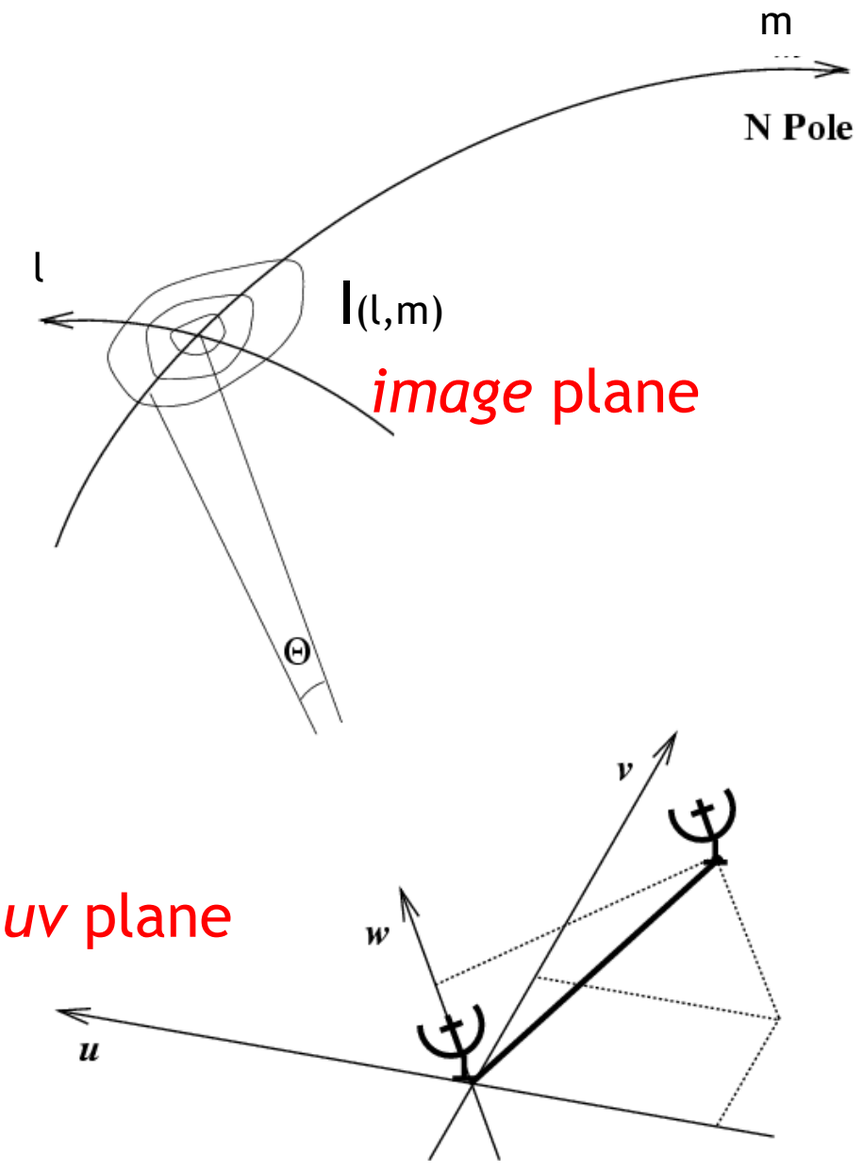

- We can now rely on a century of effort by mathematicians on how to invert this equation, and how much information we need to obtain an image of sufficient quality. Formally, **with enough measures of V, we can derive an estimate of I.**

$$I(l,m) = \int\int V(u,v) e^{2\pi i(ul+vm)} du dv$$

NRAO

2D Fourier Transforms

(from Summer School lecture by D. Wilner)

T(x,y)

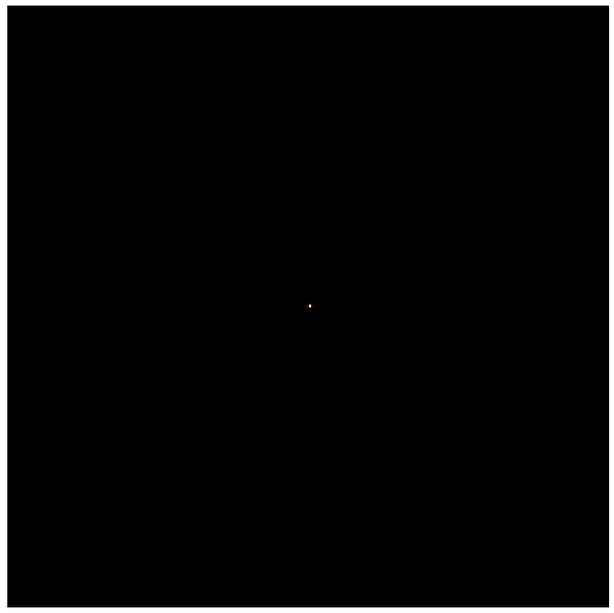

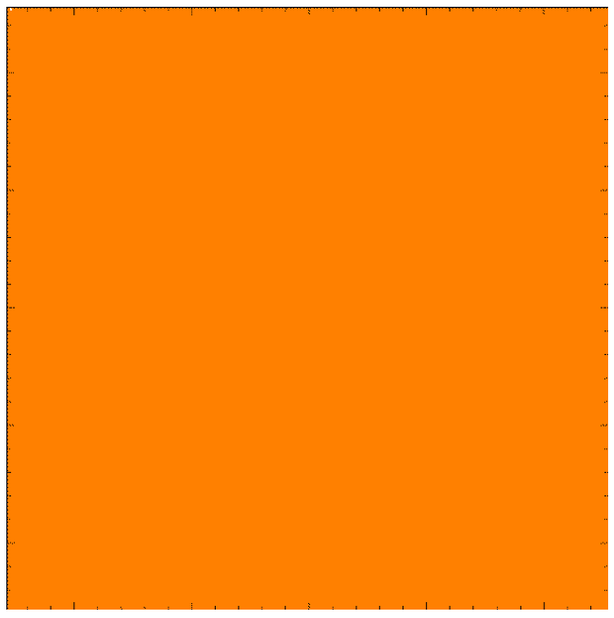

Amp{V(u,v)}

δ Function

Constant

Gaussian

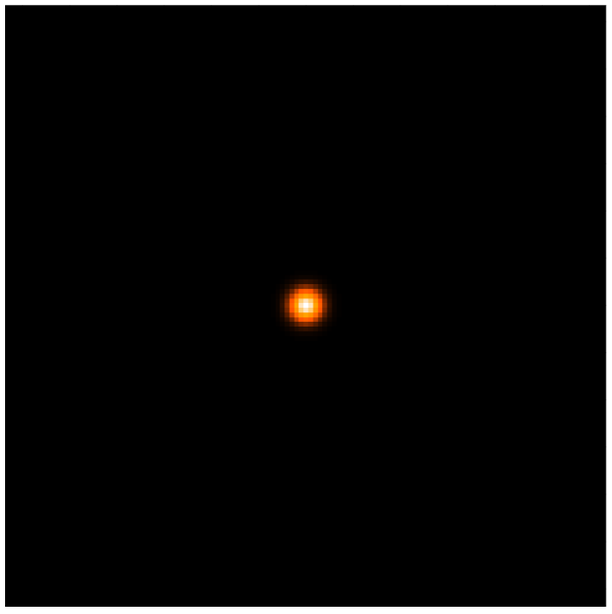

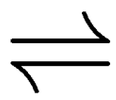

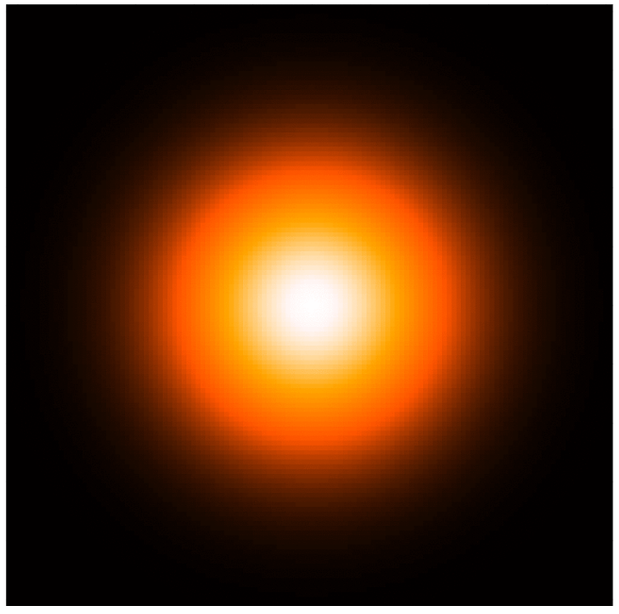

Gaussian

narrow features transform to wide features (and vice-versa)

2D Fourier Transforms

ALMA

T(x,y)

elliptical Gaussian

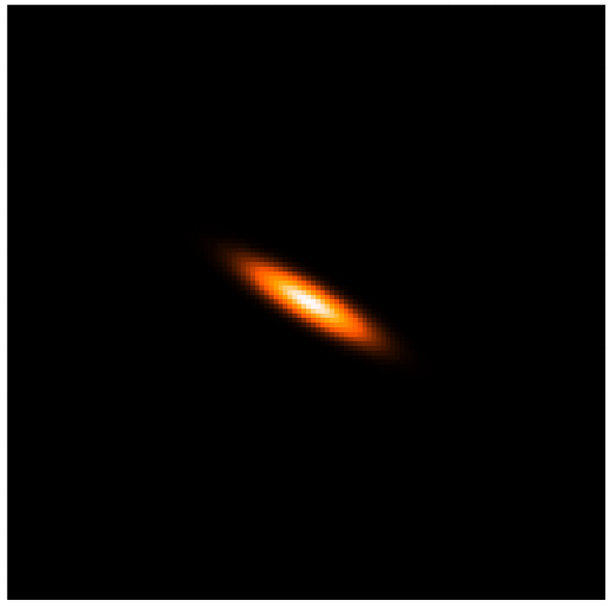

⇌

Amp{V(u,v)}

elliptical Gaussian

Disk

⇌

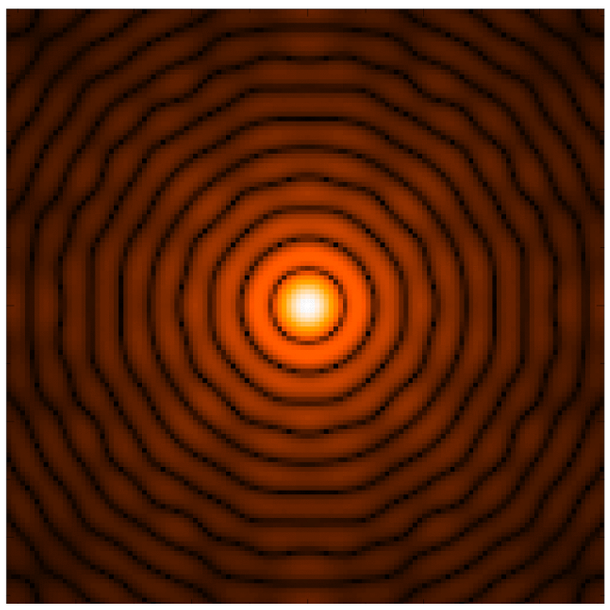

Bessel

sharp edges result in many high spatial frequencies

Visibility: Amplitude and Phase

ALMA

T(x,y) Amp{V(u,v)} Pha{V(u,v)}

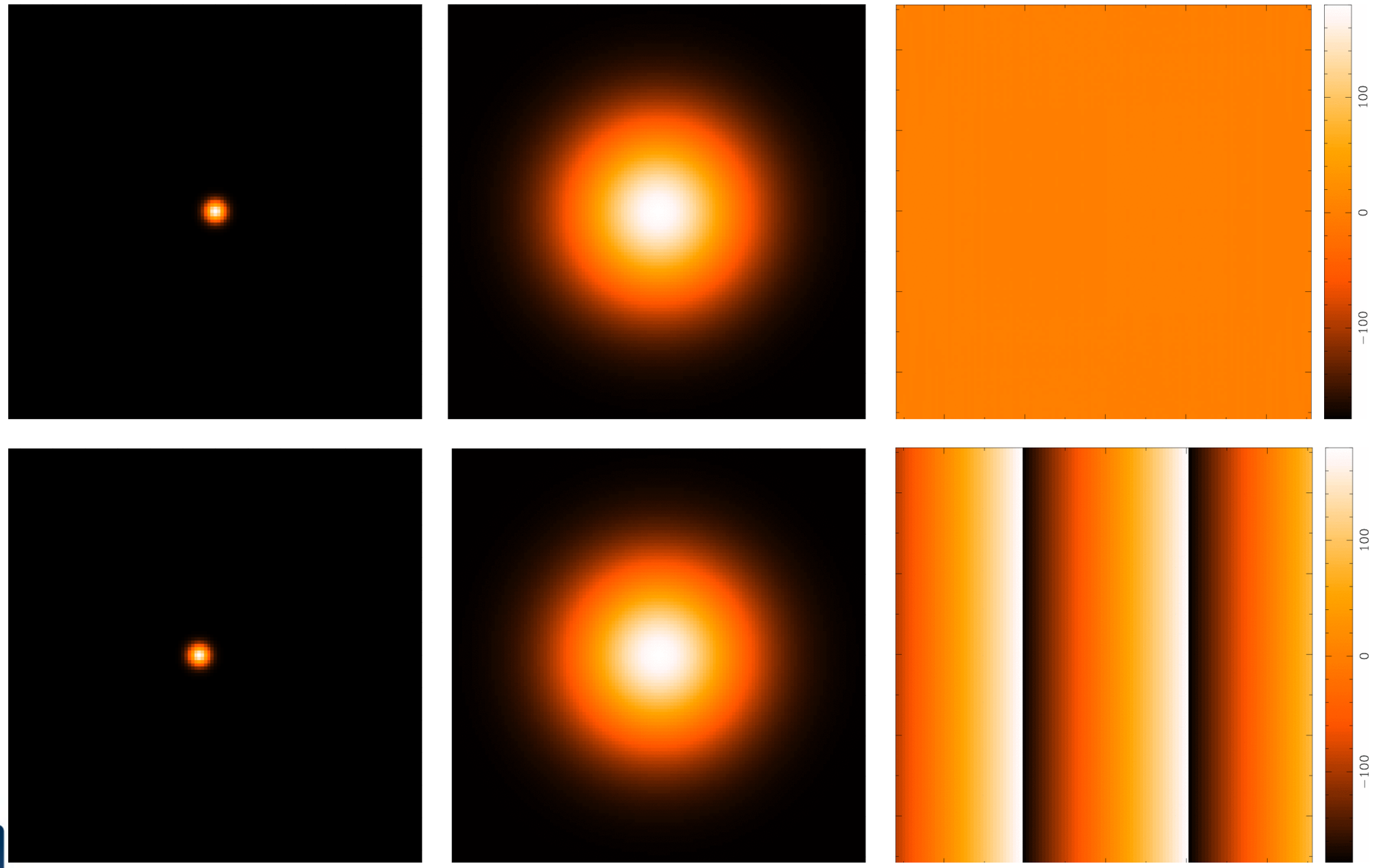

Aperture Synthesis

- **Example: 5 moveable antennas of the VLA- Let's assume are in a East-West configuration.**

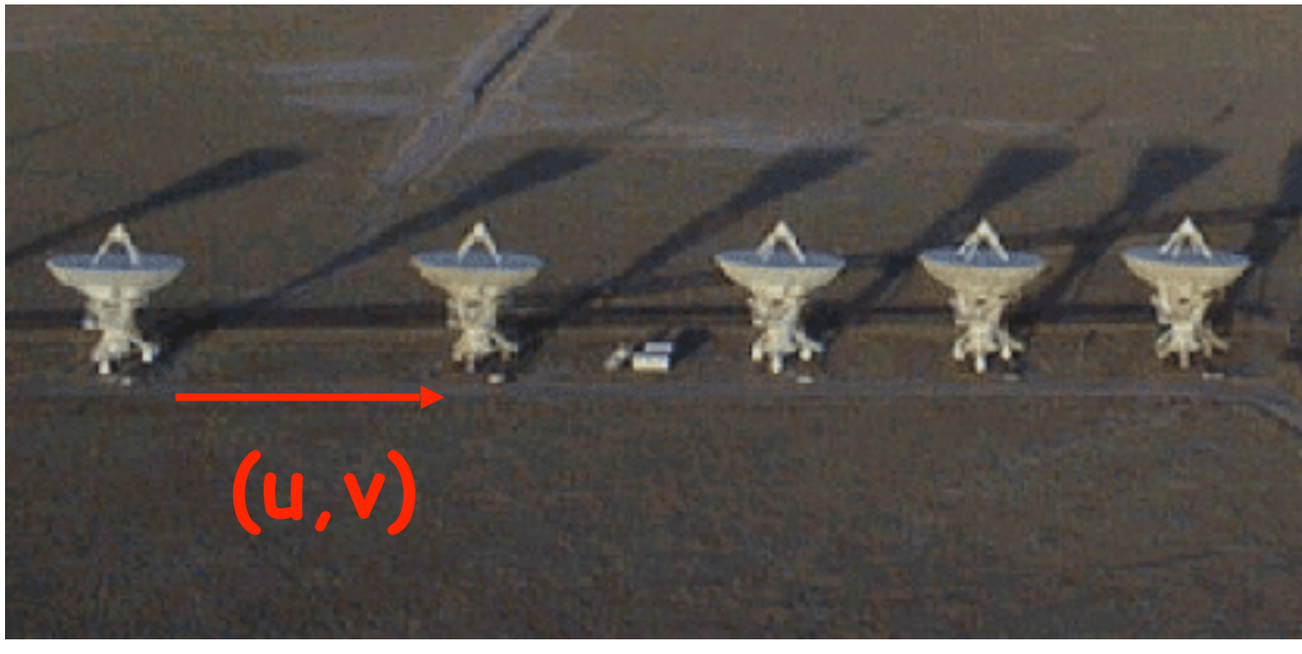

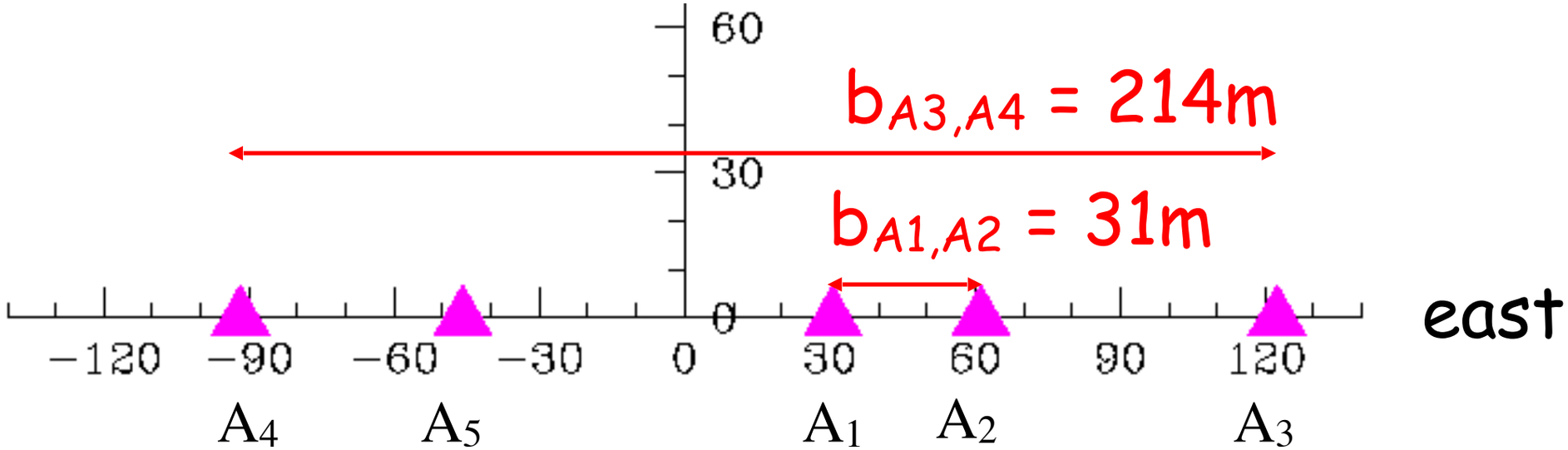

Aperture Synthesis

Number of baselines for N antennas:

$$\frac{N\,(N-1)}{2}$$

- Instantaneous (u,v) coverage near transit

- 10 baselines ranging from 31m to 214m
  ⇒ 9.1 to 63 kλ at 88 GHz (3.41mm)

- 10 baselines, 20 (u,v) points, why??:

- Visibility is a Hermitian function:
  V(u,v) =V(-u,-v)*

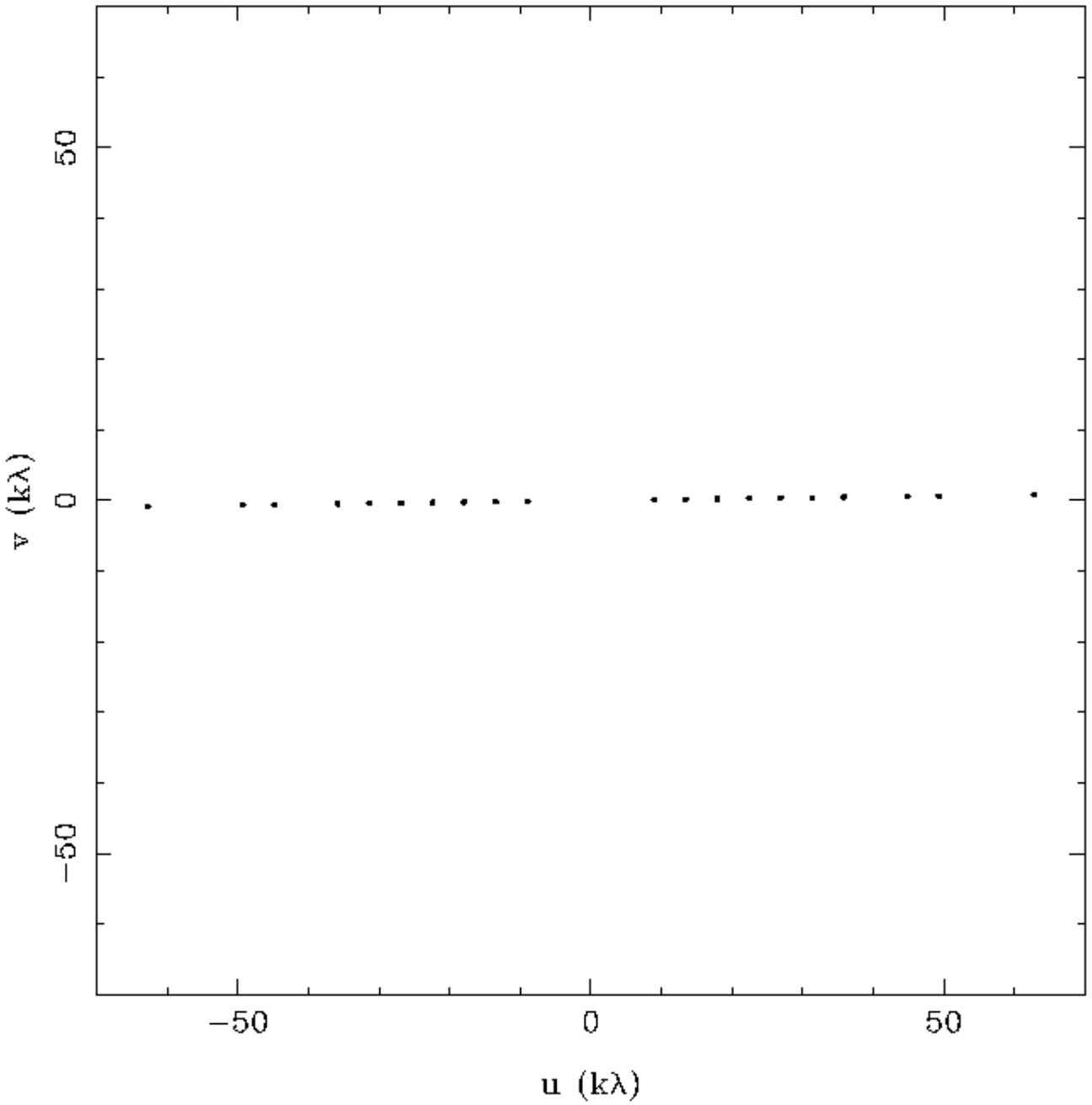

Aperture Synthesis

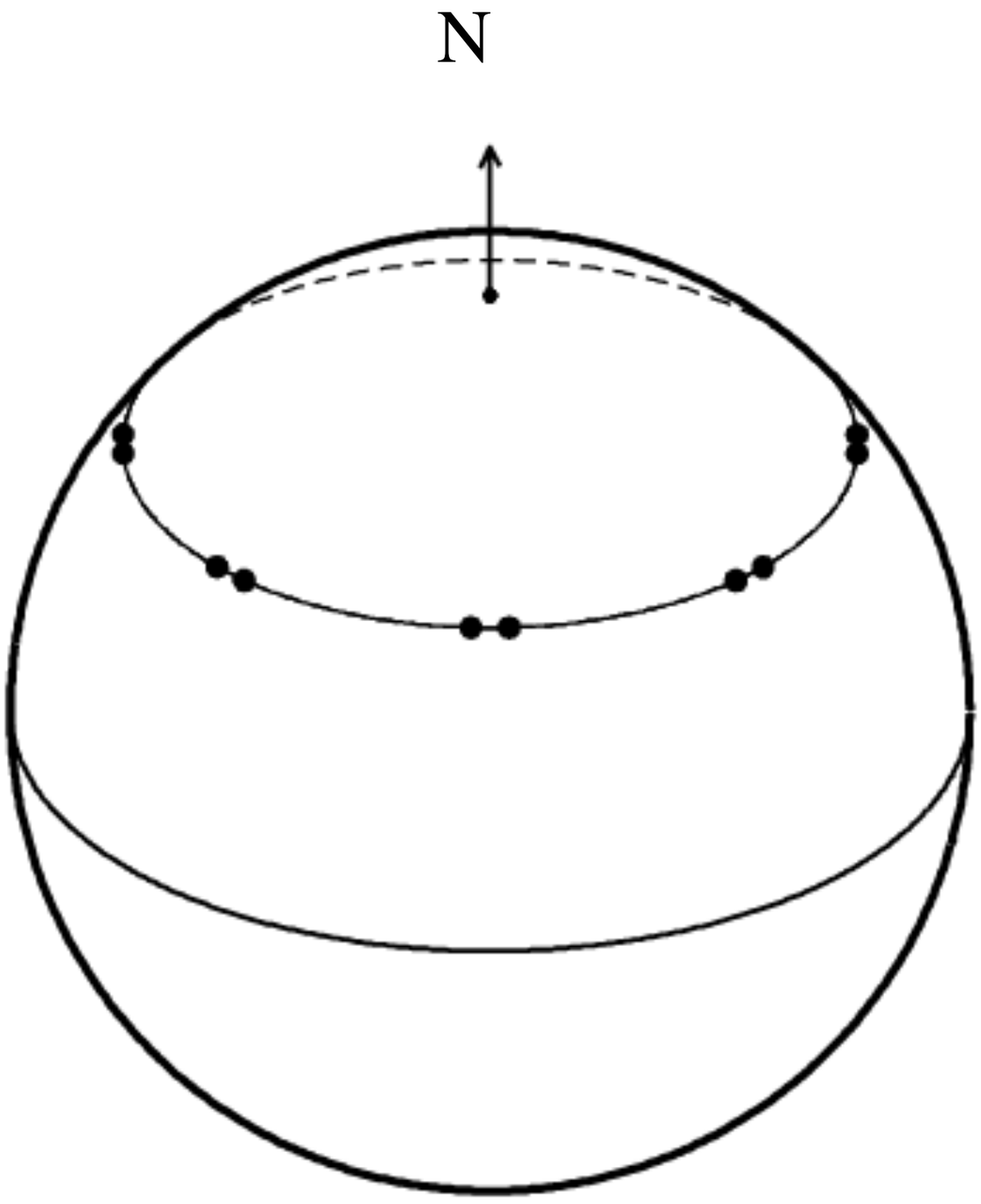

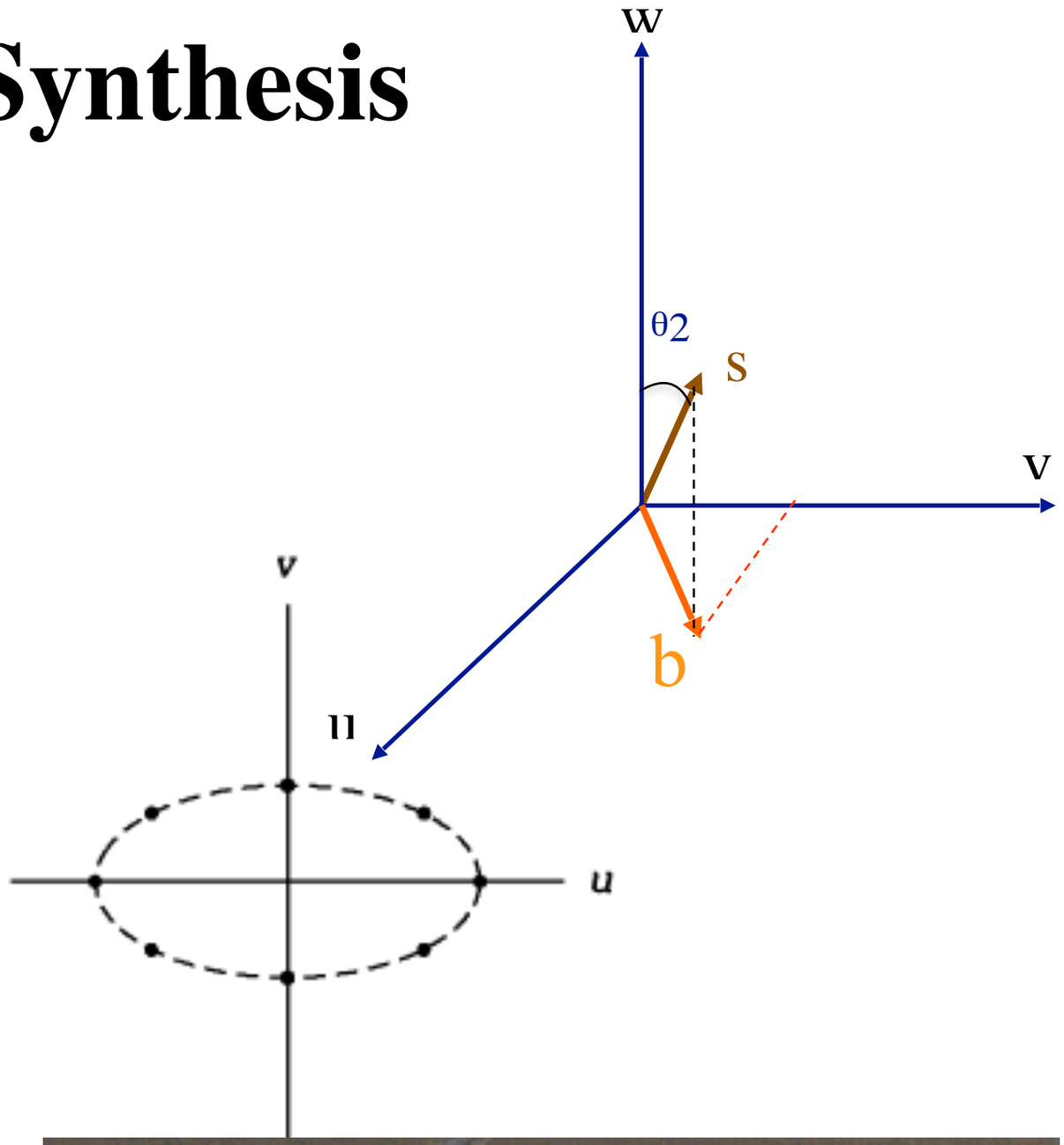

Two antennas seen from the source

Earth Rotation Aperture Synthesis!

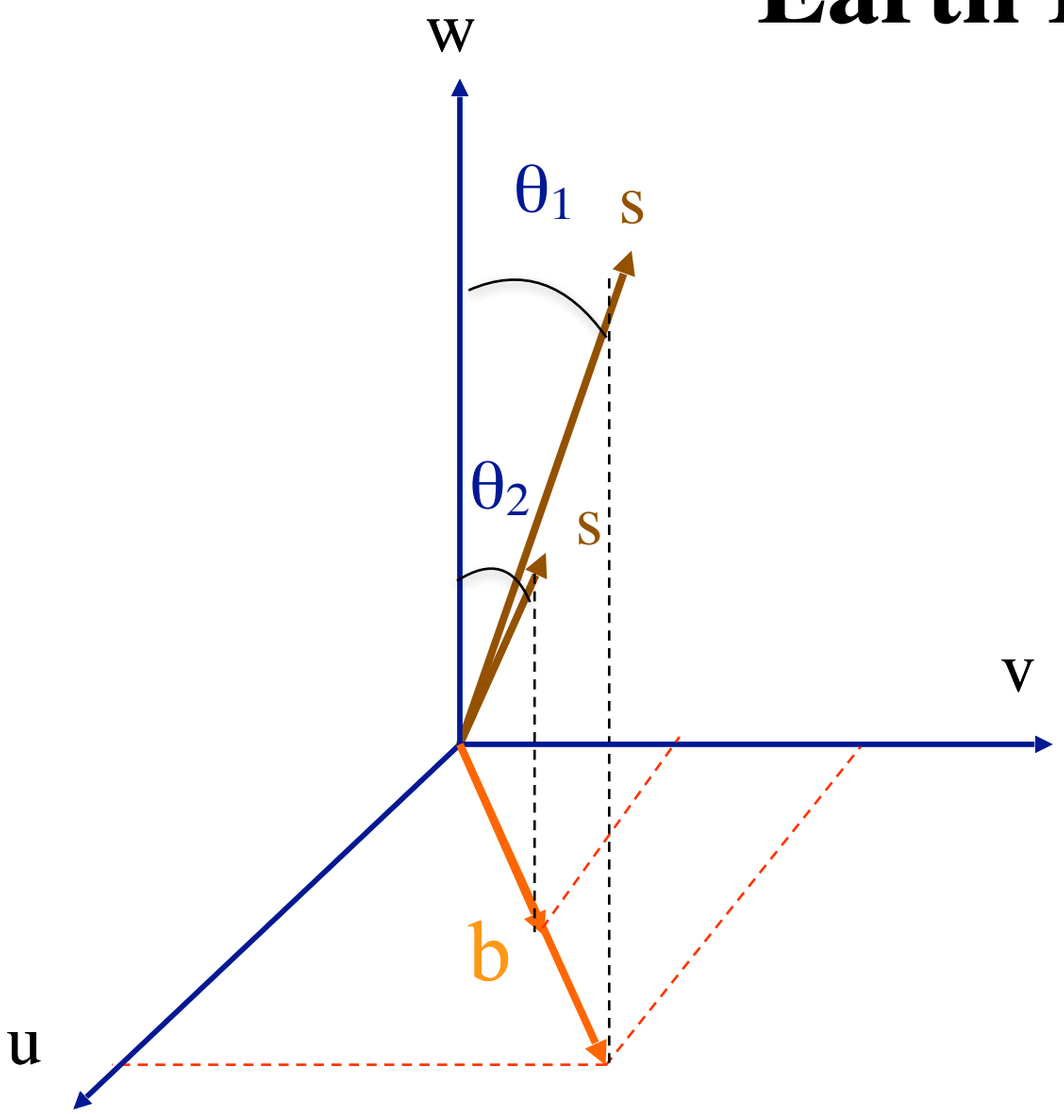

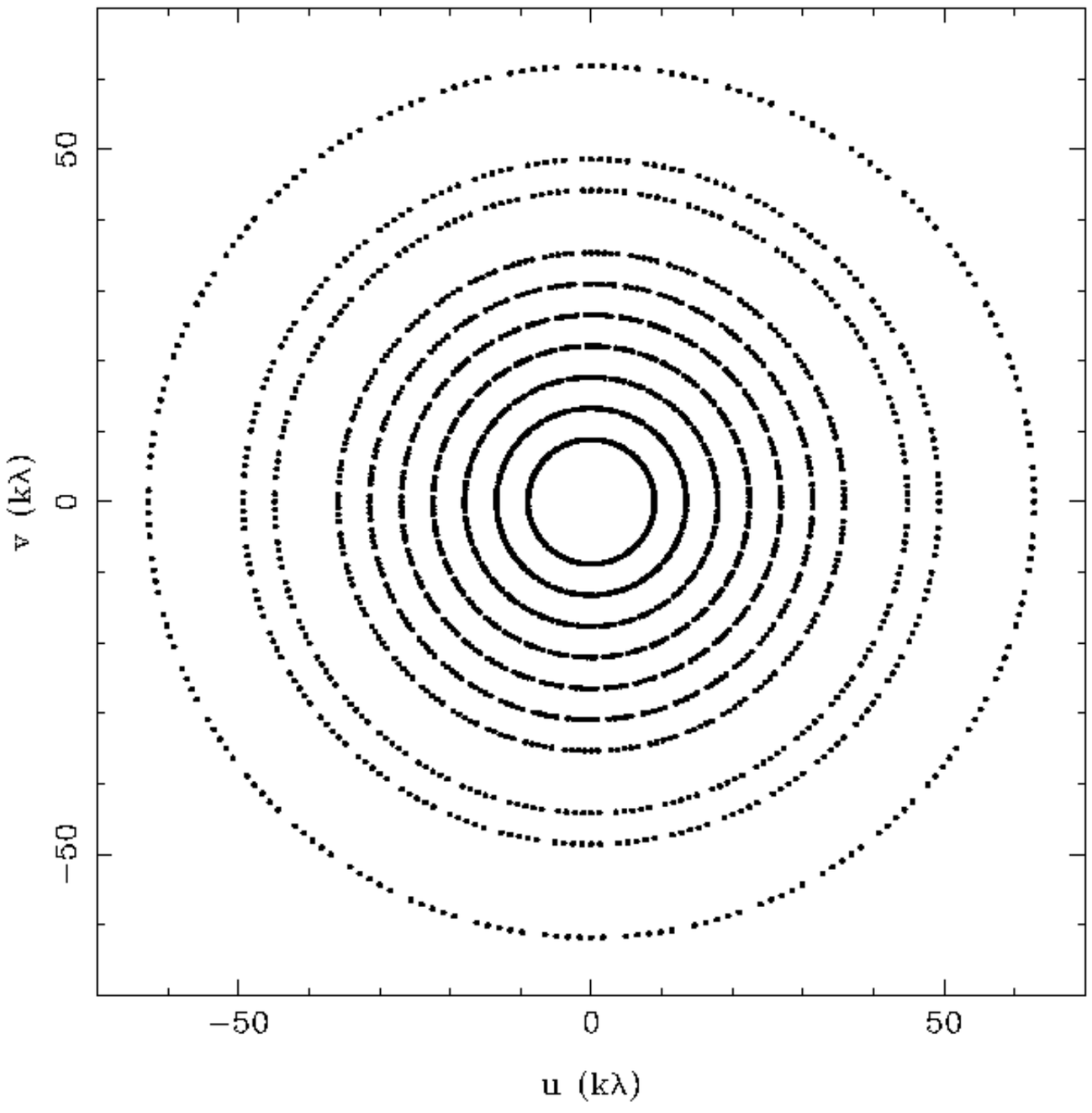

- (u,v) coverage for full 12 hour observation at declination 80º.

UV plane sampling

- For small fields of view, the visibility function is the 2-D Fourier transform of the sky brightness:

$$V(u,v) = \int\int I(l,m) e^{-2\pi i(ul+vm)} dl dm$$

- We sample the Fourier plane at a discrete number of points:

$$S(u,v) = \sum_k \delta(u-u_k)\cdot\delta(v-v_k)$$

- So the inverse transform is:

$$I^D(x,y) = F^{-1}\left[S(u,v)\cdot V(u,v)\right]$$

- Applying the Fourier convolution theorem:

$$I^D(x,y) = B(x,y)\otimes I(x,y)$$

- where B is the point spread function:

$$B(x,y) = F^{-1}\left[S(u,v)\right]$$

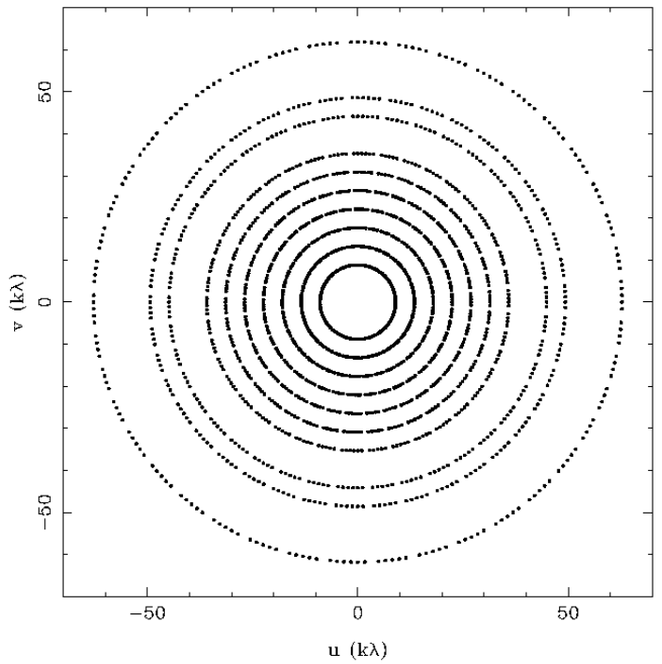

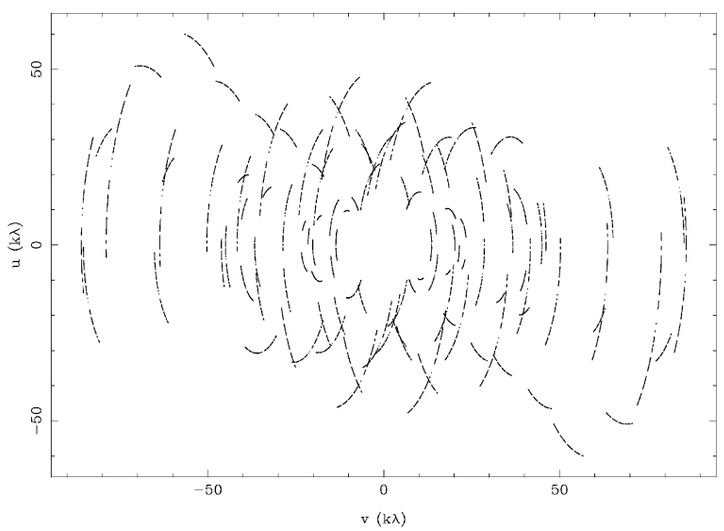

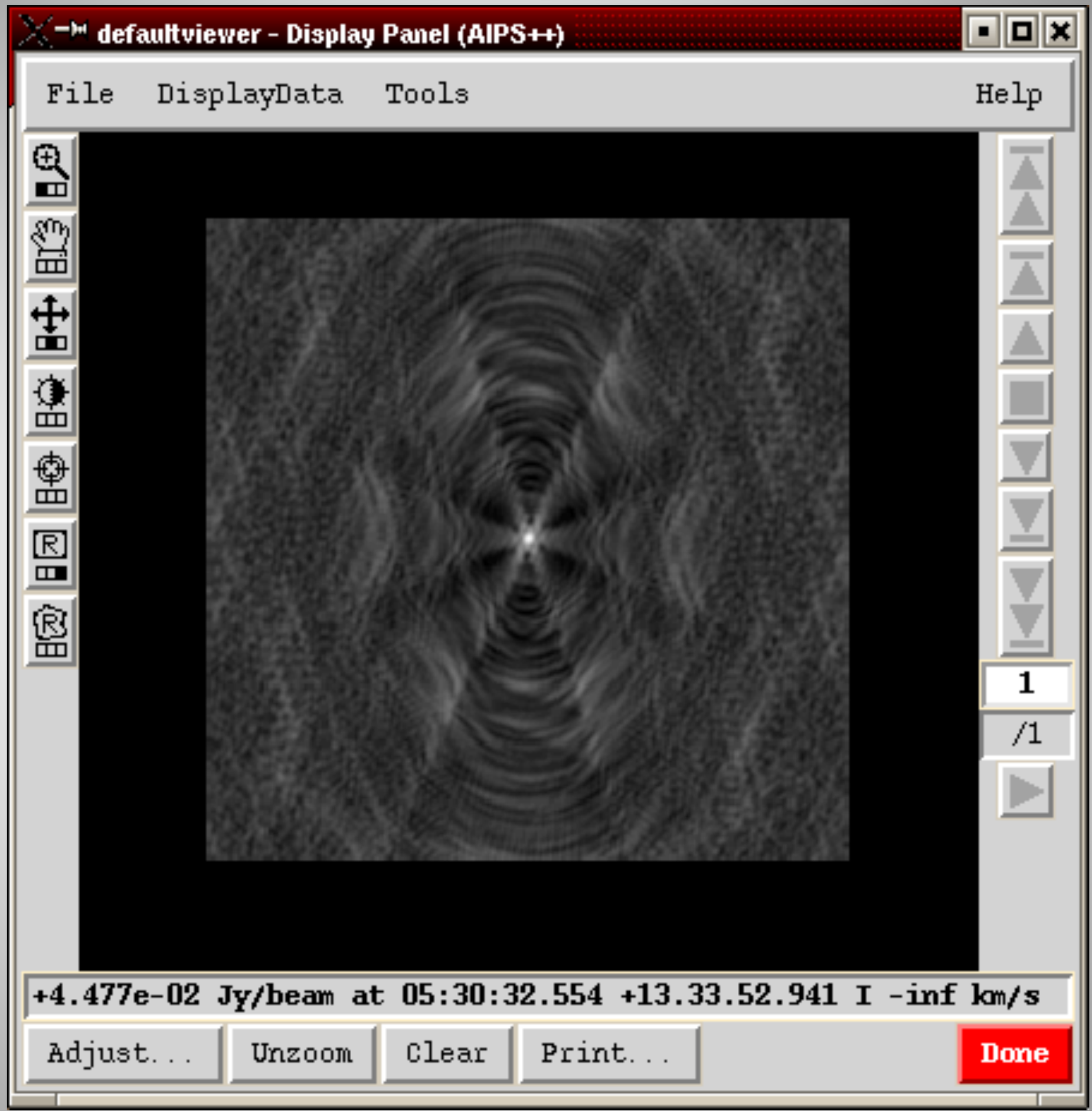
defaultviewer - Display Panel (AIPS++)
File
DisplayData
Tools
Help
1
/1
+4.477e-02 Jy/beam at 05:30:32.554 +13.33.52.941 I -inf km/s
Adjust...
Unzoom
Clear
Print...
Done

Aperture Synthesis

- **Simulated (u,v) coverage for a single dish telescope of diameter 200m.**

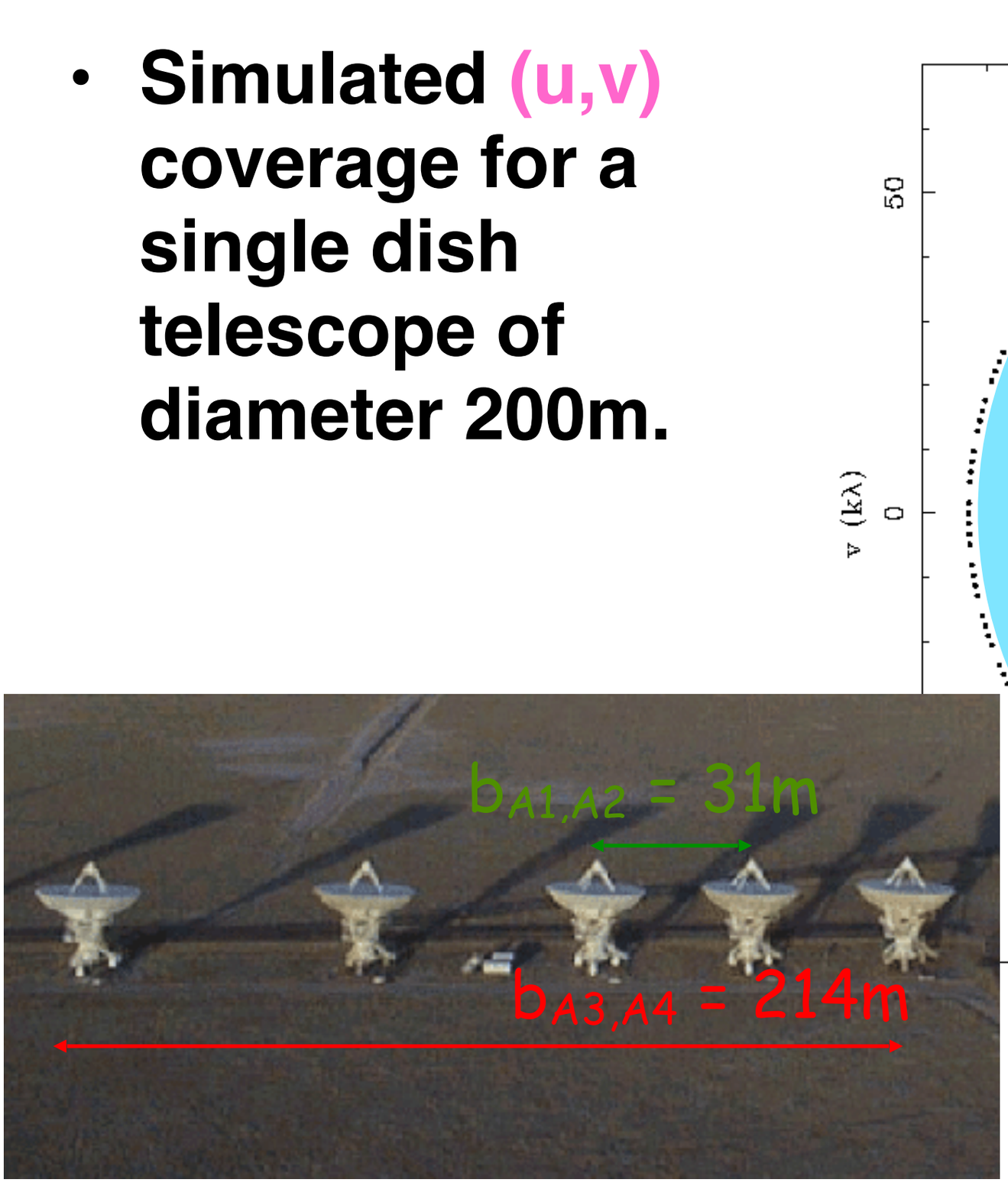

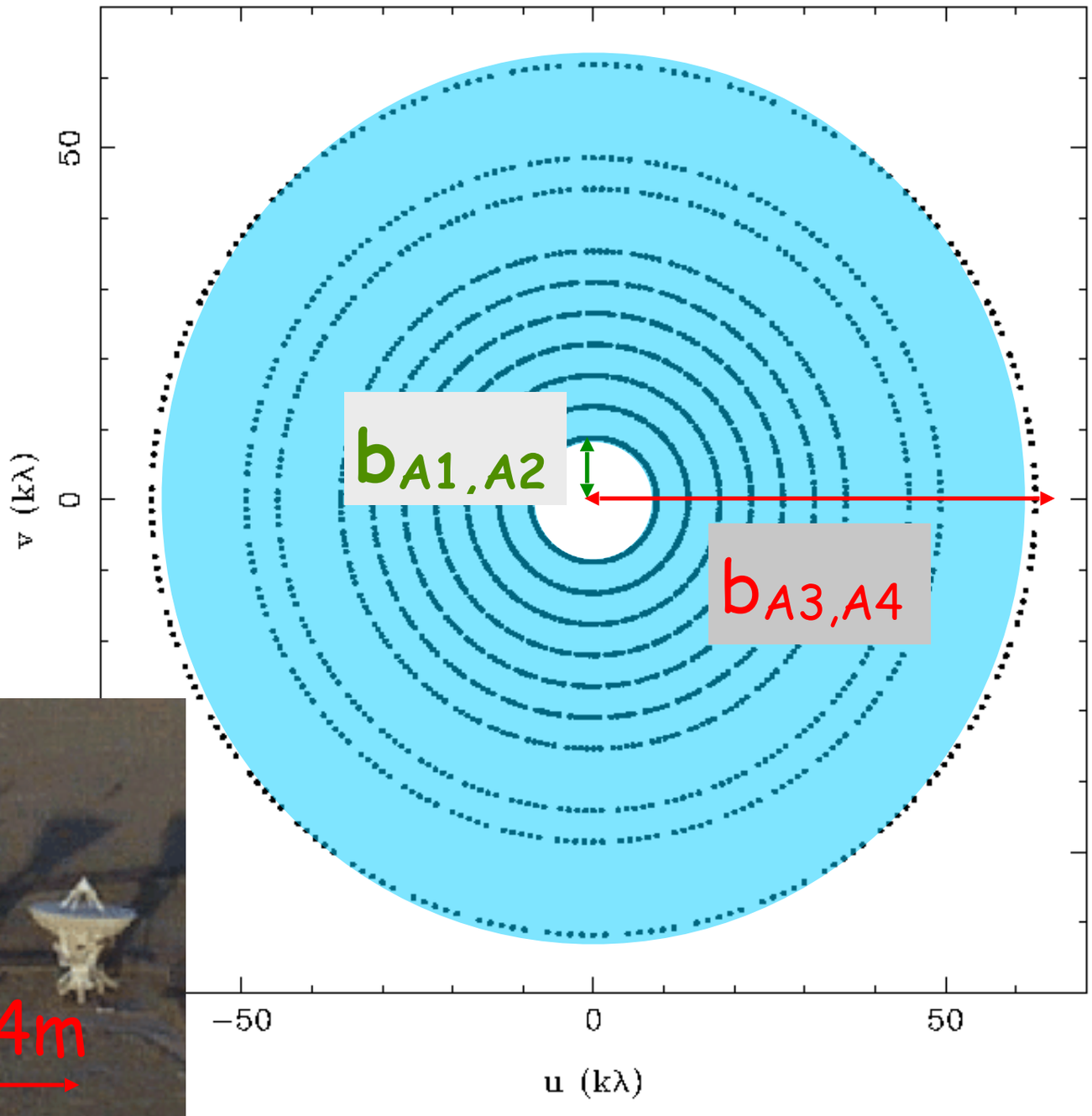

Response of an aperture synthesis telescope for two Gaussian-like astronomical objects

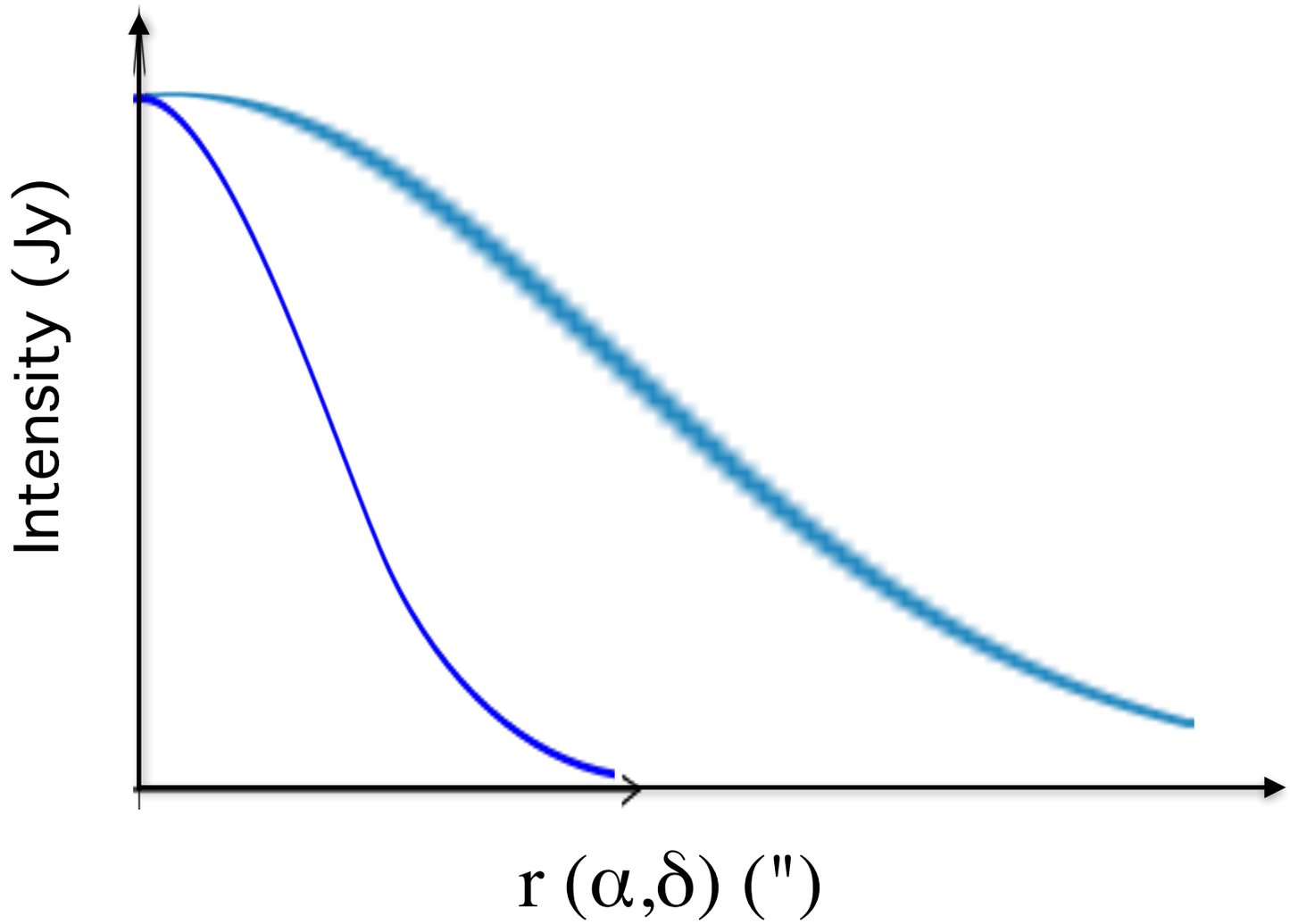

Response of an aperture synthesis telescope for two Gaussian-like astronomical objects

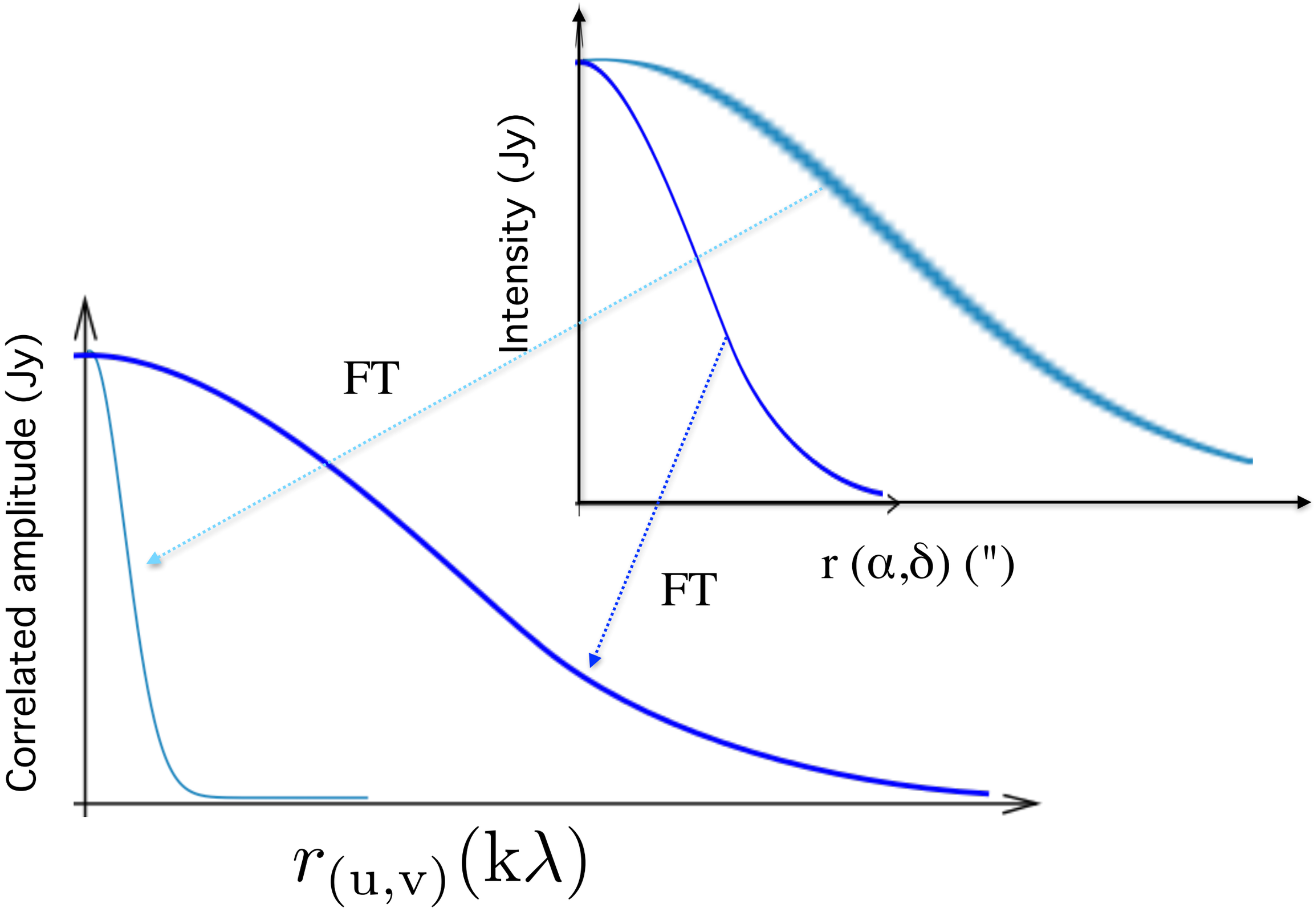

Response of an aperture synthesis telescope for two Gaussian-like astronomical objects

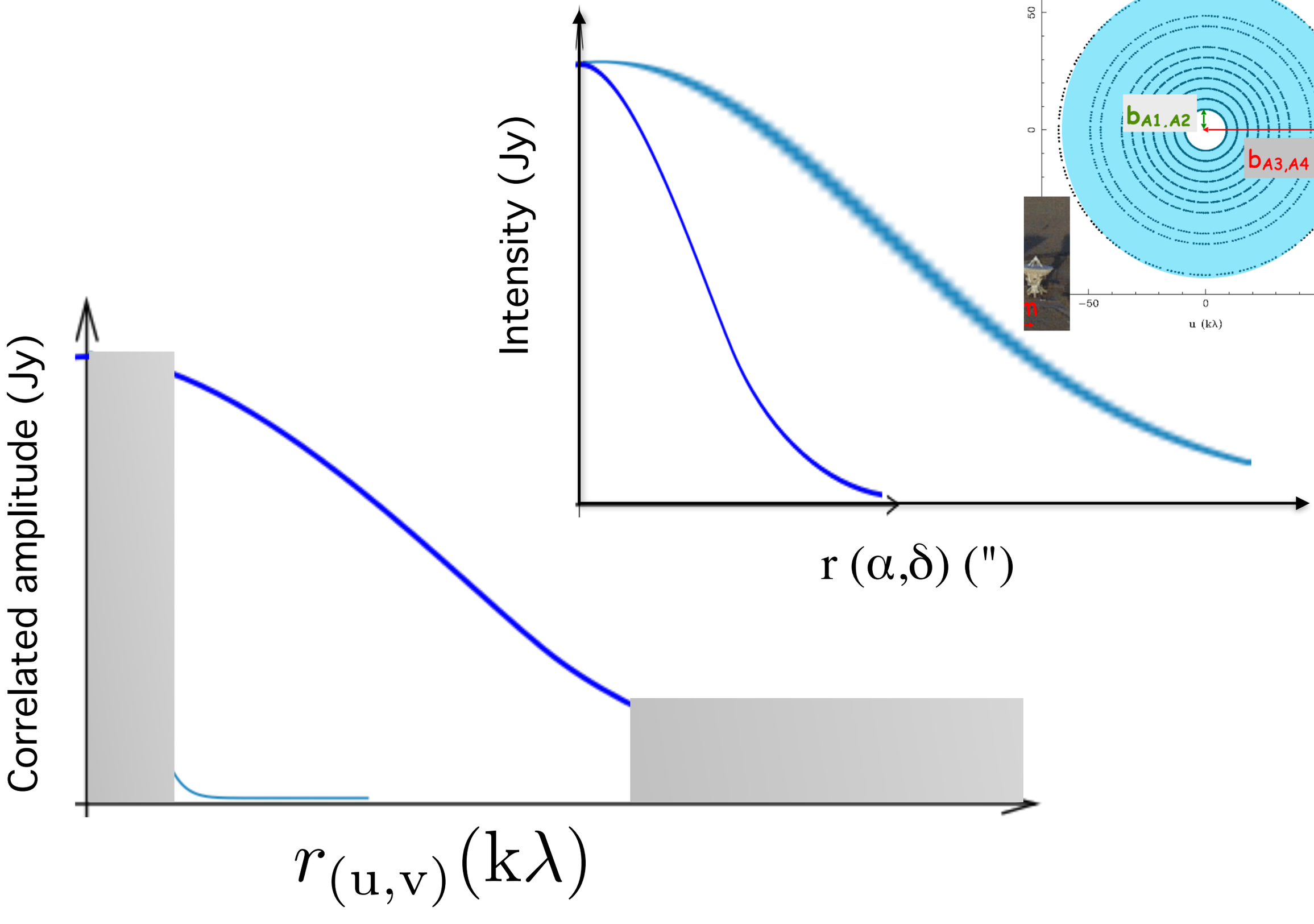

DecoInvolution • Imaging: Inverse Fourier Transform and Clean

Source

Dirty Beam

$$I^D(x,y) = B(x,y) \otimes I(x,y)$$

Dirty map

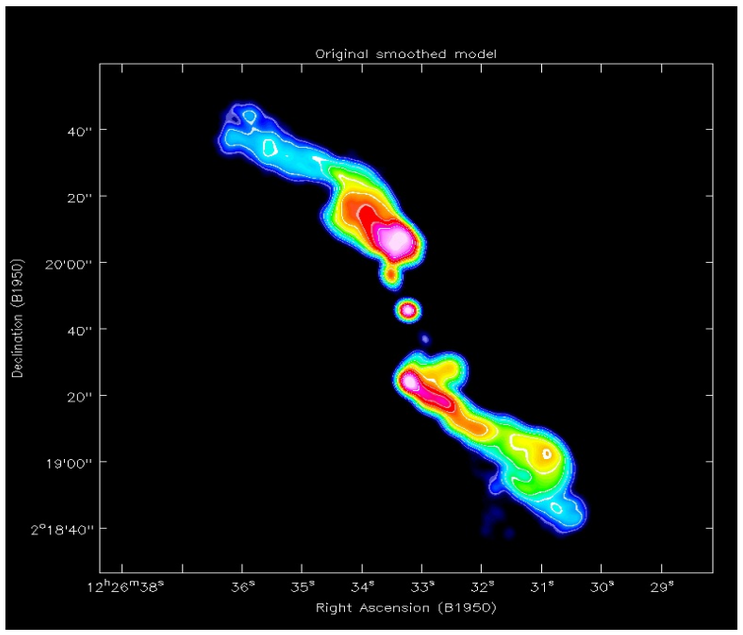

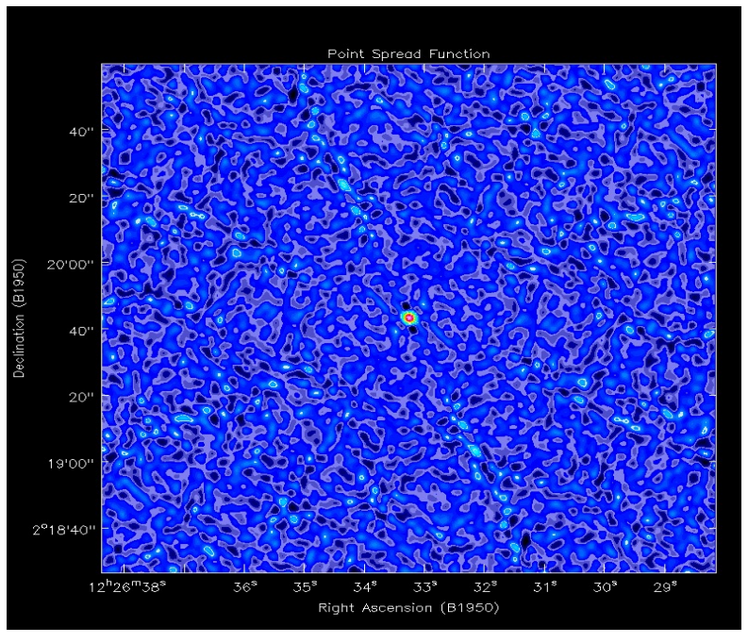

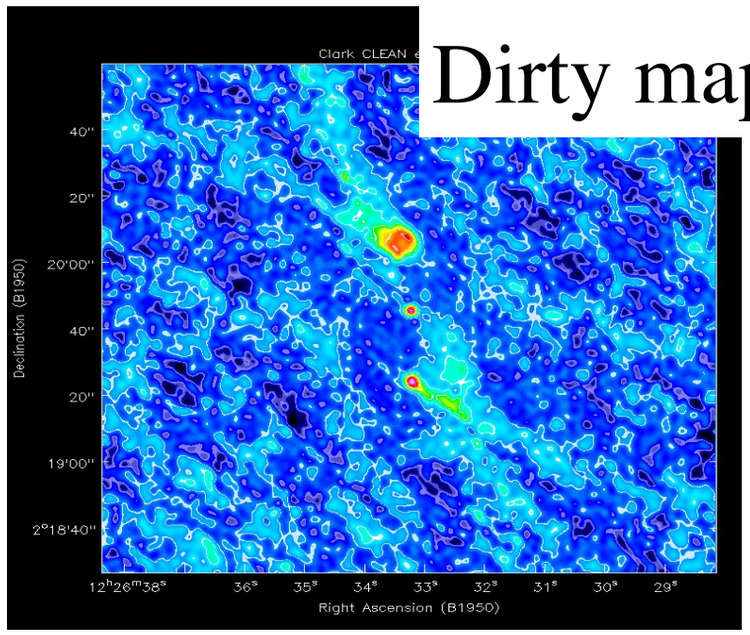

Deconvolved images, using 3 different techniques

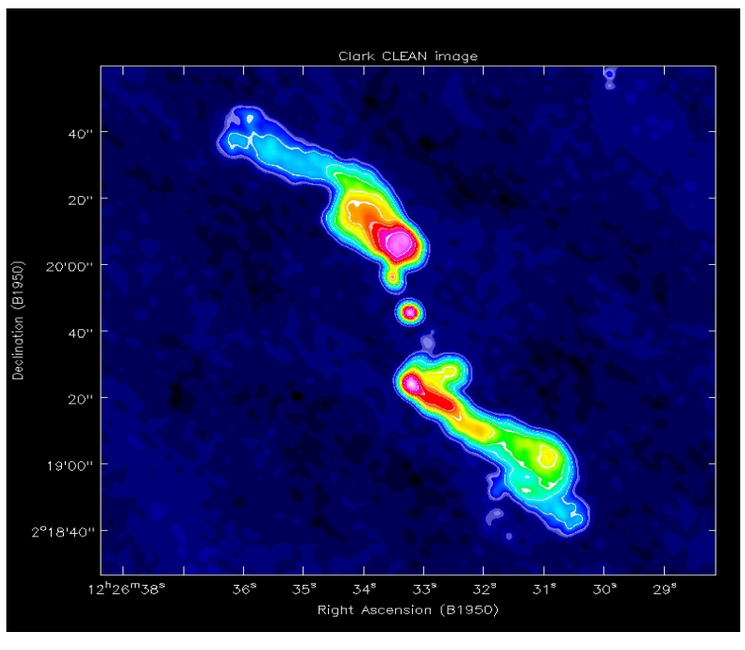

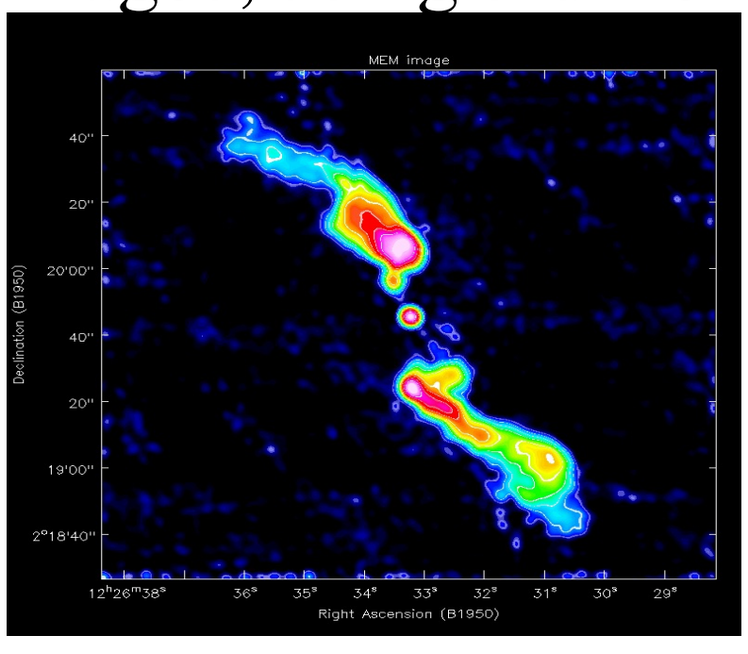

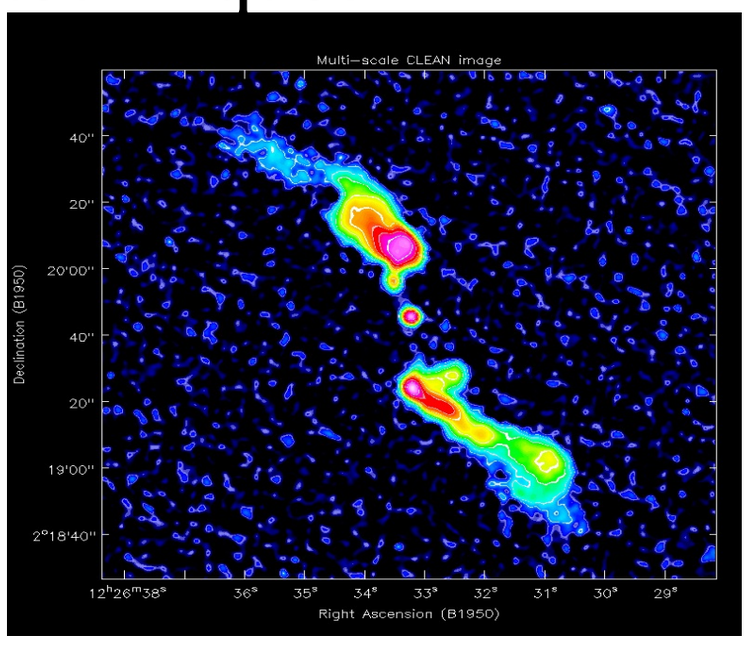

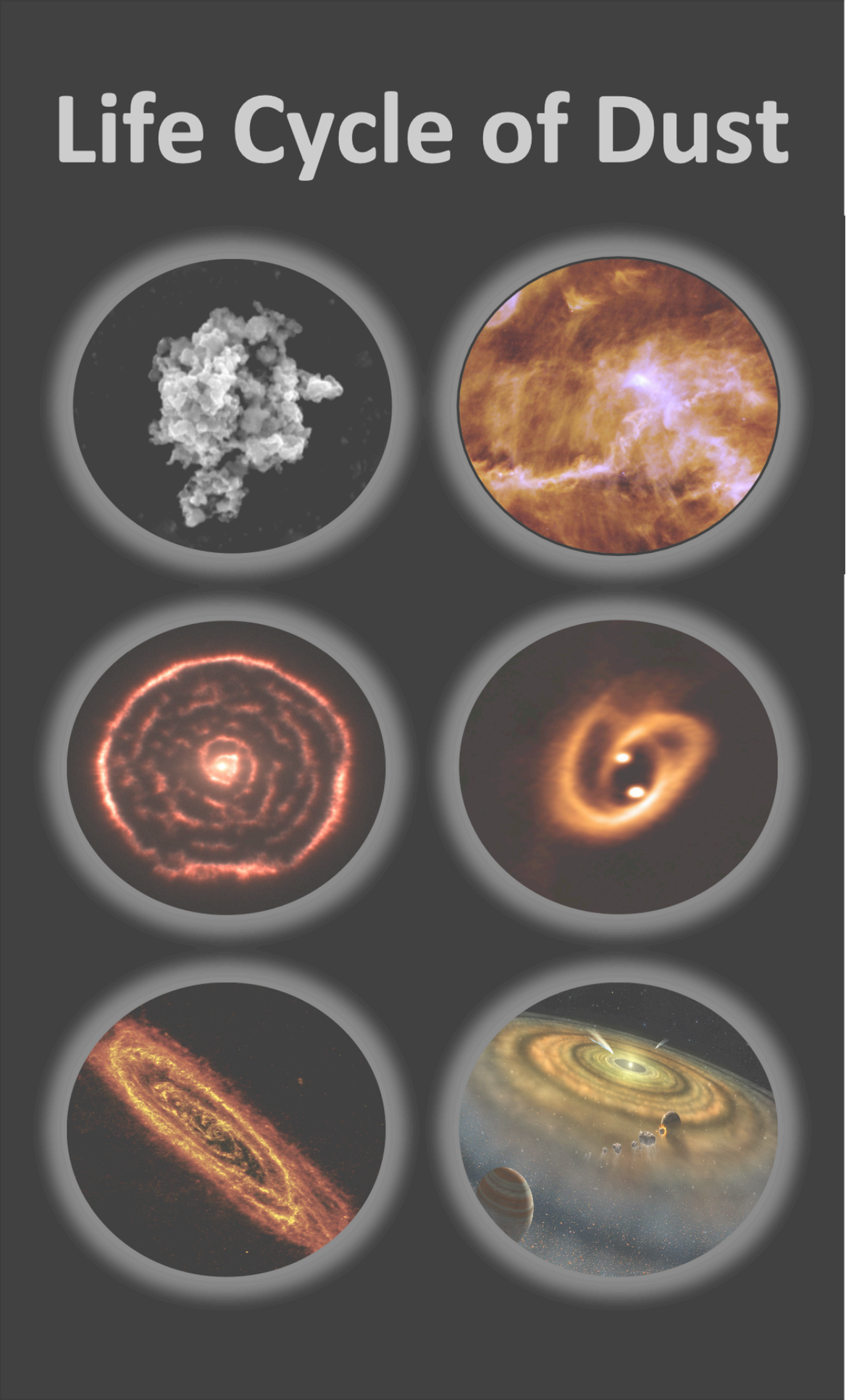

★ Facilities from Radio to Optical

•

●

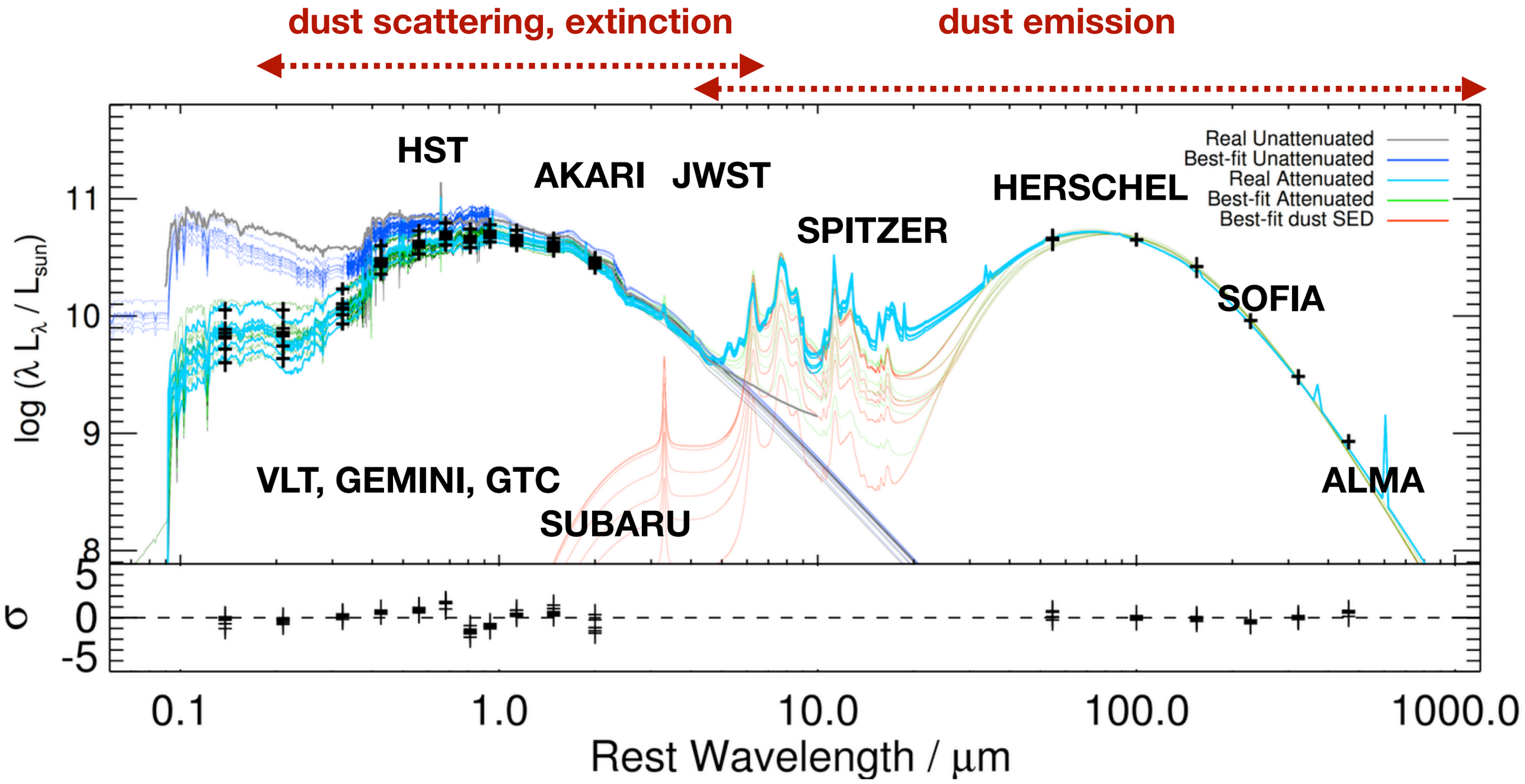
dust scattering, extinction
dust emission
HST
AKARI
JWST
SPITZER
HERSCHEL
SOFIA
ALMA
VLT, GEMINI, GTC
SUBARU
Real Unattenuated
Best-fit Unattenuated
Real Attenuated
Best-fit Attenuated
Best-fit dust SED
log (λ L_λ / L_sun)
11
10
9
8
σ
5
0
-5
0.1
1.0
10.0
100.0
1000.0
Rest Wavelength / μm

https://irsa.ipac.caltech.edu/frontpage/

NASA/IPAC Infrared Science Archive

IRSA | Data sets | Search | Tools | Help

Login

Search for Source

Name or Coordinates

Search

Radius 30 arcsec

Guide for Solar System Observers

Search Catalog: WISE

Search

ZTF Data Release 18

The eighteenth public data release from the Zwicky Transient Facility contains approximately 49.6 million images, 768 billion source detections extracted from these images, and 4.70 billion light curves.

Past News

Featured Images

Catalogs

IRSA Viewer

Finder Chart

{https://} VO/API

Spitzer

WISE

SOFIA

IRTF

2MASS

Herschel

Planck

More

Contribute Data

Documentation

Video Tutorials

Help Desk

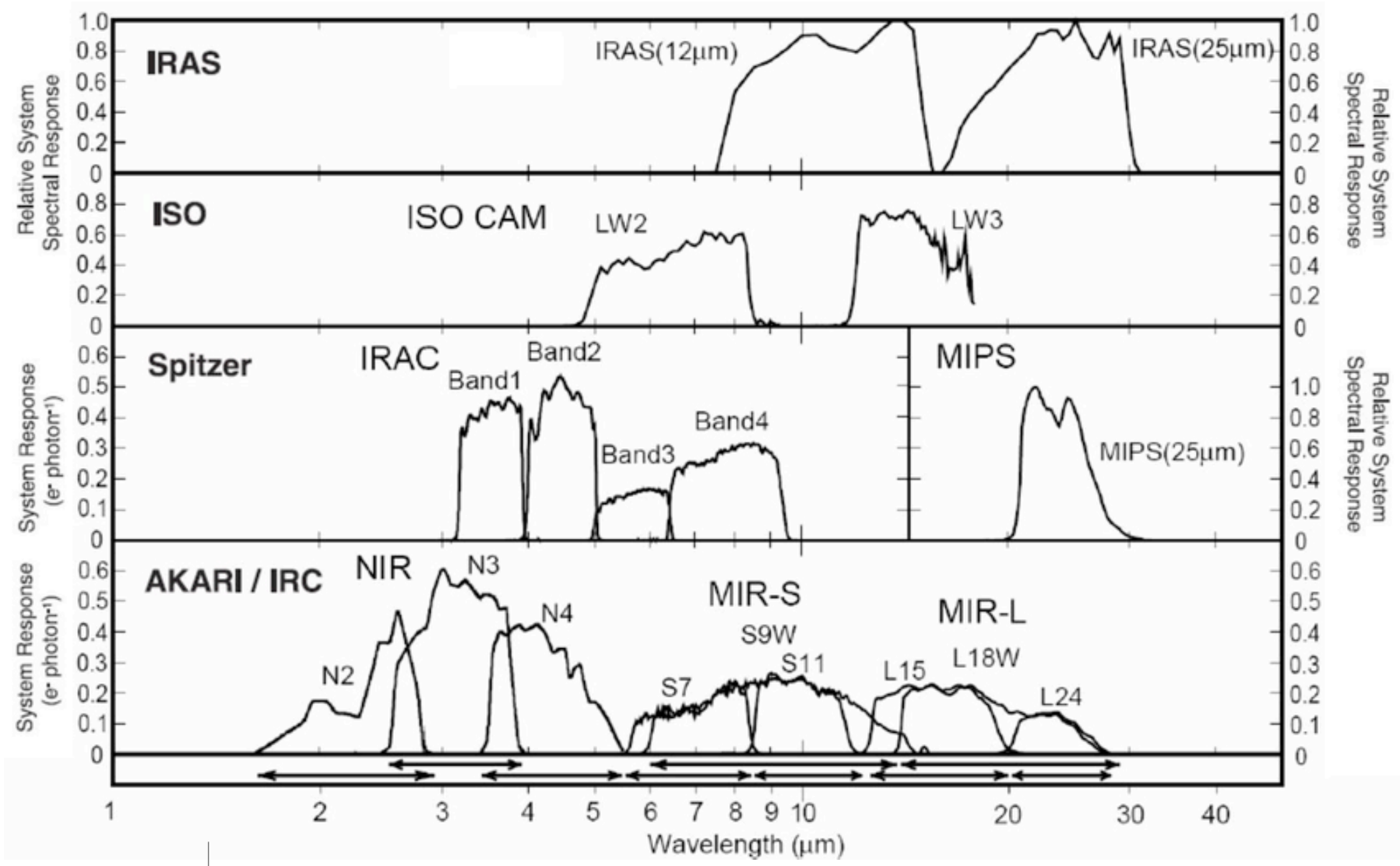
IRAS
IRAS(12μm)
IRAS(25μm)
ISO
ISO CAM
LW2
LW3
Spitzer
IRAC
Band1
Band2
Band3
Band4
MIPS
MIPS(25μm)
AKARI / IRC
NIR
N2
N3
N4
MIR-S
S7
S9W
S11
MIR-L
L15
L18W
L24
Relative System Spectral Response
System Response (e⁻ photon⁻¹)
Wavelength (μm)

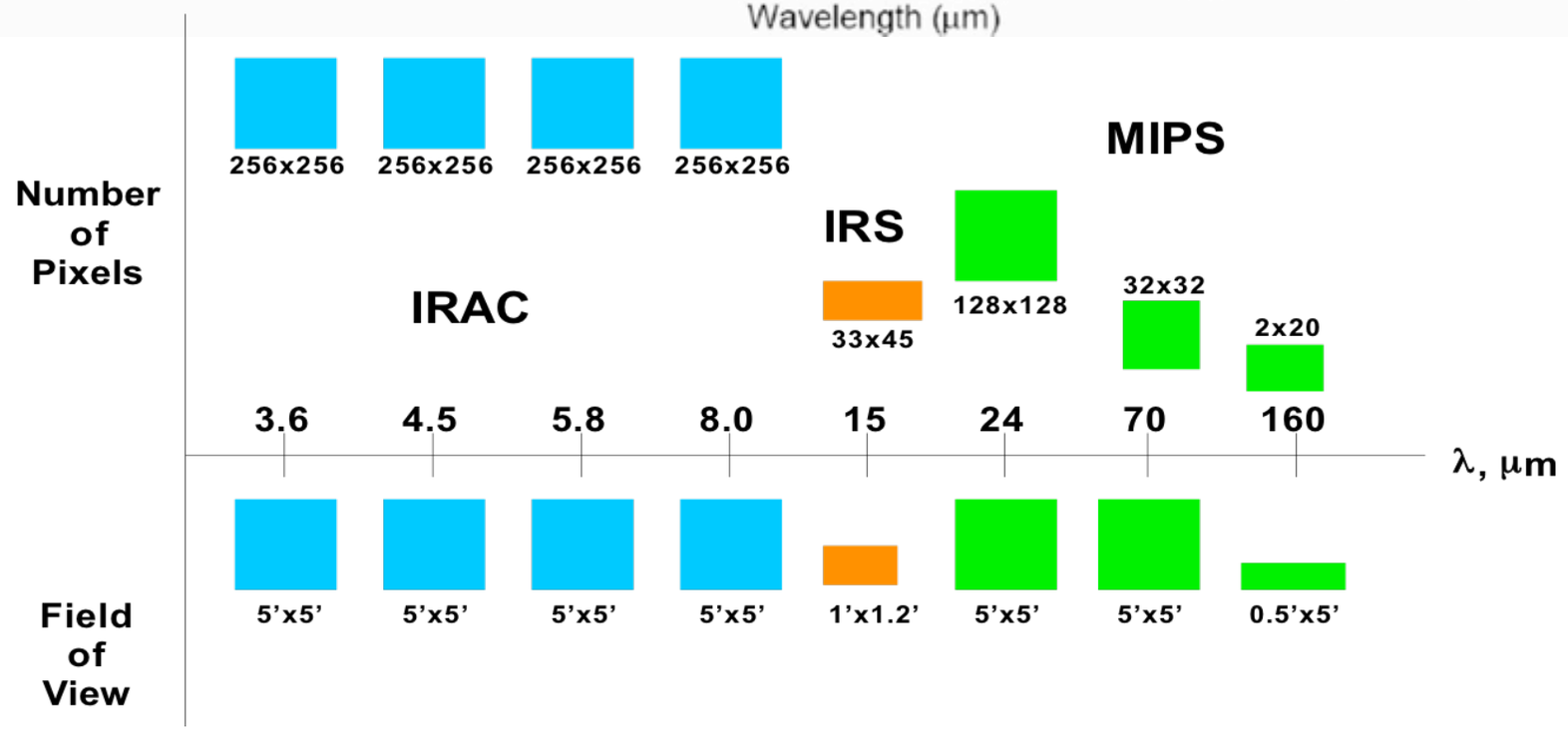
Number of Pixels
256x256
256x256
256x256
256x256
IRAC
IRS
33x45
128x128
MIPS
32x32
2x20
3.6
4.5
5.8
8.0
15
24
70
160
λ, μm
Field of View
5'x5'
5'x5'
5'x5'
5'x5'
1'x1.2'
5'x5'
5'x5'
0.5'x5'

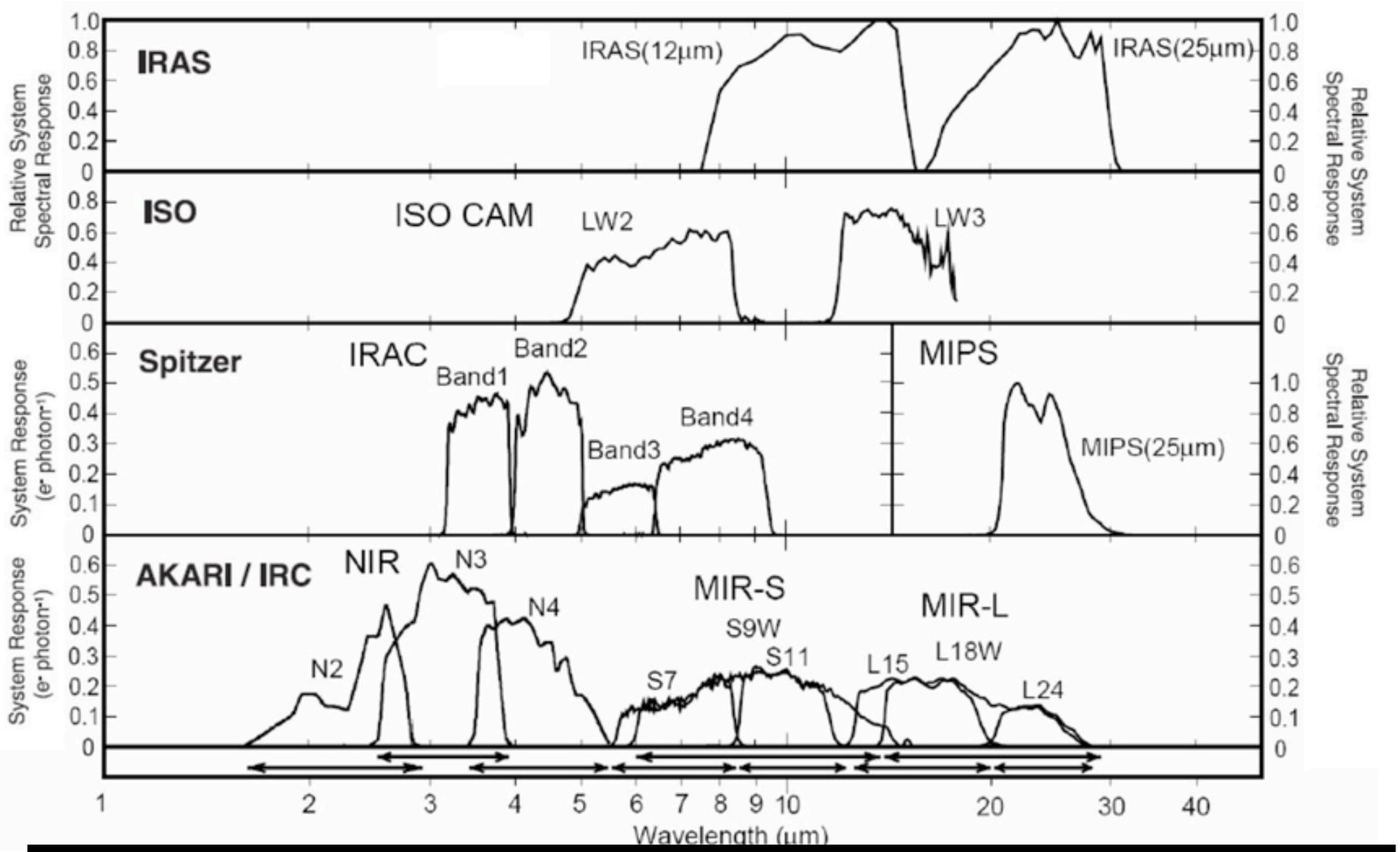
IRAS
IRAS(12μm)
IRAS(25μm)
ISO
ISO CAM
LW2
LW3
Spitzer
IRAC
Band1
Band2
Band3
Band4
MIPS
MIPS(25μm)
AKARI / IRC
NIR
N2
N3
N4
MIR-S
S7
S9W
S11
MIR-L
L15
L18W
L24
Relative System Spectral Response
System Response (e⁻ photon⁻¹)
Wavelength (μm)

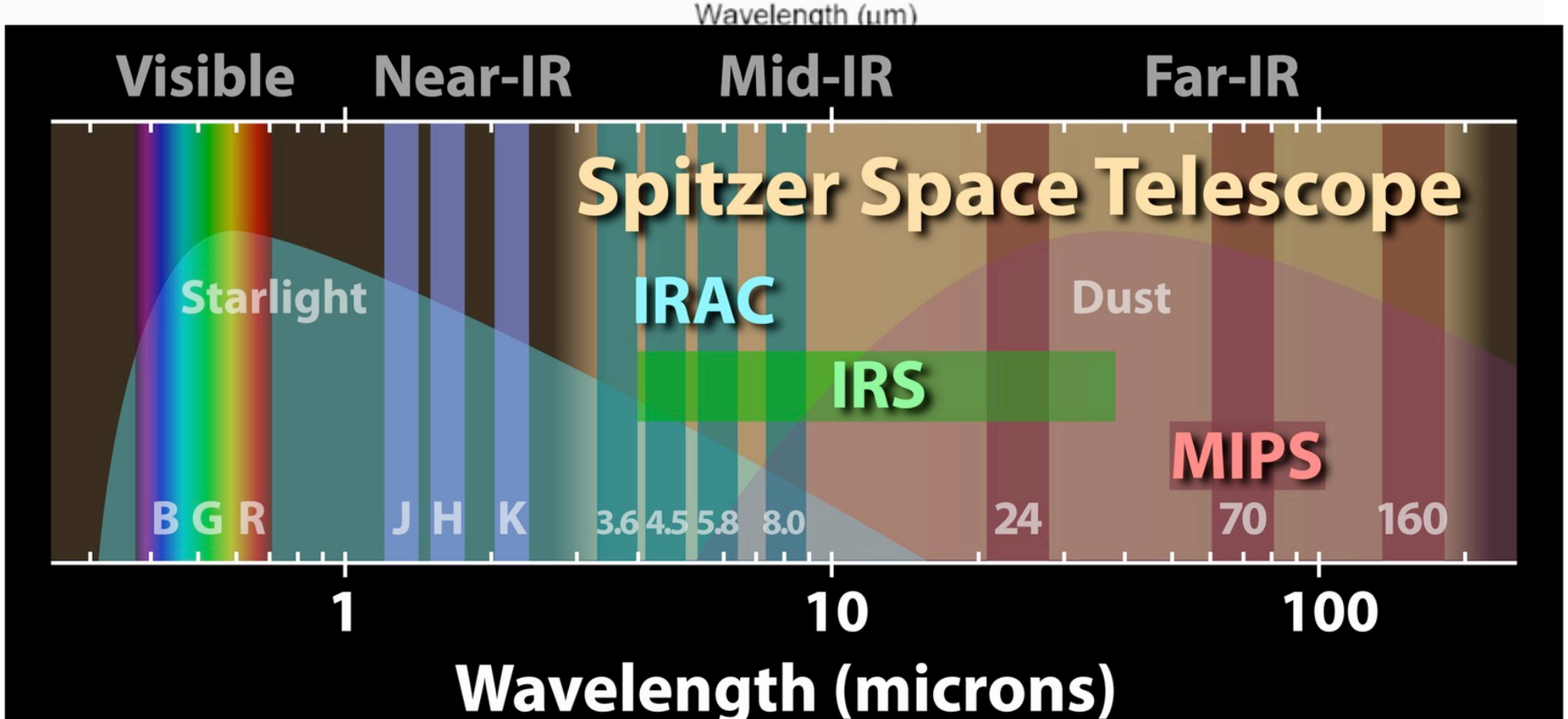
Visible
Near-IR
Mid-IR
Far-IR
Spitzer Space Telescope
Starlight
IRAC
Dust
IRS
MIPS
B G R
J H K
3.6 4.5 5.8 8.0
24
70
160
1
10
100
Wavelength (microns)

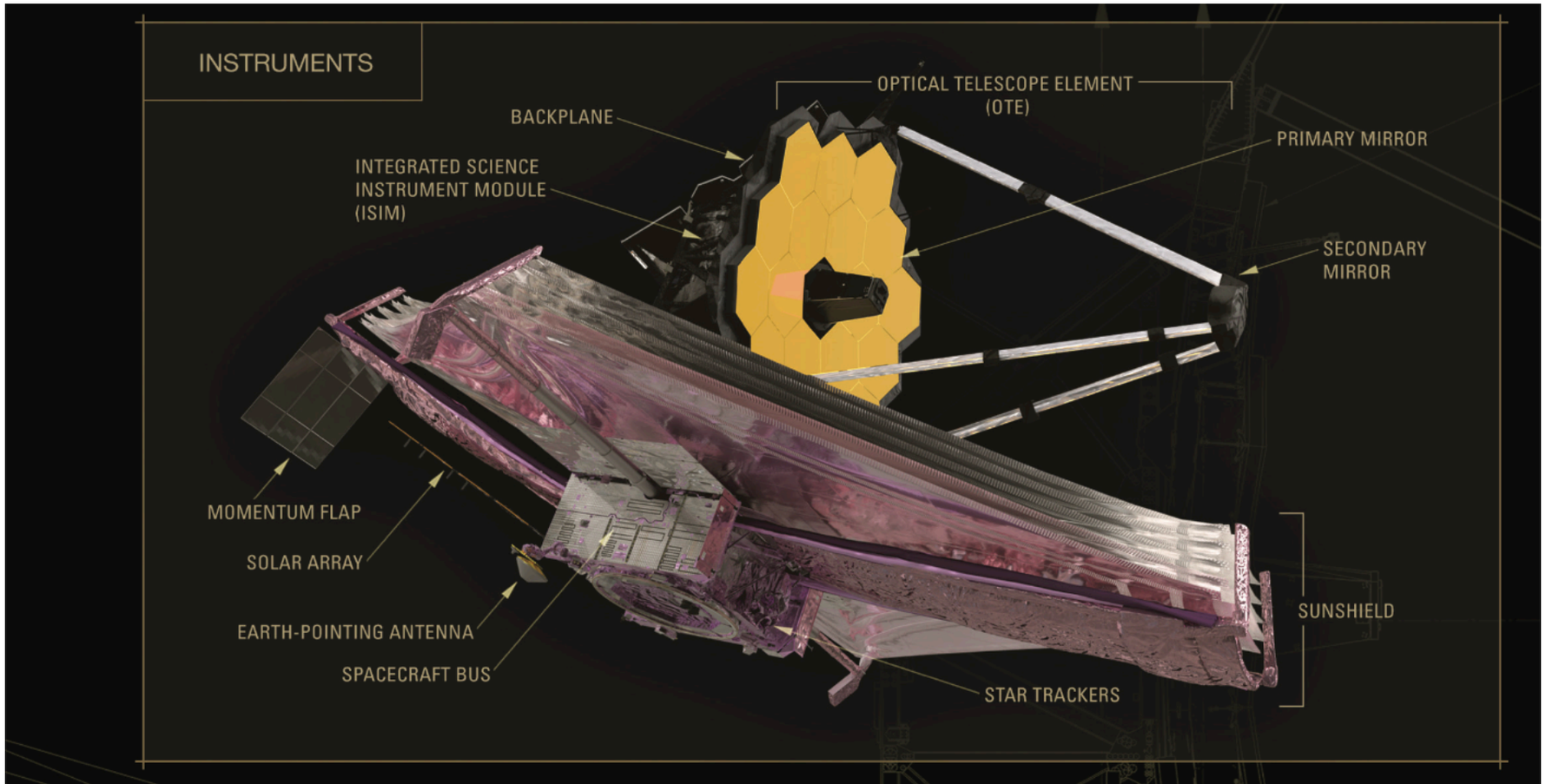

WEBB SPACE TELESCOPE

Observatory

Webb is NASA's largest and most powerful space science telescope ever constructed. Webb's enormous size and frigid operating temperature present extraordinary engineering challenges. After launching from French Guiana, the observatory will travel to an orbit about one million miles away from Earth and undergo six months of commissioning in space—unfolding its mirrors, sunshield, and other smaller systems; cooling down; aligning; and calibrating. Astronomers worldwide will then be able to conduct scientific observations to broaden our understanding of the universe. Webb will also complement the science achieved by other NASA missions.

Partners

Quick Facts

PRIMARY MIRROR SIZE: 21.3 feet (6.5 meters) across

MIRROR SHAPE: The mirror is comprised of 18 gold-plated hexagonal deployable segments

SUNSHIELD: Webb's five-layer deployable sunshield is the size of a tennis court

INSTRUMENTS: Webb has four science instruments: Near-Infrared Camera (NIRCam), Near-Infrared Spectrograph (NIRSpec), Mid-Infrared Instrument (MIRI), and Near-Infrared Imager and Slitless Spectrograph (NIRISS) with the Fine Guidance Sensor (FGS)

WAVELENGTHS: Visible, Near Infrared, Mid Infrared (0.6-28.5 micrometers)

Single-dish telescopes @ mm & submm

Nobeyama 45m

- 2 receivers (3, 7 mm)
- BEARS camera of 25 pixels at 3 mm (line/continuum)
- NOBA camera of 7 pixels at 2 mm (Δv=30GHz)

IRAM 30m

- 4 receivers (1,2,3 mm)
- Camera HERA of 9 pixels at 1mm (line)
- NIKA camera at 2mm and 1mm (continuum)

LMT 50m

- receivers 3.1 →1.4 mm
- Camera TolTEC: 1.1, 1.4, 2.0 mm with 500, 1200, 2000 pixels

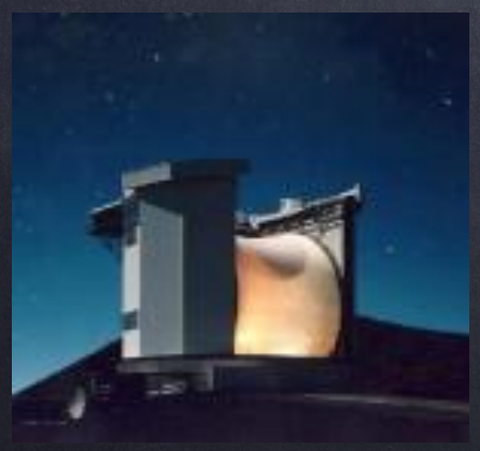

JCMT 15m

- receivers 0.42 →1.4 mm
- Camera SCUBA2 with 10^4 pixels at 0.45 & 0.85 mm

APEX 15m

- 4 receivers 1 & 0.3 mm
- Camera at 0.8mm

Main single-dish antenna at mm/submm

Telescope	Diameter (m)	Freq. (GHz)	λ (mm)	HPBW (")	Latitude (deg)
IRAM	30	70-345	4-0.7	35-7	+37
APEX	12	230-1200	1.3-0.3	30-6	-22
JCMT	15	210-710	2-0.2	20-10	+20
Herschel	3.5	500-2000	0.6-0.1	43-11	space

Single-dish telescopes at cm

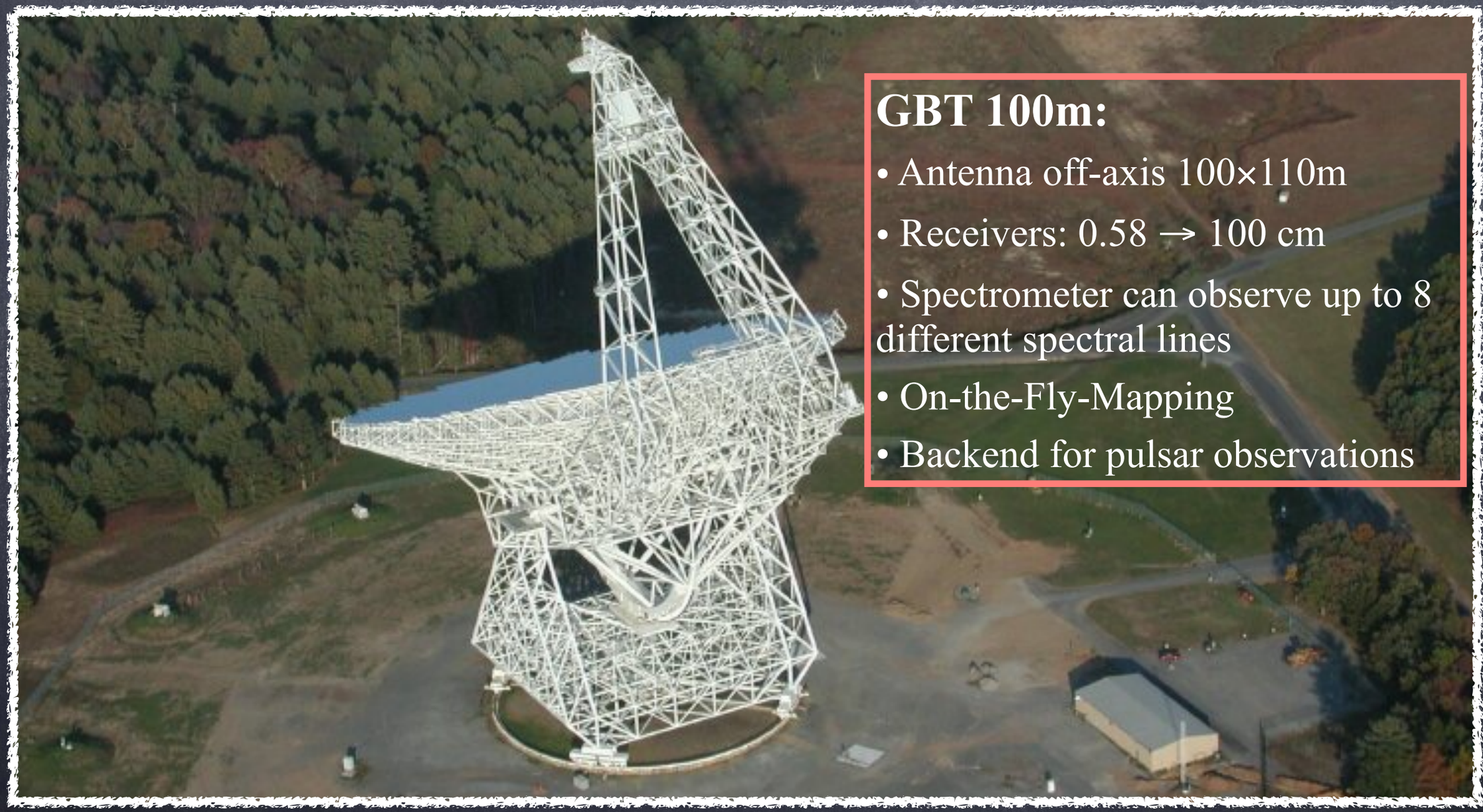

GBT 100m:

- Antenna off-axis 100×110m
- Receivers: 0.58 → 100 cm
- Spectrometer can observe up to 8 different spectral lines
- On-the-Fly-Mapping
- Backend for pulsar observations

ALMA Overview

- A global partnership to deliver a transformational millimeter/submillimeter interferometer
  - North America (US, Canada, Taiwan)
  - Europe (ESO)
  - East Asia (Japan, Taiwan)
  - In collaboration with Chile

- 5000m (16,500 Ft) site in Chilean Atacama desert

- Main Array: 50 x 12m antennas
  + Total Power Array 4 x 12m
  + Atacama Compact Array (ACA): smaller array of 12 x 7m antennas

- Total shared cost ~1.3 Billion ($US2006)

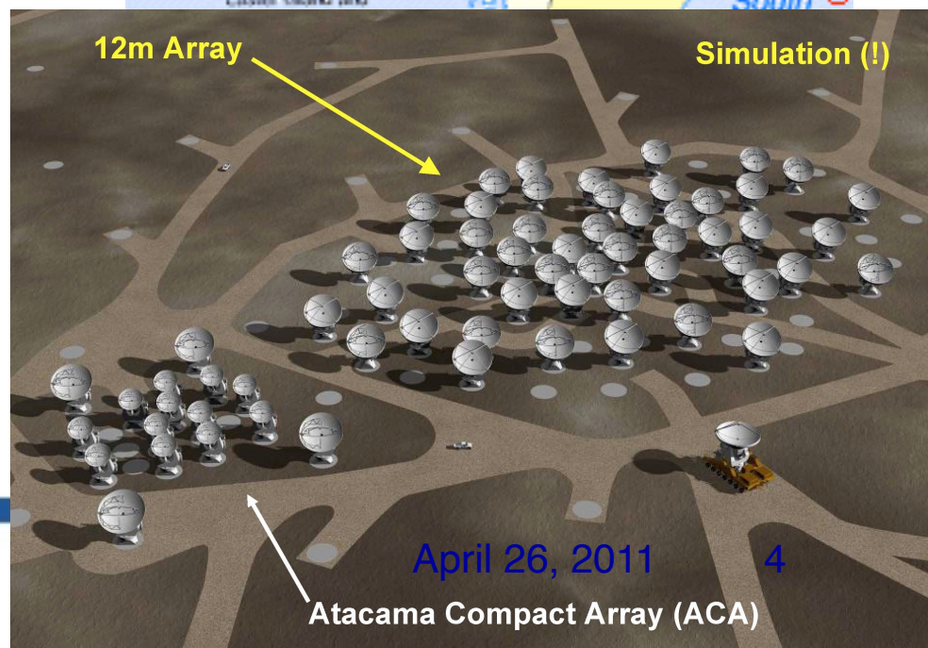

ALMA Overview

- Baselines up to 15 km (0.015" at 300 GHz) in "zoom lens" configurations
- Sensitive, precision imaging 84 to 950 GHz (3 mm to 315 μm)
- State-of-the-Art low-noise, wide-band SIS receivers (8 GHz bandwidth)
- Flexible correlator with high spectral resolution at wide bandwidth
- Full polarization capabilities
- Estimate 1 TB/day archived
- A resource for ALL astronomers

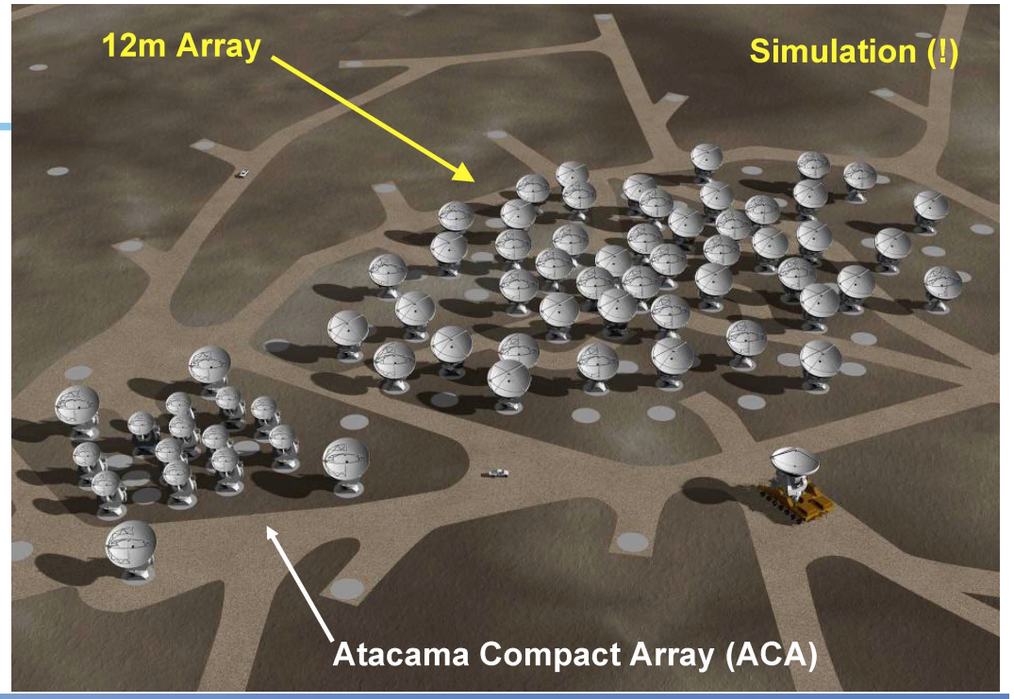

ALMA is 10-100 times more sensitive and have 10-100 times better angular resolution compared to previous millimeter interferometers

ALMA Receiver Bands

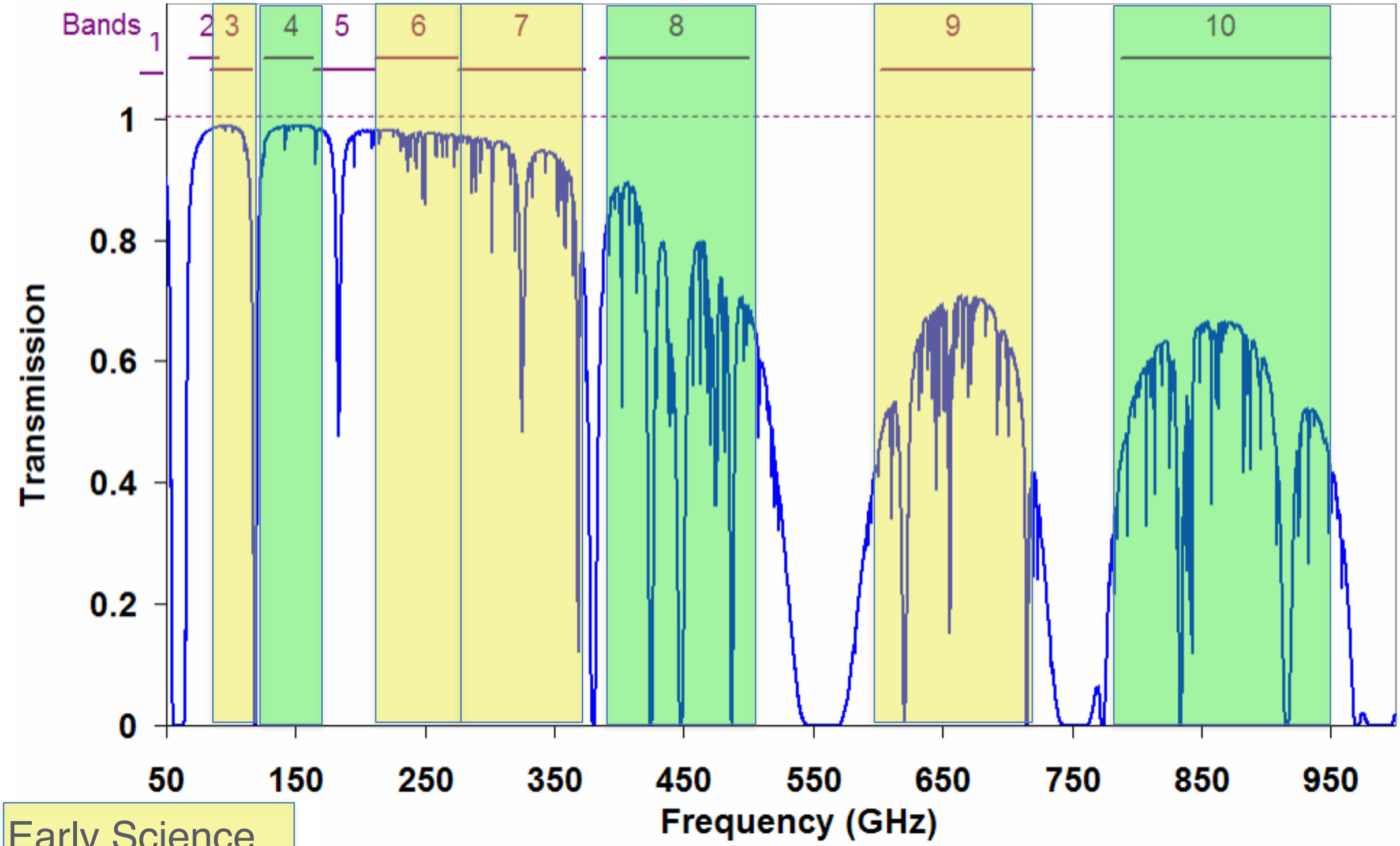

Early Science

Full Operations

Maximum Angular Scale

ALMA

Band	Frequency (GHz)	Primary beam (“)	Maximum Angular Scale (“) Compact	Extended
3	84-116	72 - 52	20	10
6	211-275	29 - 22	9	4.5
7	275-373	22 - 16	6	3
9	602-720	10 – 8.5	3	1.5

- **Smooth** structures larger than MAS are completely resolved out
- Begin to lose total recovered flux for objects on the order of half MAS

→ Need additional observations with a single-dish or a more compact array with smaller antennas

NRAO

Technical Information
The Telescopes

SKAO

The SKA telescopes are made up of arrays of antennas – SKA-mid observing mid to high frequencies and SKA-low observing low frequencies – to be spread over long distances. The SKA is to be constructed in phases: A first phase in South Africa and Australia, with a later expansion representing a significant increase in capabilities and expanding into other African countries, with the component in Australia also being expanded.

SKA1-Mid
the SKA's mid-frequency telescope

Location: South Africa

Frequency range:
350 MHz
to
15.4 GHz
with a goal of 24 GHz

197 dishes
(including 64 MeerKAT dishes)

Maximum baseline:
150km

SKA1-Low
the SKA's low-frequency telescope

Location: Australia

Frequency range:
50 MHz
to
350 MHz

131,072
antennas spread between
512 stations

Maximum baseline:
~74km

SKA1 Telescope Expected Performance – Imaging

Nominal frequency	110 MHz	300 MHz	770 MHz	1.4 GHz	6.7 GHz	12.5 GHz
Range [GHz]	0.05-0.35	0.05-0.35	0.35-1.05	0.95-1.76	4.6-8.5	8.3-15.4
Telescope	Low	Low	Mid	Mid	Mid	Mid
FoV [arcmin]	327	120	109	60	12.5	6.7
Max. resolution [arcsec]	9.7	3.5	0.7	0.3	0.06	0.03
Max. bandwidth [MHz]	300	300	700	810	3900	2 x 2500
Cont. rms, 1hr [μJy/beam] [a]	26	14	4.4	2	1.3	1.2
Line rms, 1hr [μJy/beam] [b]	1850	800	300	140	90	85
Resolution range for cont. & line rms [arcsec] [c]	12-600	6-300	1-145	0.6-78	0.13-17	0.07-9
Channel width (uniform resolution across max. bandwidth) [kHz]	5.4	5.4	13.4	13.4	80.6	80.6
Narrowest bandwidth, zoom [kHz]	3.9	3.9	3.1	3.1	3.1	3.1
Finest zoom channel width [Hz]	226	226	210	210	210	210

Captura de Pantalla